SELF-ASSEMBLED MONOLAYERS ON SILICON: DEPOSITION AND SURFACE CHEMISTRY

Małgorzata Adamkiewicz

A Thesis Submitted for the Degree of PhD
at the
University of St Andrews

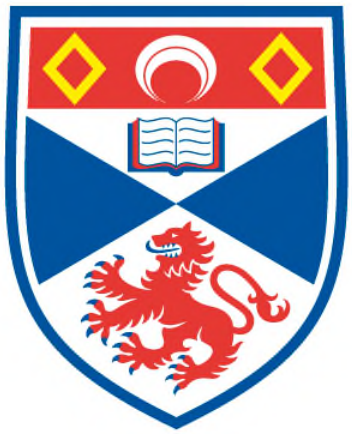

2013

Self-Assembled Monolayers on Silicon – Deposition and Surface Chemistry

School of Chemistry

Małgorzata Adamkiewicz

This thesis is submitted for the degree of
Doctor of Philosophy at the University of St Andrews

Supervisors: Dr Georg Hähner

Prof. David O'Hagan

June 2013

1. Candidate's declaration

I, Małgorzata Adamkiewicz, hereby certify that this thesis, which is approximately 32,000 words in length, has been written by me, that it is the record of my work carried out by me and that it has not been submitted in any previous application for a higher degree.

I was admitted as a research student in September 2009 and as candidate for the degree of PhD in September 2010, the higher study for which this is a record was carried out in the University of St Andres between 2009 and 2013.

Date: Signature of Candidate:

2. Supervisor's declaration

I, hereby certify that the candidate has fulfilled the conditions of the Resolution and Regulations appropriate for the degree of Doctor of Philosophy in the University of St Andrews and that the candidate is qualified to submit this thesis in application for that degree.

Date: Signatures of Supervisors:

3. Permission for electronic publication

In submitting this thesis to the University of St Andrews I understand that I am giving permission for it to be made available for use in accordance with the regulations of the University Library for the time being in force, subject to any copyright vested in the work not being affected thereby. I also understand that the title and the abstract will be published, and that a copy of the work may be made and supplied to any *bona fide* library or research worker, that my thesis will be electronically accessible for personal or research use unless exempt by award of an embargo as requested below, and that the library has the right to migrate my thesis into new electronic forms as required to ensure continued access to the thesis. I have obtained any third-party copyright permissions that may be required in order to allow such access and migration, or have requested the appropriate embargo below.

The following is an agreed request by candidate and supervisor regarding the electronic publication of this thesis:

Embargo on both all of printed copy and electronic copy for the same fixed periods of two years on the following ground: publication would preclude future publication.

Date: Signature of Candidate:

Signatures of Supervisors:

Acknowledgements

First and foremost, I would like to thank my supervisor Dr Georg Hähner for his supervision, encouragement and advice during my PhD studies. I would like to thank Prof. David O'Hagan for co-supervision, all his help and support over the last three years and for giving me the opportunity to join his research group.

I would also like to thank Dr Tony O'Hara from MEMSStar and SPIRIT Studentship for funding this project.

I would particularly like to express my appreciation to Dr Neil Keddie and Dr Stephen Francis for all the helpful discussions and suggestions along the way, and for answering all my questions.

Thanks are also due to Dr Tomas Lebl and Mrs Melanja Smith for their assistance with solution NMR spectroscopy and Mrs Caroline Horsburgh for the mass spectroscopy. I would also like to acknowledge Prof. Peter Cumpson for the XPS analysis, Prof. Manfred Buck for allowing me to use an AFM microscope and Prof. Ifor Samuel for opportunity to use an ellipsometer. I am also grateful to Dr Zhe She and Dr Yue Wang for passing on their knowledge.

I would also like to thank all the members in the O'Hagan and Hähner group, both past and present, who I encountered during my studies. Thanks are also to Dr Michael Corr for his careful proof reading and Nouchali, Jason, Nawaf, Maciej and Yi for their friendship and support.

I am also immensely grateful for the love and support of my parents and sisters. Finally, I would like to thank Krzysztof for his patience, understanding, motivation and support.

dla Rodziców

Abstract

Fabrication of surfaces with versatile functional groups is an important research area. Hence, it is essential to control and tune the surface properties in a reliable manner. Vinyl-terminated self-assembled monolayers (SAMs) offer significant flexibility for further chemical modification and can serve as a versatile starting point for tailoring of surface properties. Here a synthetic route for the preparation of vinyl-terminated trichlorosilane self-assembling molecules: 9-decenyltrichlorosilane (CH_2=CH-$(CH_2)_8$-$SiCl_3$), 10-undecenyltrichlorosilane (CH_2=CH-$(CH_2)_9$-$SiCl_3$), and 14-pentadecenyltrichlorosilane (CH_2=CH-$(CH_2)_{13}$-$SiCl_3$) is presented. These molecules were used for the preparation of SAMs in either liquid or vapour phase processes. Commercially available methyl-terminated self-assembling molecules: decyltrichlorosilane (CH_3-$(CH_2)_9$-$SiCl_3$) and octadecanetrichlorosilane (CH_3-$(CH_2)_{17}$-$SiCl_3$) were used as controls. The resultant films were characterised by X-ray photoelectron spectroscopy (XPS), contact angle analysis, ellipsometry, and atomic force microscopy (AFM).

Well defined, vinyl-terminated SAMs were further chemically modified with carbenes (:CCl_2, :CBr_2, :CF_2) and hexafluoroacetone azine (HFAA). The reactions were performed in the liquid or the vapour phase. The resulting SAMs were characterised using the same methods as for the vinyl-terminated monolayers. Successful modification was confirmed by the appearance of new signals in the XPS spectrum, with simultaneous changes in water contact angle values and unchanged thickness values. Methyl-terminated SAMs were also exposed to carbenes and HFAA as a control system. These are the first examples of C-C bond formation on SAMs in the vapour phase.

Abbreviations

AFM	- atomic force microscopy
AHTMS	- (17-aminoheptadecyl)trimethoxysilane
AMP	- ammonia/peroxide mixture
ASAP	- atmospheric solids analysis probe mass spectrometry
ATR	- attenuated total reflectance
BTEAC	- benzyltriethylammonium chloride
CA	- contact angle
CI	- chemical ionisation
CM	- cross metathesis
CuAAC	- copper catalysed azide alkyne cycloaddition
DCM	- dichloromethane
DI water	- deionised water
DMF	- dimethylformamide
E_B	- binding energy
E_K	- kinetic energy
ESCA	- electron spectroscopy for chemical analysis
ESI	- electrospray ionisation
Et_2O	- diethyl ether
EtOAc	- ethyl acetate
FDTS	- 1H,1H,2H,2H-perfluorodecyltrichlorosilane
HFAA	- hexafluoroacetone azine
HFPO	- hexafluoropropene oxide
HMP	- hydrochloric/peroxide mixture
HO-TEMPO	- 4-hydroxy-2,2,6,6-tetramethylpiperidine 1-oxyl
IR-CRDS	- infrared cavity ring-down spectroscopy
λ	- mean free path
MCPBA	- *meta*-chloroperoxybenzoic acid
MDFA	- methyl 2,2-difluoro-2-(fluorosulfonyl)-acetate
MEMS	- microelectromechanical systems
Me	- methyl
NEMS	- nanoelectromechanical systems
NMR	- nuclear magnetic resonance

OTS	- octadecanetrichlorosilane
Piranha Solution	- sulfuric acid/peroxide mixture
PMA	- ethanolic solution of phosphomolybdic acid
PTC	- phase transfer catalysis
RAIRS	- reflection-absorption infrared spectroscopy
RMS	- root mean square
rt	- room temperature
SAM	- self-assembled monolayer
SC-1	- standard clean 1
SC-2	- standard clean 2
S_N2	- nucleophilic substitution
t-BuOK	- potassium *tert*-butoxide
TEMPO	- 2,2,6,6-tetramethylpiperidine 1-oxyl
TFDA	- trimethylsilyl 2,2-difluoro-2-(fluorosulfonyl)acetate
THF	- tetrahydrofuran
TLC	- thin layer chromatography
TML	- trichloromethyllithium
$TMSCF_3$	- trifluoromethyltrimethylsilane
TMSCl	- trimethylsilyl chloride
XPS	- X-ray photoelectron spectroscopy

Contents

1. Self-Assembled Monolayers and Their Chemical Modification by Surface Reactions

Surface science focuses on the investigation of physical and chemical phenomena that occur at interfaces, *e.g.* solid-gas, solid-liquid. By means of nanotechnology surface properties can be tuned for example by the formation and chemical modification of self-assembled monolayers (SAMs).[1] SAMs are relatively easy to prepare and offer significant flexibility for introducing new chemical functionalities.[2, 3] This feature makes self-assembly a versatile and unique modification method, which can be applied widely, for example in the design of biosensors.[4, 5] In this Chapter the current state of the art in liquid phase deposition as well as a review of surface reactions will be discussed.

1.1. Self-Assembled Monolayers

SAMs are ultrathin organic films formed by spontaneous adsorption of a surfactant onto a solid substrate.[6, 7] A schematic representation of a SAM is shown in **Figure 1.1**.

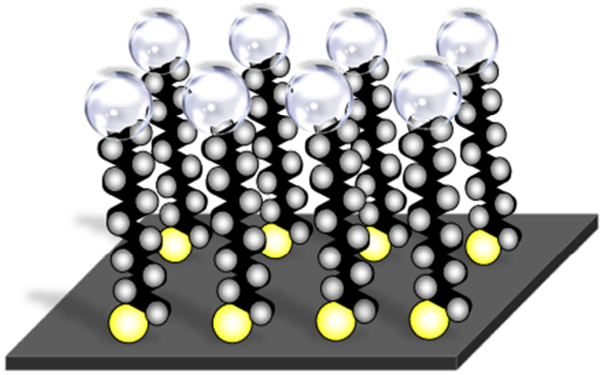

Figure 1.1. Schematic representation of a SAM.

SAMs can be formed from a variety of active self-assembling molecules on a number of different surfaces. Some of the best studied self-assembly systems are thiols on gold[8-11] and alkylsilanes on silicon.[12-16] Alkylsilane self-assembly is attractive due to the ability to generate chemically and physically stable, covalently attached films on surfaces such as SiO_x/Si, Si and glass.[7, 13-16] SAMs on silicon have been shown to have various

applications in fields such as: protein adsorption,[17-19] cell adhesion,[20] bioactive surfaces,[21] nanotechnology,[22] biosensors,[4, 5] chemical sensors,[22, 23] protective coatings,[24, 25] thin-film technology,[25, 26] microelectronics,[27] optoelectronics[28, 29] and others.[30-32]

Three different components can be distinguished in a self-assembling molecule used in SAM formation. These are a head group, a spacer, and a terminal functional group (**Figure 1.2**).

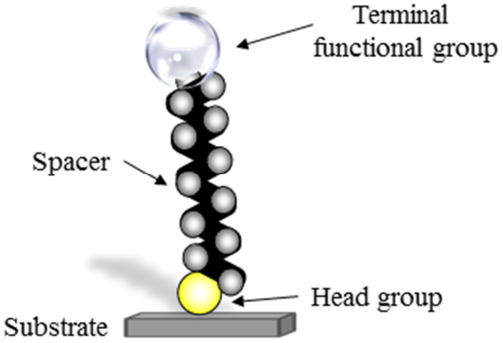

Figure 1.2. Construction of the self-assembling molecule.

The head group (reactive site) is a functionality with a strong affinity to a particular substrate.[33] If silicon oxide is the substrate, head groups such as trichlorosilane (-$SiCl_3$), trimethoxysilane (-$Si(OCH_3)_3$) or triethoxysilane (-$Si(OCH_2CH_3)_3$) have been used, the first being the most reactive.[7] When the reactive head group comes into contact with the substrate, a hydrolysis reaction of the Si-R (R = Cl, OCH_3, OCH_2CH_3) bonds occur, involving water present on the oxide's surface.[3, 34] The silanes attach *via* hydrogen bonds to the surface silanol groups and then a condensation reaction leads to covalent attachment and cross-linking between adjacent molecules (**Scheme 1.1**).[3, 22, 35]

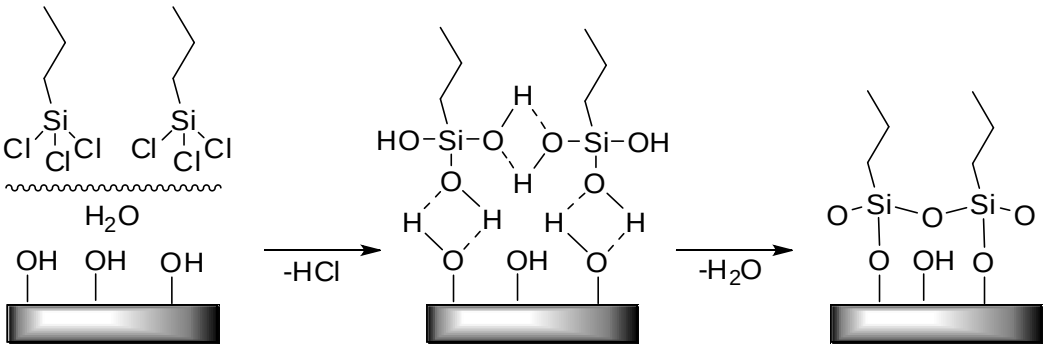

Scheme 1.1. Schematic representation of the proposed mechanism of the silanisation reaction.[3]

Silberzan *et al.*,[3] also indicated that the silane molecules form a polymerised network, where molecules are linked to each other, with only a few anchoring bonds linking them to the surface. The presence of the cross-linked network of Si-O-Si bonds explains why wafers modified with alkylsiloxane monolayers exhibit roughness which is similar or lower than for unmodified substrates.[22]

The spacer is generally an alkyl chain[36] or an aromatic ring[37] (**Figure 1.2**). It plays a crucial role in the packing/ordering of the molecules on the surface.[38] Longer alkyl chains (minimum 11 carbons)[39] result in the formation of closely-packed monolayers.[2, 40]

Finally, the terminal functional group (**Figure 1.2**) defines the properties of the surface. The chemical properties of a film can be tuned by introducing different terminal functional groups, either by deposition of self-assembling molecules with a modified end group, or by chemical transformation of the terminal group after the SAM film has been formed.[41]

1.2. Deposition of SAMs

SAMs can be prepared by immersion of a substrate into a solution of surface-active surfactant molecules (**Scheme 1.2**).

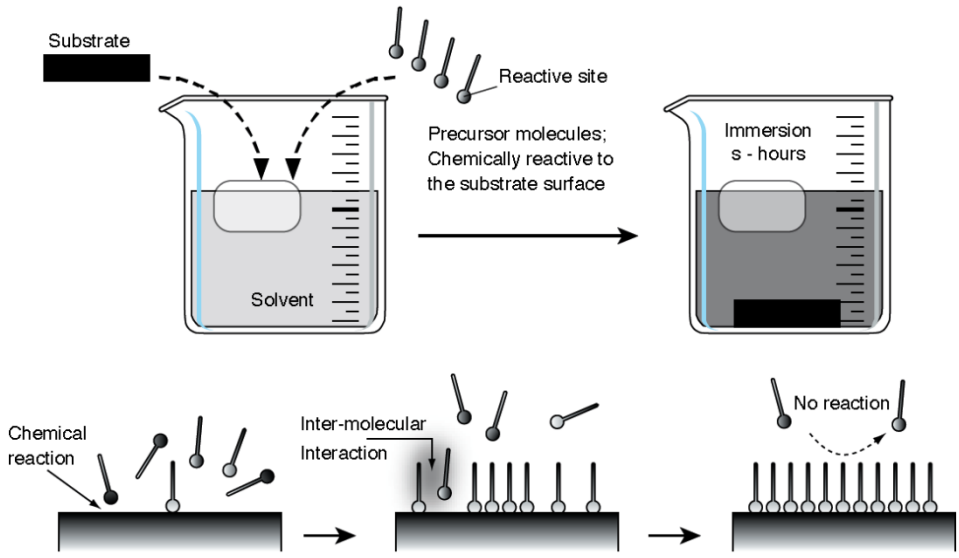

Scheme 1.2. Preparation of SAMs in the liquid phase (reprinted with permission from S. C. Tjong, *Nanocrystalline Materials: Their Synthesis-Structure-Property- Relationships and Applications*, Elsevier, Oxford, 2006. Copyright © 2006 Elsevier B. V.).[42]

The mechanism of SAM formation is shown in **Scheme 1.2**. First, the self-assembling molecules chemisorb onto the surface with their reactive head groups -SiR_3 (R = Cl, OCH_3, OCH_2CH_3) facing the surface.[42] The molecules organise *via* inter-molecular interactions between their spacers. SAM formation stops when the self-assembling molecules have reacted with all accessible reactive groups on the surface (**Scheme 1.2**). The thickness of a closely-packed and ordered SAM is determined by the length of the self-assembling molecule and the angle at which it is oriented relative to the surface.

The experimental modification of silicon substrates with SAMs *via* a silanisation reaction is relatively simple, but reproducing a well-defined monolayer is rather difficult due to the large number of parameters that influence the quality of the SAMs.[3, 38, 43] Thus, factors such as water content, type of surfactant, age and concentration of the solution, deposition time, temperature and the type of solvent must be carefully controlled.

The amount of water present in the surfactant solution or on the hydroxylated surface needs to be precisely controlled in order to obtain high-quality SAMs. In the absence of water, incomplete monolayers are formed.[44, 45] However, too much water causes excessive polymerisation of the trichlorosilanes in solution and results in deposition of polysiloxane on the surface rather than anchoring bonding.[7, 13, 46-50]

Self-assembling molecules, with different spacer lengths and types of reactive head group, also affect the overall SAM quality. Bierbaum *et al.*,[51] reported that the ordering behaviour of *n*-alkyltrichlorosilane films depends on the alkyl chain length. The optimum molecular length is eighteen carbons in order to obtain a monolayer with alkyl chains in all *trans*-conformation, oriented perpendicular to the surface. Moreover, short alkyl chain silanes with three[51] or eight[40, 52] carbons form disordered films. Long alkyl chain silanes with thirty[51] carbons form less ordered films.

Organosilane surfactants can have one (R_3SiX), two (R_2SiX_2) or three ($RSiX_3$) hydrolysable groups.[53, 54] Monochlorosilanes are able to form only one covalent bond to the surface and the obtained films are disordered due to strong repulsion between the 'R' groups of adjacent head groups (**Scheme 1.3**).[45] Dichlorosilanes can form covalent bonds to the surface as well as vertical polymerisation structures (**Scheme 1.3**).[53]

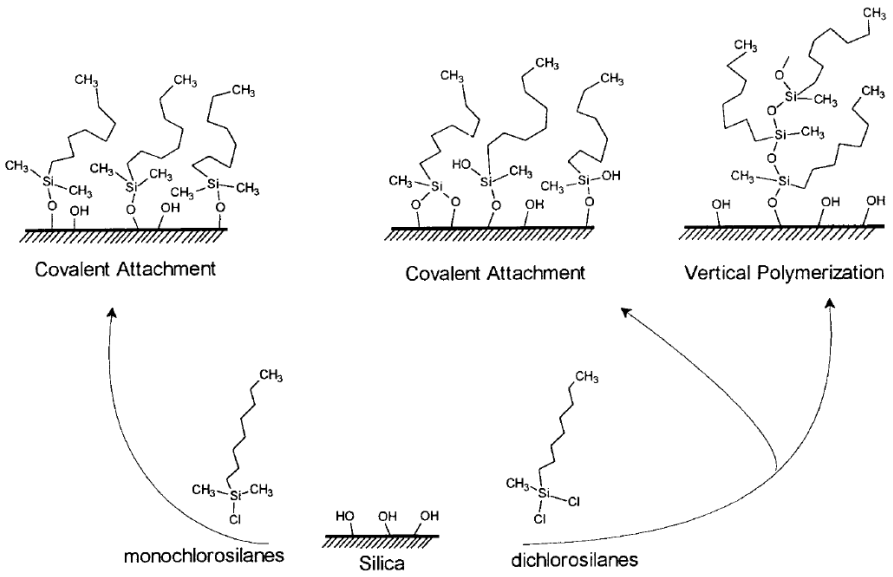

Scheme 1.3. Possible products of the reaction of monochlorosilanes and dichlorosilanes with silicon dioxide surfaces (reprinted with permission from A. Y. Fadeev and T. J. McCarthy, *Langmuir*, 2000, **16**, 7268-7274. Copyright © 2000, American Chemical Society).[53]

Trichlorosilanes are able to form densely-packed monolayers due to their ability to cross-polymerise. However, covalent attachments and vertical polymerisation are also possible (**Scheme 1.4**), thus the deposition parameters must be carefully controlled.[53]

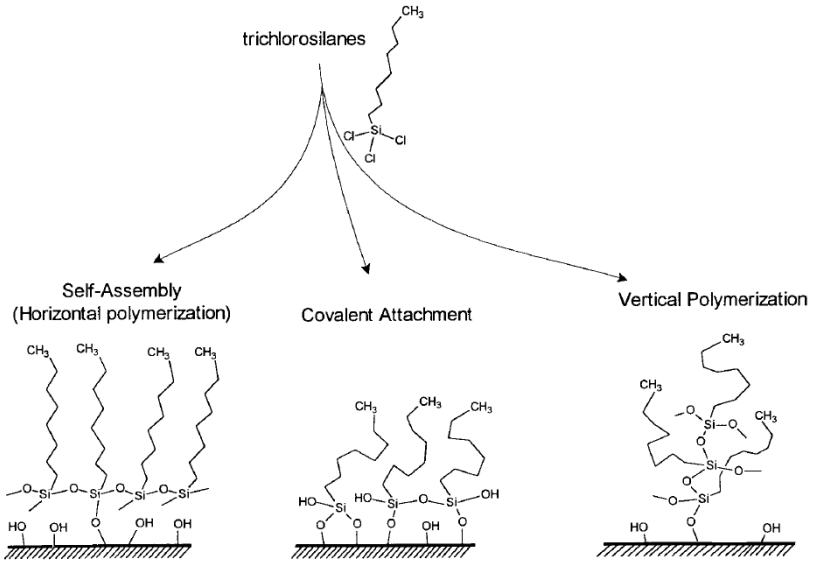

Scheme 1.4. Possible products of the reaction of trichlorosilanes with silicon dioxide surfaces (reprinted with permission from A. Y. Fadeev and T. J. McCarthy, *Langmuir*, 2000, **16**, 7268-7274. Copyright © 2000, American Chemical Society).[53]

The concentration of the precursor solution is crucial for SAM growth and its final quality.[55-57] Desbief *et al.*,[58] reported that an increase of the concentration (from 10^{-2} M to

2.5×10^{-1} M) caused formation of a less ordered film, which manifested itself by lower contact angle values (contact angle analysis, see Chapter 2). The authors concluded that at high concentrations too many molecules may deposit at the same time, thus their self-reorganisation might be difficult.[58] Ito *et al.*,[59] also investigated different solution concentrations in SAM formation. They found that at lower concentrations (<1 mM), incomplete monolayers were produced, while at higher concentrations (>5 mM), multilayers were formed.

Vallant *et al.*,[60] examined how the 'age' of the solution (*i.e.* time between solution preparation and immersion of the substrate) influenced monolayer formation. They tested SAM films prepared from a freshly made solution as well as from a solution stored for 2 h in a sealed vessel. The obtained results indicated that when an 'old' solution was used in the deposition process, large polymeric aggregates were present on the surface.[61, 62]

Influence of the deposition time[63] on SAM formation was studied by Liu *et al.*[64] They found that for adsorption times longer than 6 h, no changes in water contact angles were observed in the examined *n*-alkylsilane SAMs.

Silberzan *et al.*,[3] observed that the deposition rate could be affected by temperature. An optimal quality of octadecanetrichlorosilane (OTS) monolayer was achieved in 2 min at 18 °C, while a 24 h reaction time did not lead to a satisfactory result at 30 °C. Brzoska[34, 65] found that surface coverage was poor when deposition was performed at high temperature (~60 °C, 10 min). Moreover, the optimal deposition temperature *T* depends linearly on *n*-alkyl chain length and increases by 3.5 ± 0.5 °C for each additional CH_2 group (**Figure 1.3**).

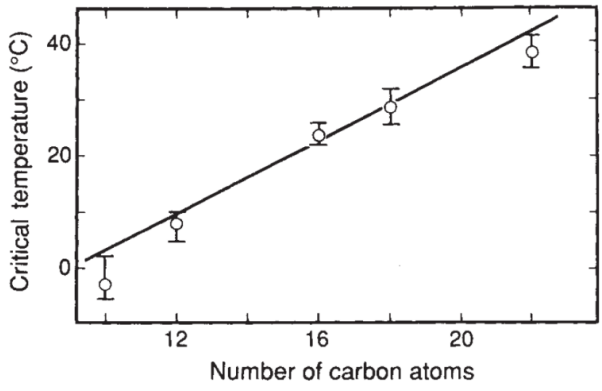

Figure 1.3. The optimal deposition temperature *T* against the chain length *n* of the *n*-alkyltrichlorosilane (reprinted with permission from Macmillan Publishers Ltd: Nature Publishing Group, J. B. Brzoska, N. Shahidzadeh and F. Rondelez, *Nature*, 1992, **360**, 719-721, copyright © 1992).[34]

Parikh *et al.*,[31] studied the effect of preparation temperature, in the range of 5-65 °C, on the structures of OTS monolayers on oxidised silicon substrates. They observed that the optimum deposition temperature of OTS films was 28 ± 0.5 °C. Above this temperature a gradual decrease of the film thicknesses was measured with increasing temperature. Moreover, Carraro *et al.*,[66, 67] observed that SAM formation can be initiated by three different mechanisms at different temperatures; island growth at low temperatures (T < 16 °C), homogenous growth at high temperatures (T ≥ 40 °C), and a mixed regime at intermediate temperatures (**Figure 1.4**).[58, 66]

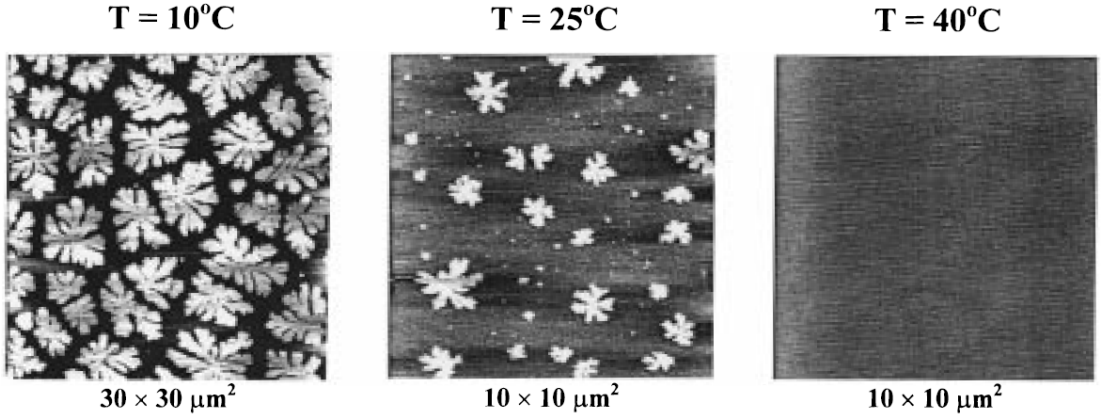

Figure 1.4. AFM images of partial SAMs grown at 10, 25 and 40 °C for 30 s (reprinted with permission from C. Carraro, O. W. Yauw, M. M. Sung and R. Maboudian, *J. Phys. Chem. B*, 1998, **102**, 4441-4445. Copyright © 1998, American Chemical Society).[66]

Rozlosnik *et al.*,[68] investigated the effect of solvent polarity on the formation of OTS SAMs on silicon. They found that different solvents affect the water solubility and hence, SAM creation. Deposition of OTS from dodecane solutions resulted in multi-layered films. In contrast, the use of heptane as a solvent, caused the formation of high-quality monolayers. Cheng *et al.*,[69] used four solvents: hexadecane, toluene, chloroform and dichloromethane for SAM preparations. Very smooth, monolayer films were obtained when either hexadecane or toluene were used in the deposition process. They also claimed that lower polarity solvents resulted in better molecular packing and smoother OTS films.

It is surprising that dodecane and hexadecane, which both belong to the same family (non-polar, linear hydrocarbons) affected the quality of monolayers in a different way. This is another indication that preparation conditions are critical for SAMs formation. More detail will be discussed in Chapter 4.

1.3. Surface chemistry

The properties of the surface of a substrate can be tuned by deposition of ultrathin films, formed from self-assembling molecules carrying different functionalities. A functional group can be introduced either before or after deposition. For example, Bierbaum *et al*.,[51] reported that amino silane films prepared from (17-aminoheptadecyl)trimethoxysilane [AHTMS, $NH_2(CH_2)_{17}Si(OCH_3)_3$] formed completely disordered SAMs. Otherwise, ordered and well-defined layers can be obtained by deposition of a molecule containing a terminal azide or cyanide group, followed by subsequent reduction to the corresponding amine.[22, 70-72] The aim of this section is to present a selection of reactions used for surface modification such as nucleophilic substitution, reactions involving double bonds, click chemistry, Diels-Alder reactions as well as modifications in the vapour phase.

1.3.1. Nucleophilic substitution

Nucleophilic substitution reactions are an important class of reactions in organic and inorganic chemistry.[73] The replacement of a leaving group by a nucleophile takes place on a positively or partially positively charged atom. Nucleophiles are either negatively charged or neutral species with a free pair of electrons *e.g.* hydroxide, bromide, azide and cyanide ions, water, ammonia and others.[73]

In 1988, Balachander and Sukenik[74] recognised the potential for using nucleophilic substitution reactions in the preparation of amine-terminated SAMs. Two years later the same research group presented a series of new trichlorosilane SAMs, obtained by nucleophilic displacement of Br in pre-functionalised films with either CN or SCN or N_3. Moreover, subsequent treatment with $LiAlH_4$ yielded the corresponding -SH and -NH_2 moieties (**Scheme 1.5**).[70] The conversion was monitored by IR spectroscopy, X-ray photoelectron spectroscopy (XPS, see Chapter 2) and contact angle analysis. Quantitative displacement of the bromine atoms was confirmed by the disappearance of the Br signal from the XPS spectrum.

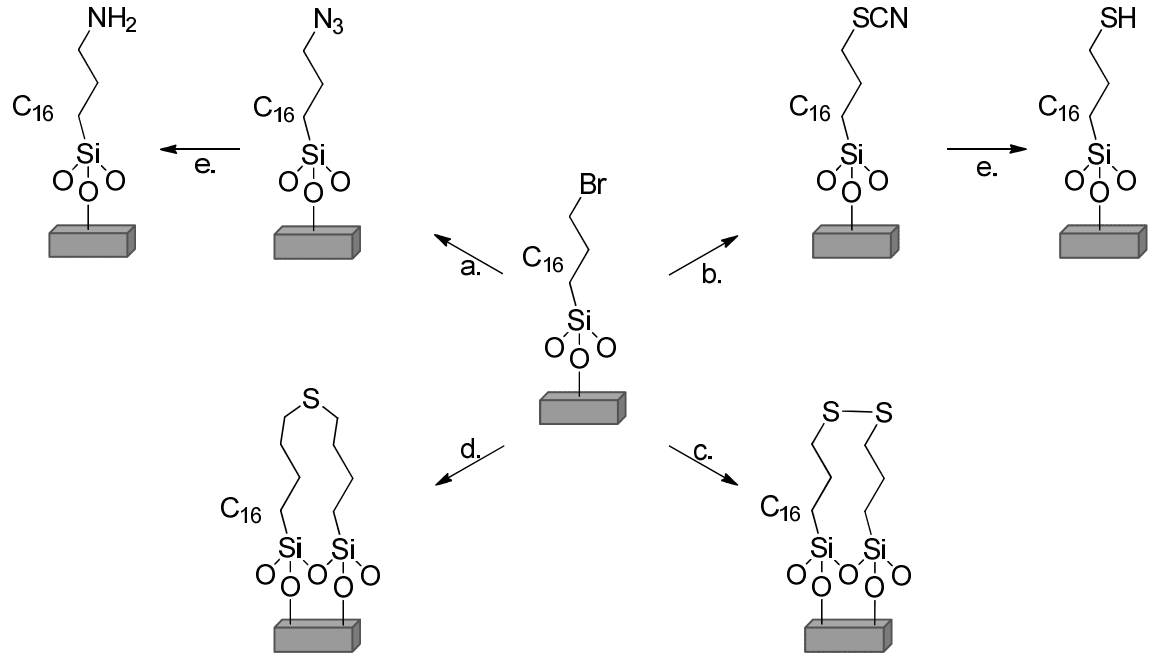

Scheme 1.5. Schematic representation of nucleophilic substitution reactions on bromine-terminated monolayers and further modification towards -NH_2 and -SH moieties. (a) NaN_3, DMF, rt, 24 h; (b) KSCN, DMF, rt, 20 h; (c) Na_2S_2, EtOH, reflux, 2 h; (d) Na_2S DMF, 24 h; (e) $LiAlH_4$, Et_2O, rt, 24 h.[70]

Nucleophilic substitution reactions between halide-terminated SAMs and anionic nucleophiles (*e.g.* azide, thiocyanate, thiolate and iodine) were also studied by Fryxell[75] and Koloski,[76] while formation of a dense amine-functionalised SAM (*via* reduction of azide-terminated SAM) was investigated by Ofir[77] and Heise,[78] due to its potential to graft polypeptides onto the substrate.[5, 79, 80]

In 1993, Lee and co-workers[81] investigated the selective attachment of peptides onto halide-terminated surfaces. The reaction involved nucleophilic substitution of the halide by the thiol group from cysteine moieties of tri- and nona-peptides. The yields increased as follows:

$$RCl < RBr < RI$$

which is consistent with leaving group abilities in S_N2 reactions.[73] This methodology represented a powerful tool for the controlled attachment of peptides or proteins to solid substrates, a strategy used for biosensors and immunosensors.

Moreover, the nucleophilic substitution of -Br by -N_3 also represents an important surface reaction, as azide functional groups can be used for further post-modification reactions.[71, 78, 82, 83]

1.3.2. Reactions involving double bonds

The first chemical reaction directly on SAMs was reported by Netzer and Sagiv.[12] They performed hydroxylation of terminal vinyl groups by hydroboration/oxidation (BH_3, H_2O_2) reactions. The products were then used for anchoring another monolayer. Preparation of a double layered SAM is not possible in a one-step procedure, due to the high reactivity of the trichlorosilane head groups towards the hydroxyl groups. Thus, reactions on pre-functionalised SAMs became a convenient method for multi-layered SAM formation on oxidised surfaces.[2]

In 1989, Wasserman *et al.*,[13, 84] described simple reactions on vinyl-terminated monolayers resulting in hydroxyl-, carboxylic acid- and bromine-terminated films (**Scheme 1.6**, a, b and c). Recently, Song and co-workers[85] performed an epoxidation reaction on double bonds of covalently grafted polynorbornene films on SiO_2/Si substrates (**Scheme 1.6**, d). In both cases, the successful modification was confirmed by lower water contact angles of the modified films compared to the starting monolayers, while the thicknesses remained largely unchanged.

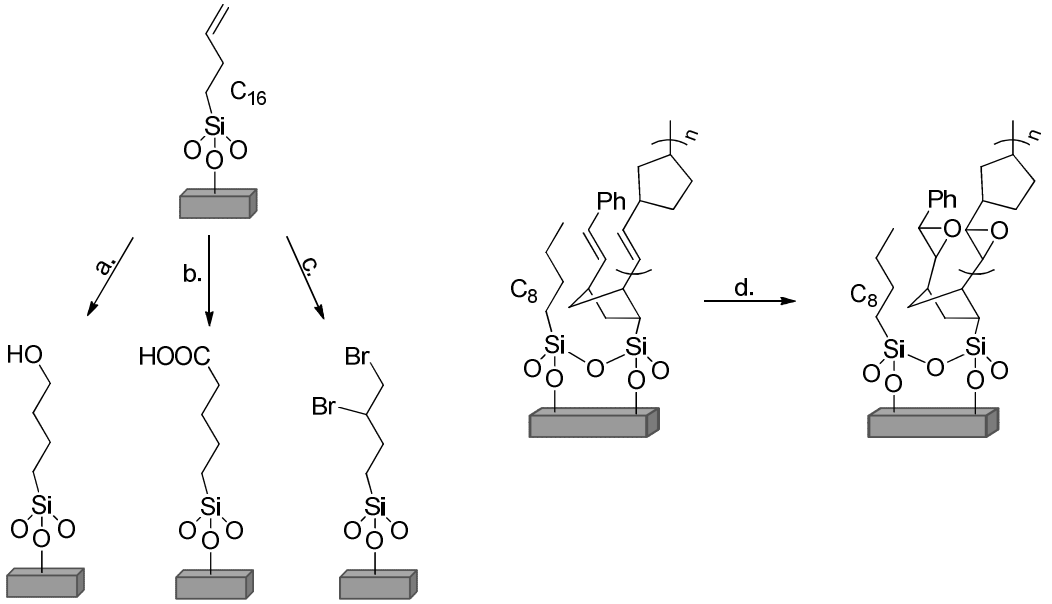

Scheme 1.6. The formation of -OH, -COOH and -Br terminated self-assembled monolayers, as well as epoxidation of polynorbornene films. (a) BH_3 and H_2O_2,[13] (b) $KMnO_4$,[13] (c) 2% Br_2 in DCM,[13] (d) MCPBA.[85]

Maoz *et al.*,[86] presented a microwave-induced formation of imide bilayers (**Scheme 1.7**). In the first step vinyl-terminated groups were oxidised to a carboxylic acid.[87, 88] Then, the carboxylic acid monolayer was used to form a bilayer with

octadecylamine through electrostatic/hydrogen-bonding interactions.[87, 88] Exposure of a self-assembled amine-acid salt bilayer to microwaves resulted in the formation of an imide bilayer. The transformation induced by microwaves was a promising tool for the unusual surface modification and a novel route for the fabrication of new types of organised film structures *e.g.* biological membranes.

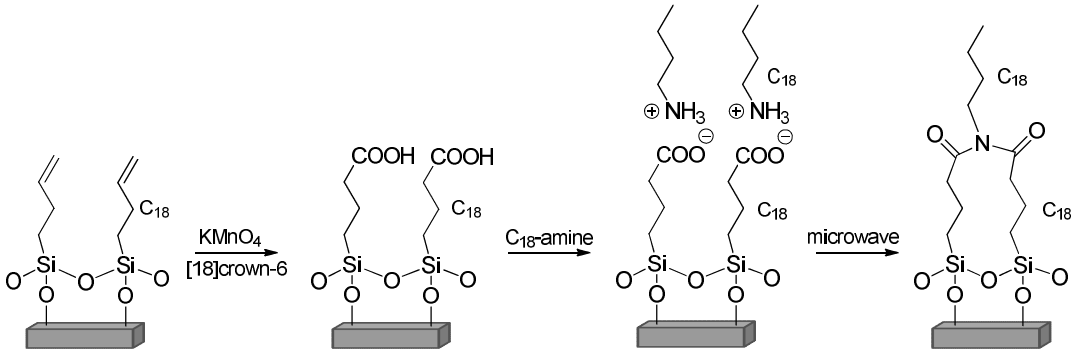

Scheme 1.7. Schematic representation of the microwave-induced conversion of a vinyl-terminated self-assembled monolayer into an imide bilayer.[86]

In 2000, Wang and co-workers[89] demonstrated a convenient route to the covalent bonding of phosphorylocholine groups to solid substrates using vinyl-terminated SAMs. The resultant monolayers were biocompatible and prohibited the deposition of enzymes and proteins.

Siegenthaler *et al.*,[90] published work on chemical surface modification *via* radical C-C bond-forming reactions. They performed a carboaminoxylation reaction on alkene-terminated SAMs using HO-TEMPO-malonate (4-hydroxy-2,2,6,6-tetramethylpiperidine 1-oxyl malonate) as a C-radical precursor (**Scheme 1.8**). The reaction could be carried out under neutral conditions and many functional groups were tolerated *e.g.* complex molecules with biological functionalities such as TEMPO-biotin conjugates.

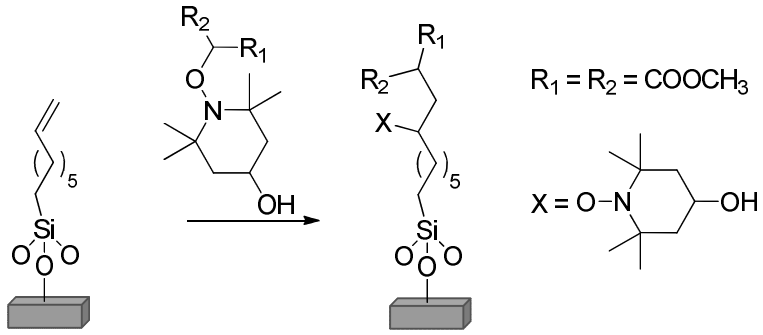

Scheme 1.8. Radical carboaminoxylation of 7-octenyl SAMs using HO-TEMPO-malonate.[90]

In 2003, Lee and co-workers[91] studied the reactivity of undec-10-ene thiol SAMs (on gold) towards olefin cross-metathesis (CM). Olefin metathesis is an organic reaction in which two starting olefins in the presence of a catalyst form two new alkenes, due to the exchange of the double-bond carbons (**Scheme 1.9**).[73]

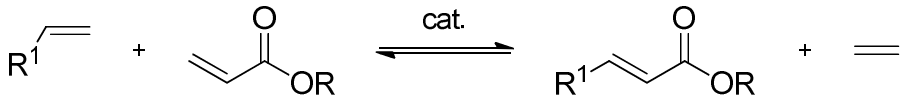

Scheme 1.9. Schematic of an olefin cross-metathesis.[73]

The successful conversion of vinyl-terminated SAMs into *α,β*-unsaturated carbonyl groups was monitored by IR spectroscopy, X-ray photoelectron spectroscopy and contact angle analysis.

In 2006, Dutta *et al*.,[92] reported functionalisation and patterning of olefin-terminated monolayers on a silicon substrate through cross metathesis. The reaction was performed on a mixed monolayer formed from di-olefin $CH_2=CH(CH_2)_9O(CH_2)_9CH=CH_2$ and 1-octadecene. The terminal vinyl groups were extended above the methyl groups in order to be easily accessible for the Grubbs catalyst and alkenes from the solution. Otherwise, the vinyl-terminated molecules might be too closely packed and thus the double bonds would not be accessible for interaction with the catalyst (**Scheme 1.10**, a). The olefins exposed on a monolayer could either react with each other (**Scheme 1.10**, b) or with alkenes from solution resulting in a functionalised monolayer (**Scheme 1.10**, c).

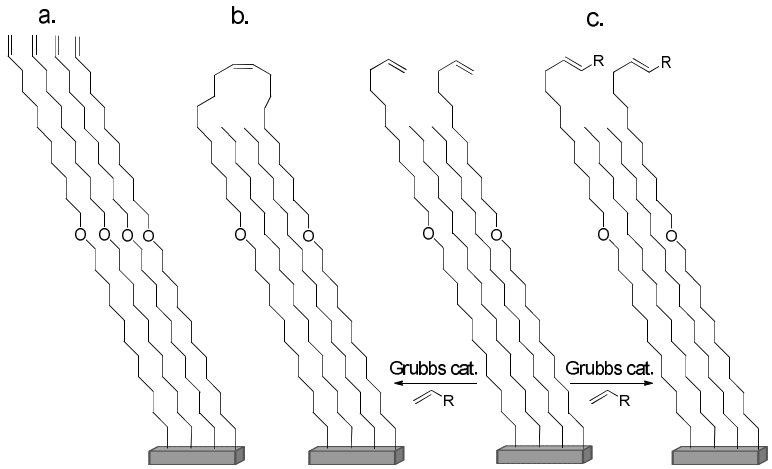

Scheme 1.10. The possible outcomes for the reaction of mixed-monolayers with Grubbs catalyst and an olefin in solution (reprinted with permission from S. Dutta, M. Perring, S. Barrett, M. Mitchell, P. J. A. Kenis and N. B. Bowden, *Langmuir*, 2006, **22**, 2146-2155. Copyright © 2006, American Chemical Society).[92]

In order to obtain the highest conversion in cross metathesis (**Scheme 1.10**, c) the reaction conditions as well as the composition of the monolayer (1:1 ratio of di-olefin and 1-octadecene in solution, used in deposition process) must be strictly controlled.

The reported examples clearly indicate the potential of vinyl-terminated SAMs as starting films for further modification and introduction of new functionalities to solid substrates.

1.3.3. Click chemistry

Copper(I)-catalysed 1,3-dipolar cycloaddition of azides to terminal acetylenes is known as the 'click' reaction and it represents a versatile and useful method in organic chemistry.[93, 94] The reaction has also found an application in the functionalisation of inorganic surfaces.[38, 95] The introduction of 1,2,3-triazole moieties into the monolayer can be achieved in two ways. The first method uses acetylene terminated substrates for coupling with azide functionalised molecules,[96, 97] while the second method involves azide terminated substrates and terminal acetylene self-assembling molecules.[98-100]

An azide terminated monolayer can be obtained by nucleophilic substitution of -Br with $-N_3$. Lummerstorfer and Hoffmann[101] prepared 11-azido-undecylsiloxane monolayers *via* substitution of a Br-terminated SAM. Subsequent coupling with various acetylenes yielded 1,2,3-triazoles (**Scheme 1.11**). Quantitative coupling was obtained when the reaction was performed at 70 °C for 24 h, without catalytic activation.

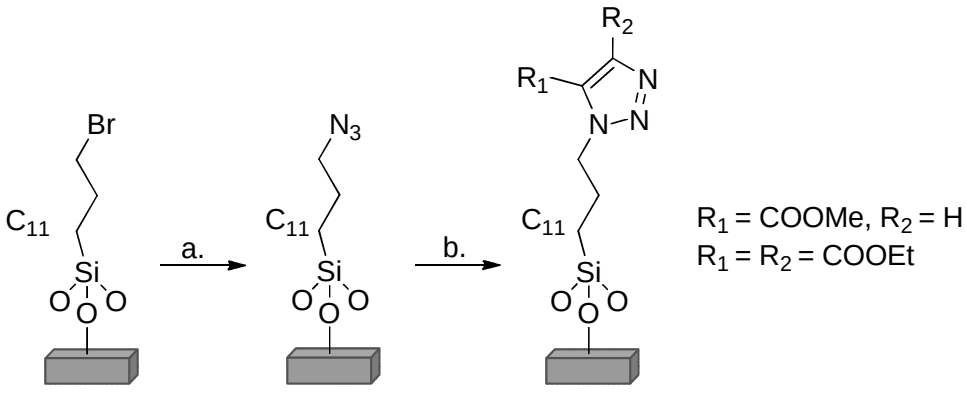

Scheme 1.11. Formation of 1,2,3-triazole-terminated SAMs. (a) Nucleophilic substitution with NaN_3, (b) cycloaddition with *bis*(ethoxycarbonyl) and methoxycarbonyl acetylene (R_1-C≡C-R_2).[101]

Two different methods can be used to obtain acetylene-terminated monolayers. The first one employs chlorination of hydrogenated silicon and subsequent reaction with

HC≡C-Na.[102] In the second method, either 1,8-nonadiyene[97, 103] or 1,6-heptadiyene[104] reacts with hydrogenated Si substrates. The use of 1,8-nonadyiene was reported by Ciampi and co-workers.[103, 105] Their SAMs were further modified by CuAAC reactions in order to obtain 1,2,3-triazole monolayers (**Scheme 1.12**). The characterisation and reaction conversion was monitored by IR spectroscopy and optical reflectivity measurements, which revealed the presence of the desired functionalities. According to the authors[103, 105] surface modification *via* 'click' reactions could be applied to produce functionalised surfaces in silicon-based sensing devices and implantable biomaterials.[105]

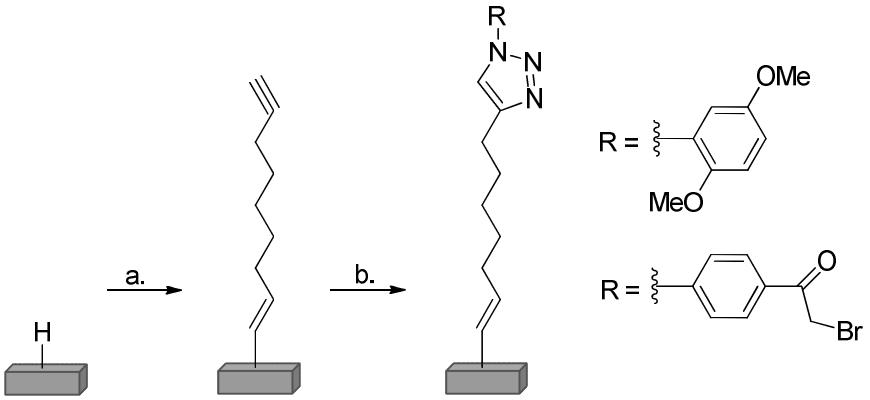

Scheme 1.12. Schematic representation of the 1,3-dipolar cycloaddition onto hydrogenated Si substrates. (a) The preparation of an alkyne-terminated monolayer from 1,8-nonadiyene, (b) R-N_3 cycloaddition with acetylene functionalised molecules.[105]

1.3.4. Diels-Alder reactions

Another candidate for surface modification is the Diels-Alder cycloaddition.[38] In this reaction a conjugated diene is reacted with a substituted alkene (dienophile) to form a cyclohexene ring system.[73] The Diels-Alder reaction has been used to immobilise biomolecules (oligonucleotides, peptides) on *e.g.* glass or gold substrates.[38, 95] Recently, Dirlam *et al.*,[106] reported a reversible Diels-Alder cycloaddition reaction on a glass substrate. The reaction is temperature-dependent and reversible by controlling the temperature of the system.[106] The hydrophobic dienophile (fluorinated maleimide) was attached to a surface pre-coated with a hydrophilic electrophile (3-aminopropylsiloxane SAM modified with 2-furoyl chloride). Thermal treatment of the modified surface cleaved the Diels-Alder 'functional group' resulting in a hydrophilic substrate (**Scheme 1.13**). The reaction was monitored by contact angle analysis. A water contact angle of 70 ± 3° was observed for the electrophile-terminated SAM (**Scheme 1.13**, a) and this value increased to

101 ± 9° after cycloaddition with the hydrophobic dienophile (**Scheme 1.13**, b). Thermal cleavage of the hydrophobic dienophile resulted in regeneration of a hydrophilic state, CA 70 ± 6° (**Scheme 1.13**, c). This methodology is a convenient way of controlling surface properties by introducing various functionalities to a substrate. As a result, the wetting properties are modified.

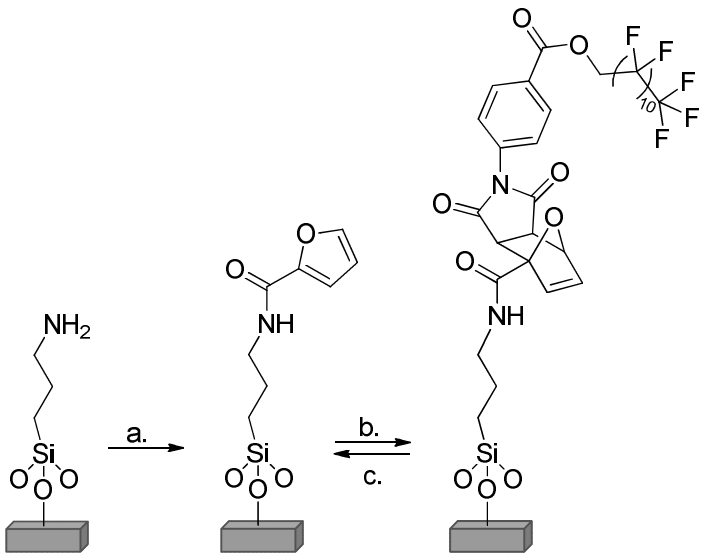

Scheme 1.13. Preparation of Diels-Alder functionalised surface. (a) 2-Furoyl chloride, (b) fluorinated maleimide, THF, rt, 24 h, (c) toluene, reflux, 24 h.[106]

1.3.5. Modification in the vapour phase

Vapour phase chemical modifications are much more difficult to control than solution phase reactions and only a few examples have been published to date. Ozonolysis is one of the most studied gas-phase reactions, used to modify inorganic substrates coated with SAMs.[107-109]

In 2004, Dubowski and co-workers[107] investigated the interactions of gas-phase ozone with unsaturated self-assembled monolayers deposited on an Attenuated Total Reflection (ATR) silicon crystal. The SAMs oxidation was monitored in real time by FTIR spectroscopy and the gas phase products of the ozonolysis were analysed by Infrared Cavity Ring-Down spectroscopy (IR-CRDS). The ATR-FTIR spectra revealed that upon exposure to ozone, the vinyl groups quickly oxidised to form carbonyls. Some were proven to be -COOH groups, which was indicated by formation of an ammonium salt after the product was exposed to NH_3 vapour. However, on SAMs exposed to ozone, a significant amount of aldehyde was formed in addition to the carboxylic acid. This was confirmed by IR-CRDS spectroscopy, which indicated a higher level of RCHO than RCOOH.

In 2005, Fiegland *et al.*,[108] studied the reaction of C=C terminated SAMs on gold exposed to gas-phase ozone. The authors found that reactions between ozone and vinyl-groups proceed through the formation of a -COOH moiety and its subsequent conversion into inter-chain carboxylic acid anhydride, which was revealed by Reflection-Absorption Infrared Spectra (RAIRS).

In 2008, Hallen and Hallen[109] developed a high yielding method for the production of carboxyl-terminated SAMs on silicon, by oxidising 10-undecenylsiloxane monolayers with gas-phase ozone, followed by hydrolysis in deionised water. The conversion of the reaction was monitored by contact angle analysis and ellipsometry measurements. Carboxyl-terminated SAMs exhibited a water contact angle of 16°, which decreased from ~100° for an unmodified film. Ellipsometry results showed the presence of a full monolayer after modification.

Apart from ozonolysis, a vapour phase modification of SAMs *via* a free radical was also reported. In 1997, Baker and Walting[110] investigated SAM functionalisation by free radical bromination reactions in both the liquid and vapour phases. The liquid phase reaction was performed using Br_2/CCl_4, while in the vapour phase process, SAMs were exposed to gaseous Br_2 in a sealed container. In both cases, wafers were irradiated for 6 h using a tungsten lamp, which resulted in brominated monolayers. SAM degradation was also observed in both cases, however, degradation in the vapour phase occurred much faster. Additionally, in comparison to 16-bromohexadecylsiloxane SAMs,[74] monolayers produced by Baker and Walting[110] were less organised, due to variable distribution of bromine across the alkyl chains (**Scheme 1.14**).

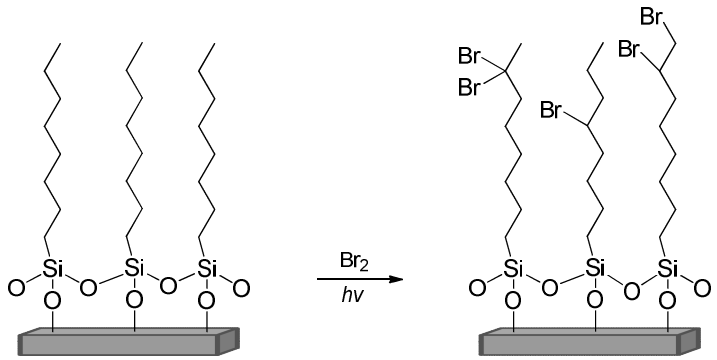

Scheme 1.14. Schematic representation of a bromination reaction of hexadecylsiloxane monolayer. The bromination was performed either in liquid Br_2/CCl_4 or in vapour Br_2.[110]

1.4. Aims of the project

The functionalisation of a surface containing a self-assembled monolayer is potentially very valuable as such a modification can alter surface properties. Alkylsiloxane SAMs are of particular interest, because they form chemically and physically stable films on various substrates.

Many different deposition methods have been investigated in order to reliably produce stable and ordered SAMs with a defined quality. In all the reported examples, liquid processes have been explored in detail. Although the preparation of SAMs on silicon substrates is relatively easy, reproducing well-defined monolayers is difficult due to various parameters that must be strictly controlled.[3] Thus, the first part of the thesis focuses on the development of a vapour phase deposition method of vinyl-terminated trichlorosilanes onto the silicon substrate. Vapour phase deposition can eliminate some disadvantages of liquid processes *e.g.* polymeric organosilane aggregates do not vaporise and, hence, do not deposit onto the surface. Moreover, this method can provide more homogenous coatings.[54, 111]

Apart from the deposition of vinyl-terminated self-assembled molecules, direct surface chemistry on the terminal double bond is explored. Surface chemistry gives various possibilities of introducing new functional groups onto the surface. However, an efficient reaction in traditional solution chemistry might not necessarily be successful on a solid substrate, due to the reduced mobility and accessibility of the immobilised molecules.[22] The majority of the reactions discussed in the Introduction were performed in the liquid phase and only a few reports describe surface chemistry in the vapour phase. In all cases the vapour phase reactions (*e.g.* ozonolysis) did not give satisfactory results *i.e.* several functional groups were formed in one process. Moreover, few solution reactions led to the formation of new C-C bonds on the surface, and to the best of our knowledge, no example of a C-C bond formation has been reported in the vapour phase. Thus, the potential of carbene chemistry in order to modify vinyl-terminated SAMs in both the liquid and vapour phases will be explored. The development of a surface modification process in which all steps (deposition and chemical surface modification) can be performed in the vapour phase is of great interest, as vapour phase processes can be easily adapted and are preferred for industrial scale coating processes.

1.5. Literature

1. M. A. Van Hove, *Catal. Today*, 2006, **113**, 133-140.
2. N. Herzer, S. Hoeppener and U. S. Schubert, *Chem. Commun.*, 2010, **46**, 5634-5652.
3. P. Silberzan, L. Leger, D. Ausserre and J. J. Benattar, *Langmuir*, 1991, **7**, 1647-1651.
4. N. K. Chaki and K. Vijayamohanan, *Biosens. Bioelectron.*, 2002, **17**, 1-12.
5. D. Samanta and A. Sarkar, *Chem. Soc. Rev.*, 2011, **40**, 2567-2592.
6. A. Ulman, *An Introduction to Ultrathin Organic Films from Langmuir-Blodgett to Self-Assembly*, Academic Press, San Diego, 1991.
7. A. Ulman, *Chem. Rev.*, 1996, **96**, 1533-1554.
8. R. G. Nuzzo and D. L. Allara, *J. Am. Chem. Soc.*, 1983, **105**, 4481-4483.
9. M. D. Porter, T. B. Bright, D. L. Allara and C. E. D. Chidsey, *J. Am. Chem. Soc.*, 1987, **109**, 3559-3568.
10. S. E. Creager and G. K. Rowe, *Anal. Chim. Acta*, 1991, **246**, 233-239.
11. N. Bonnet, D. O'Hagan and G. Hahner, *Chem. Commun.*, 2007, 5066-5068.
12. L. Netzer and J. Sagiv, *J. Am. Chem. Soc.*, 1983, **105**, 674-676.
13. S. R. Wasserman, Y. T. Tao and G. M. Whitesides, *Langmuir*, 1989, **5**, 1074-1087.
14. R. Maoz and J. Sagiv, *J. Colloid Interface Sci.*, 1984, **100**, 465-496.
15. J. Gun, R. Iscovici and J. Sagiv, *J. Colloid Interface Sci.*, 1984, **101**, 201-213.
16. J. Gun and J. Sagiv, *J. Colloid Interface Sci.*, 1986, **112**, 457-472.
17. S. Morgenthaler, C. Zink and N. D. Spencer, *Soft Matter*, 2008, **4**, 419-434.
18. J. Genzer, K. Efimenko and D. A. Fischer, *Langmuir*, 2006, **22**, 8532-8541.
19. C. Hoffmann and G. E. M. Tovar, *J. Colloid Interface Sci.*, 2006, **295**, 427-435.
20. D. A. Stenger, J. H. Georger, C. S. Dulcey, J. J. Hickman, A. S. Rudolph, T. B. Nielsen, S. M. McCort and J. M. Calvert, *J. Am. Chem. Soc.*, 1992, **114**, 8435-8442.
21. C. S. Dulcey, J. H. Georger, V. Krauthamer, D. A. Stenger, T. L. Fare and J. M. Calvert, *Science*, 1991, **252**, 551-554.
22. S. Onclin, B. J. Ravoo and D. N. Reinhoudt, *Angew. Chem., Int. Ed.*, 2005, **44**, 6282-6304.
23. S. Flink, F. van Veggel and D. N. Reinhoudt, *Adv. Mater.*, 2000, **12**, 1315-1328.
24. T. O. Salami, Q. Yang, K. Chitre, S. Zarembo, J. Cho and S. R. J. Oliver, *J. Electron. Mater.*, 2005, **34**, 534-540.
25. K. L. Choy, *Prog. Mater. Sci.*, 2003, **48**, 57-170.
26. J. D. Swalen, D. L. Allara, J. D. Andrade, E. A. Chandross, S. Garoff, J. Israelachvili, T. J. McCarthy, R. Murray, R. F. Pease, J. F. Rabolt, K. J. Wynne and H. Yu, *Langmuir*, 1987, **3**, 932-950.
27. D. K. Aswal, S. Lenfant, D. Guerin, J. V. Yakhmi and D. Vuillaume, *Anal. Chim. Acta*, 2006, **568**, 84-108.
28. A. Ulman, *Adv. Mater.*, 1990, **2**, 573-582.
29. B. Pignataro, A. Licciardello, S. Cataldo and G. Marletta, *Mater. Sci. Eng. C*, 2003, **23**, 7-12.
30. E. Ruckenstein and Z. F. Li, *Adv. Colloid Interface Sci.*, 2005, **113**, 43-63.
31. A. N. Parikh, D. L. Allara, I. B. Azouz and F. Rondelez, *J. Phys. Chem.*, 1994, **98**, 7577-7590.
32. M. K. Chaudhury and G. M. Whitesides, *Science*, 1992, **255**, 1230-1232.
33. N. R. Glass, R. Tjeung, P. Chan, L. Y. Yeo and J. R. Friend, *Biomicrofluidics*, 2011, **5**, 36501-365017.

34. J. B. Brzoska, N. Shahidzadeh and F. Rondelez, *Nature*, 1992, **360**, 719-721.
35. R. R. Rye, G. C. Nelson and M. T. Dugger, *Langmuir*, 1997, **13**, 2965-2972.
36. H. Brunner, T. Vallant, U. Mayer, H. Hoffmann, B. Basnar, M. Vallant and G. Friedbacher, *Langmuir*, 1999, **15**, 1899-1901.
37. C. Combellas, F. Kanoufi, J. Pinson and F. I. Podvorica, *J. Am. Chem. Soc.*, 2008, **130**, 8576-8577.
38. J. J. Gooding and S. Ciampi, *Chem. Soc. Rev.*, 2011, **40**, 2704-2718.
39. Y. Barness, O. Gershevitz, M. Sekar and C. N. Sukenik, *Langmuir*, 2000, **16**, 247-251.
40. Z. H. Jin, D. V. Vezenov, Y. W. Lee, J. E. Zull, C. N. Sukenik and R. F. Savinell, *Langmuir*, 1994, **10**, 2662-2671.
41. N. Herzer, C. Haensch, S. Hoeppener and U. S. Schubert, *Langmuir*, 2010, **26**, 8358-8365.
42. S. C. Tjong, *Nanocrystalline Materials: Their Synthesis-Structure-Property-Relationships and Applications*, Elsevier, Oxford, 2006.
43. R. Tian, O. Seitz, M. Li, W. Hu, Y. J. Chabal and J. Gao, *Langmuir*, 2010, **26**, 4563-4566.
44. J. D. Le Grange, J. L. Markham and C. R. Kurkjian, *Langmuir*, 1993, **9**, 1749-1753.
45. D. L. Angst and G. W. Simmons, *Langmuir*, 1991, **7**, 2236-2242.
46. M. E. McGovern, K. M. R. Kallury and M. Thompson, *Langmuir*, 1994, **10**, 3607-3614.
47. R. W. P. Fairbank and M. J. Wirth, *J. Chromatogr. A*, 1999, **830**, 285-291.
48. R. Wang and S. L. Wunder, *Langmuir*, 2000, **16**, 5008-5016.
49. T. Vallant, J. Kattner, H. Brunner, U. Mayer and H. Hoffmann, *Langmuir*, 1999, **15**, 5339-5346.
50. D. H. Flinn, D. A. Guzonas and R. H. Yoon, *Colloids Surf. A*, 1994, **87**, 163-176.
51. K. Bierbaum, M. Kinzler, C. Woll, M. Grunze, G. Hahner, S. Heid and F. Effenberger, *Langmuir*, 1995, **11**, 512-518.
52. T. Ohtake, N. Mino and K. Ogawa, *Langmuir*, 1992, **8**, 2081-2083.
53. A. Y. Fadeev and T. J. McCarthy, *Langmuir*, 2000, **16**, 7268-7274.
54. Y. X. Zhuang, O. Hansen, T. Knieling, C. Wang, P. Rombach, W. Lang, W. Benecke, M. Kehlenbeck and J. Koblitz, *J. Microelectromech. Syst.*, 2007, **16**, 1451-1460.
55. J. Foisner, A. Glaser, J. Kattner, H. Hoffmann and G. Friedbacher, *Langmuir*, 2003, **19**, 3741-3746.
56. J. T. Woodward and D. K. Schwartz, *J. Am. Chem. Soc.*, 1996, **118**, 7861-7862.
57. C. J. Yu, A. G. Richter, J. Kmetko, S. W. Dugan, A. Datta and P. Dutta, *Phys. Rev. E*, 2001, **63**, 021205.
58. S. Desbief, L. Patrone, D. Goguenheim, D. Guerin and D. Vuillaume, *Phys. Chem. Chem. Phys.*, 2011, **13**, 2870-2879.
59. Y. Ito, A. A. Virkar, S. Mannsfeld, J. H. Oh, M. Toney, J. Locklin and Z. A. Bao, *J. Am. Chem. Soc.*, 2009, **131**, 9396-9404.
60. T. Vallant, H. Brunner, U. Mayer, H. Hoffmann, T. Leitner, R. Resch and G. Friedbacher, *J. Phys. Chem. B*, 1998, **102**, 7190-7197.
61. T. Leitner, G. Friedbacher, T. Vallant, H. Brunner, U. Mayer and H. Hoffmann, *Microchim. Acta*, 2000, **133**, 331-336.
62. M. Reiniger, B. Basnar, G. Friedbacher and M. Schleberger, *Surf. Interface Anal.*, 2002, **33**, 85-88.
63. T. Balgar, R. Bautista, N. Hartmann and E. Hasselbrink, *Surf. Sci.*, 2003, **532–535**, 963-969.

64. Y. Liu, L. K. Wolf and M. C. Messmer, *Langmuir*, 2001, **17**, 4329-4335.
65. J. B. Brzoska, I. Benazouz and F. Rondelez, *Langmuir*, 1994, **10**, 4367-4373.
66. C. Carraro, O. W. Yauw, M. M. Sung and R. Maboudian, *J. Phys. Chem. B*, 1998, **102**, 4441-4445.
67. M. M. Sung, C. Carraro, O. W. Yauw, Y. Kim and R. Maboudian, *J. Phys. Chem. B*, 2000, **104**, 1556-1559.
68. N. Rozlosnik, M. C. Gerstenberg and N. B. Larsen, *Langmuir*, 2003, **19**, 1182-1188.
69. Y.-a. Cheng, B. Zheng, P.-h. Chuang and S. Hsieh, *Langmuir*, 2010, **26**, 8256-8261.
70. N. Balachander and C. N. Sukenik, *Langmuir*, 1990, **6**, 1621-1627.
71. M.-T. Lee and G. S. Ferguson, *Langmuir*, 2001, **17**, 762-767.
72. S. Onclin, A. Mulder, J. Huskens, B. J. Ravoo and D. N. Reinhoudt, *Langmuir*, 2004, **20**, 5460-5466.
73. J. Clayden, N. Greeves and S. Warren, *Organic Chemistry*, 2 edn., Oxford University Press, Oxford New York, 2012.
74. N. Balachander and C. N. Sukenik, *Tetrahedron Lett.*, 1988, **29**, 5593-5594.
75. G. E. Fryxell, P. C. Rieke, L. L. Wood, M. H. Engelhard, R. E. Williford, G. L. Graff, A. A. Campbell, R. J. Wiacek, L. Lee and A. Halverson, *Langmuir*, 1996, **12**, 5064-5075.
76. T. S. Koloski, C. S. Dulcey, Q. J. Haralson and J. M. Calvert, *Langmuir*, 1994, **10**, 3122-3133.
77. Y. Ofir, N. Zenou, I. Goykhman and S. Yitzchaik, *J. Phys. Chem. B*, 2006, **110**, 8002-8009.
78. A. Heise, M. Stamm, M. Rauscher, H. Duschner and H. Menzel, *Thin Solid Films*, 1998, **327–329**, 199-203.
79. O. Seitz, P. G. Fernandes, R. H. Tian, N. Karnik, H. C. Wen, H. Stiegler, R. A. Chapman, E. M. Vogel and Y. J. Chabal, *J. Mater. Chem.*, 2011, **21**, 4384-4392.
80. A. Heise, H. Menzel, H. Yim, M. D. Foster, R. H. Wieringa, A. J. Schouten, V. Erb and M. Stamm, *Langmuir*, 1997, **13**, 723-728.
81. Y. W. Lee, J. Reed-Mundell, J. E. Zull and C. N. Sukenik, *Langmuir*, 1993, **9**, 3009-3014.
82. Y. Wang, J. Cai, H. Rauscher, R. J. Behm and W. A. Goedel, *Chem. Eur. J.*, 2005, **11**, 3968-3978.
83. S. Sawoo, P. Dutta, A. Chakraborty, R. Mukhopadhyay, O. Bouloussa and A. Sarkar, *Chem. Commun.*, 2008, 5957-5959.
84. S. R. Wasserman, G. M. Whitesides, I. M. Tidswell, B. M. Ocko, P. S. Pershan and J. D. Axe, *J. Am. Chem. Soc.*, 1989, **111**, 5852-5861.
85. Z. Q. Song, X. F. Su, K. K. Huang, H. Lin, F. Q. Liu and J. Tang, *Polymer*, 2011, **52**, 4456-4462.
86. R. Maoz, H. Cohen and J. Sagiv, *Langmuir*, 1998, **14**, 5988-5993.
87. R. Maoz, J. Sagiv, D. Degenhardt, H. Möhwald and P. Quint, *Supramol. Science*, 1995, **2**, 9-24.
88. R. Maoz, S. Matlis, E. DiMasi, B. M. Ocko and J. Sagiv, *Nature*, 1996, **384**, 150-153.
89. Y. L. Wang, T. J. Su, R. Green, Y. Q. Tang, D. Styrkas, T. N. Danks, R. Bolton and J. R. Liu, *Chem. Commun.*, 2000, 587-588.
90. K. O. Siegenthaler, A. Schafer and A. Studer, *J. Am. Chem. Soc.*, 2007, **129**, 5826-5827.
91. J. K. Lee, K. B. Lee, D. J. Kim and I. S. Choi, *Langmuir*, 2003, **19**, 8141-8143.

92. S. Dutta, M. Perring, S. Barrett, M. Mitchell, P. J. A. Kenis and N. B. Bowden, *Langmuir*, 2006, **22**, 2146-2155.
93. R. Huisgen, *Angew. Chem., Int. Ed.*, 1963, **2**, 565-598.
94. H. C. Kolb, M. G. Finn and K. B. Sharpless, *Angew. Chem., Int. Ed.*, 2001, **40**, 2004-2021.
95. S. Arumugam and V. V. Popik, *J. Am. Chem. Soc.*, 2011, **133**, 15730-15736.
96. R.-V. Ostaci, D. Damiron, S. Capponi, G. Vignaud, L. Leger, Y. Grohens and E. Drockenmuller, *Langmuir*, 2008, **24**, 2732-2739.
97. S. Ciampi, T. Böcking, K. A. Kilian, M. James, J. B. Harper and J. J. Gooding, *Langmuir*, 2007, **23**, 9320-9329.
98. A. G. Marrani, E. A. Dalchiele, R. Zanoni, F. Decker, F. Cattaruzza, D. Bonifazi and M. Prato, *Electrochim. Acta*, 2008, **53**, 3903-3909.
99. C. Gauchet, G. R. Labadie and C. D. Poulter, *J. Am. Chem. Soc.*, 2006, **128**, 9274-9275.
100. T. Govindaraju, P. Jonkheijm, L. Gogolin, H. Schroeder, C. F. W. Becker, C. M. Niemeyer and H. Waldmann, *Chem. Commun.*, 2008, 3723-3725.
101. T. Lummerstorfer and H. Hoffmann, *J. Phys. Chem. B*, 2004, **108**, 3963-3966.
102. R. D. Rohde, H. D. Agnew, W.-S. Yeo, R. C. Bailey and J. R. Heath, *J. Am. Chem. Soc.*, 2006, **128**, 9518-9525.
103. S. Ciampi, G. Le Saux, J. B. Harper and J. J. Gooding, *Electroanalysis*, 2008, **20**, 1513-1519.
104. L. Britcher, T. J. Barnes, H. J. Griesser and C. A. Prestidge, *Langmuir*, 2008, **24**, 7625-7627.
105. S. Ciampi, T. Böcking, K. A. Kilian, J. B. Harper and J. J. Gooding, *Langmuir*, 2008, **24**, 5888-5892.
106. P. T. Dirlam, G. A. Strange, J. A. Orlicki, E. D. Wetzel and P. J. Costanzo, *Langmuir*, 2009, **26**, 3942-3948.
107. Y. Dubowski, J. Vieceli, D. J. Tobias, A. Gomez, A. Lin, S. A. Nizkorodov, T. M. McIntire and B. J. Finlayson-Pitts, *J. Phys. Chem. A*, 2004, **108**, 10473-10485.
108. L. R. Fiegland, M. McCorn Saint Fleur and J. R. Morris, *Langmuir*, 2005, **21**, 2660-2661.
109. M. A. Hallen and H. D. Hallen, *J. Phys. Chem. C*, 2008, **112**, 2086-2090.
110. M. V. Baker and J. D. Watling, *Langmuir*, 1997, **13**, 2027-2032.
111. T. Koga, M. Morita, H. Ishida, H. Yakabe, S. Sasaki, O. Sakata, H. Otsuka and A. Takahara, *Langmuir*, 2005, **21**, 905-910.

2. Analytical Methods for Characterising Self-Assembled Monolayers

Many spectroscopic, microscopic and other characterisation techniques are employed in surface science to investigate various properties of nanostructures including self-assembled monolayers (SAMs). It is essential to have as much information as possible on the modified surfaces using a variety of analytical techniques.[1] This Chapter describes the analytical techniques used in this study such as X-ray photoelectron spectroscopy (XPS), contact angle (CA) goniometry, ellipsometry, and atomic force microscopy (AFM).

2.1. X-ray Photoelectron Spectroscopy

X-ray photoelectron spectroscopy (XPS), also known as electron spectroscopy for chemical analysis (ESCA), is a powerful method for determining the elemental composition of materials' surfaces.[2] XPS measures the kinetic energy of core level electrons ejected from a material, after irradiation of a sample with monochromatic X-rays (**Figure 2.1**).

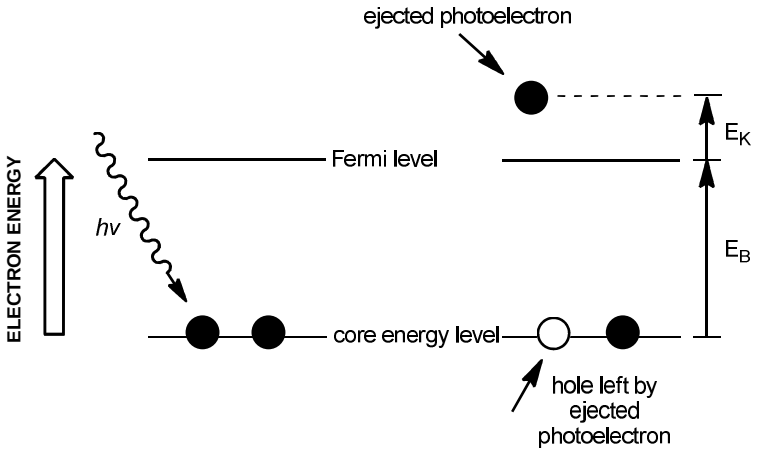

Figure 2.1. Representation of a photoelectron emission process.[3]

The electron binding energy (E_B) is the parameter which identifies the electron, in terms of its parent element and atomic energy level.[3] Based on the measured kinetic energy (E_K) of an ejected electron and knowing the energy of the incident X-ray radiation (*hv*), the binding energy (E_B) can be determined (**Equation 2.1**).

$$E_K = h\nu - E_B \qquad \textbf{Equation 2.1}$$

Each element has a characteristic set of peaks in the spectrum and peaks' positions are influenced by oxidation state of the element and its chemical environment. A typical XPS spectrum for a SiO_x/Si substrate, coated with an organic film is shown in **Figure 2.2**.

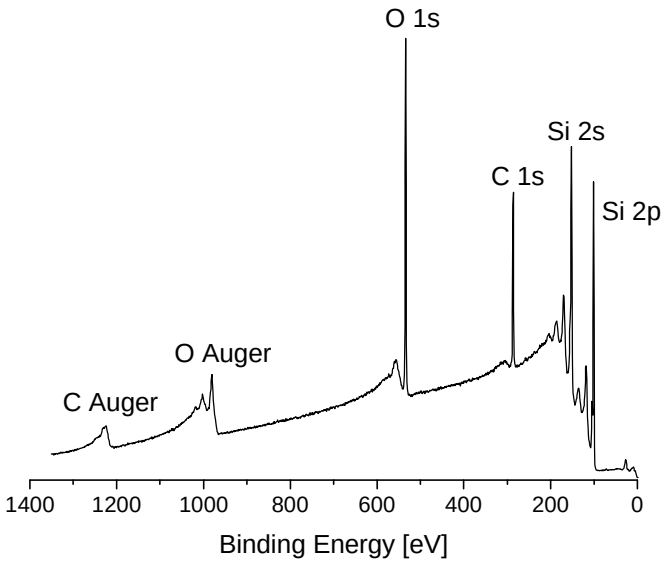

Figure 2.2. The XPS spectrum of an organic coated SiO_x/Si substrate.

The spectrum consists of narrow core-level photoelectron peaks (Si, C, O) and broad Auger peaks (C and O), while the background is formed by scattered electrons. The presence of peaks at particular E_B indicates the presence of a specific element on the surface and the intensity of the peaks is related to the concentration of the element on the surface of the sample.

The X-rays may penetrate deep into the sample, however, the escape depth of the ejected electrons is limited.[4] The electrons ejected from depths greater than a few nm have a low probability to leave the surface without an energy loss, thus they contribute to the background signal, rather than appear as a well-defined peak.[4] For this reason, XPS is a surface analytical technique used to determine the surface composition of a material only.

2.1.1. Details of XPS

X-ray photoelectron spectroscopy analysis was performed either at the University of Newcastle (NEXUS at nanoLAB) or at the University of Edinburgh.

Newcastle X-ray photoelectron spectroscopy spectra were obtained using a K-Alpha instrument (Thermo Scientific) and Al Kα radiation (1486.6 eV). During the analysis, the pressure in the instrument chamber was kept around 3×10^{-8} mbar. The detector had a takeoff angle of 90° relative to the surface. Survey spectra were recorded with the analyser pass energy set to 200 eV. Single region scans were recorded with the pass energy of the analyser set to 20 eV.

Edinburgh X-ray photoelectron spectroscopy spectra were obtained using a VG Sigma Probe (VG Scientific Ltd., UK) and Al Kα radiation (1486.6 eV). During the analysis, the pressure in the instrument chamber was kept around 1.33×10^{-8} mbar. The detector had a takeoff angle of 37° relative to the surface. Survey spectra were recorded with the analyser pass energy set to 80 eV. The number of single region scans recorded for each element was typically 20, with the pass energy of the analyser set to 10 eV.

The XPS spectra were corrected for charging by referencing the aliphatic C 1s peak of hydrocarbons to 284.6 eV. Elemental compositions of the various surfaces were determined from the area under individual elemental peaks using sensitivity factors provided with the software as well as taking the transmission function of the analyser into account. CasaXPS (Casa Software Ltd., UK) was used for the analysis. The spectra were fitted using Gaussian/Lorentzian peak shapes with a ratio of 70%/30%. A Shirley background was subtracted for the quantitative analysis.

2.2. Contact angle analysis

Contact angle (θ) is the angle measured at the three-phase interface between air, a liquid drop and a solid (**Figure 2.3**).[5, 6] Contact angle analysis measures the wettability of a surface and can indicate a chemical change at the terminal functional groups of a monolayer or the cleanliness of a surface.[1]

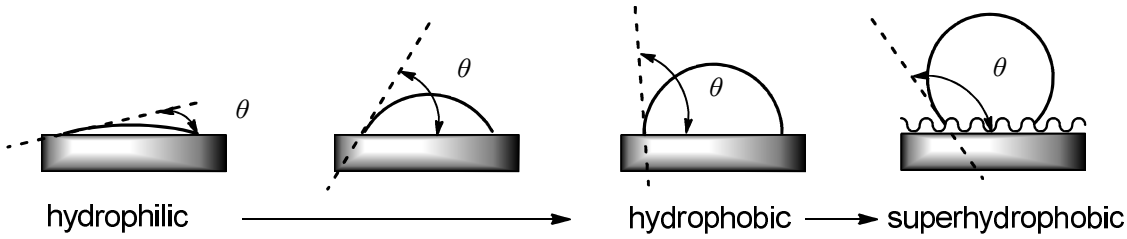

Figure 2.3. Schematic representation of different levels of wettability of surfaces (redrawn).[5]

If the water contact angle is smaller than 90°, the surface of a solid is considered hydrophilic, while a water contact angle higher than 90° represents a hydrophobic surface. Superhydrophobic materials with very rough surfaces can exhibit a water contact angle of 150° or greater, due to the presence of air pockets under the liquid droplet (**Figure 2.3**).[7] Also the presence of organic contaminants prevent wetting and result in higher contact angles.

The contact angle can be recorded either by placing a liquid droplet on the sample surface and measuring the angle (the static sessile drop method) or by measuring the angle by increasing and decreasing the liquid volume (the dynamic sessile drop method). The resulting contact angle obtained for the maximum liquid volume is referred to as the advancing angle, while the contact angle recorded for the minimum liquid volume is referred to as the receding angle (**Figure 2.4**). The difference between the advancing and receding angles (contact angle hysteresis) gives an indication of the smoothness and quality of the self-assembled monolayer.

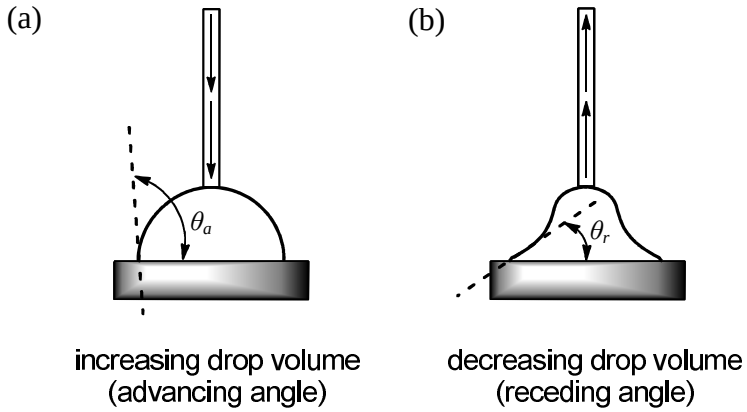

Figure 2.4. Dynamic contact angle analysis which measures (a) advancing contact angle θ_a and (b) receding contact angle θ_r.

2.2.1. Details of contact angle measurements

Water contact angles (DI water) were measured with a G10 goniometer microscope (KRÜSS GmbH, Hamburg, Germany) under ambient conditions at room temperature. Droplets of ~3 µL were dispensed from a microburette. All reported values are the average of three measurements taken from different places of the surface. The error based on the observed variation of the contact angle of the organic films prepared under identical conditions was ± 1°.

2.3. Ellipsometry

Ellipsometry is a very sensitive, non-destructive technique widely used to characterise thin films.[2] The optical properties of thin films as well as film thicknesses can be calculated by measuring changes of an elliptically polarised light beam due to the interaction with the sample (**Figure 2.5**).[8, 9]

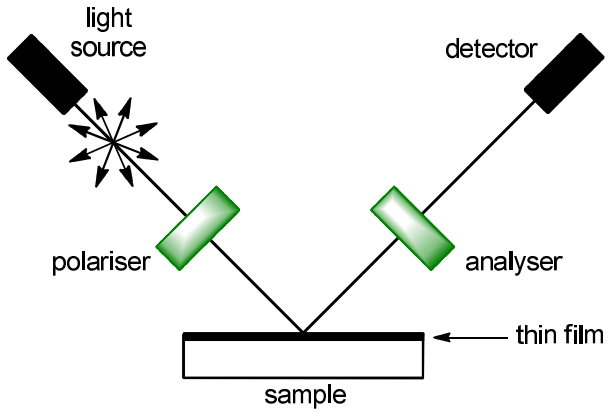

Figure 2.5. Schematic representation of an ellipsometry experiment.[10]

Ellipsometry measures the phase shift (Δ) and the amplitude component (Ψ) of the reflected light. However, to obtain the parameters of interest (thickness and optical constants) it is necessary to build a model which represents the sample with its different layers. Ψ and Δ are evaluated from the model giving a fit which is compared to the measured data. The fitting is performed by changing the model in which the thickness is modified until the experimental curves overlap with the modelled ones. The thickness of the self-assembled monolayer is found by the best fit (**Figure 2.6**).[10]

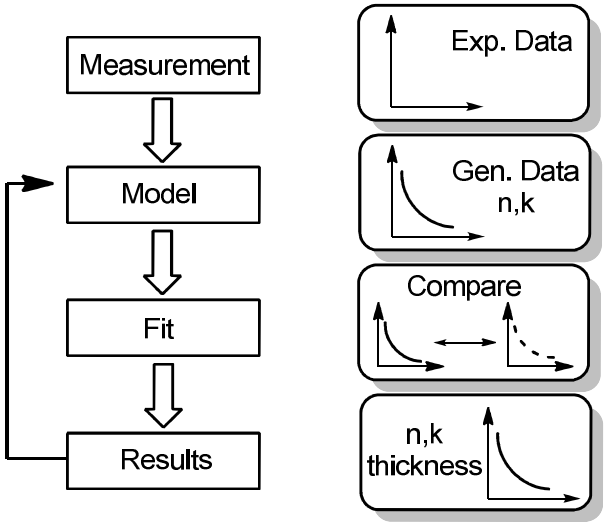

Figure 2.6. Ellipsometry procedure to determine material properties from experimental data (redrawn).[10]

2.3.1. Details of ellipsometry

The thickness of the SAMs was measured with an M-2000DI™ spectroscopic ellipsometer (J. A. Woollam Co., Inc., USA). Thickness values were extracted from fits to the data taken from 45 to 70° in steps of 5° over wavelengths from 200 to 1000 nm. The sample surface was modelled as a Si substrate with an oxide layer and a Cauchy layer.[10] The thickness of the silicon oxide after the oxidative cleaning treatment was 16 ± 1 Å (average of three samples). The thickness of the monolayer films was calculated with a refractive index of 1.45.[11, 12] The error based on the observed variation of the thickness of the organic films prepared under identical conditions was ~2 Å.

2.4. Atomic Force Microscopy

The atomic force microscope (AFM) was invented by Binnig, Quate and Gerber[13] in 1986, and can be used to image the surfaces of conducting and insulating materials on the nanometre scale. AFM measures the attractive and repulsive forces between a sharp tip, attached to a Si_3N_4 cantilever, and the surface of a sample.[14] In response to these forces, the cantilever deflects. The top of the cantilever is illuminated by a laser beam and the deflection changes the position of the reflected laser beam which is detected by a photodiode. The position of the laser beam on the photodiode is recorded by the controller electronics *via* a feedback loop and then converted into an image, which represents a map of interactions between the measured surface and the tip (**Figure 2.7**).[15, 16]

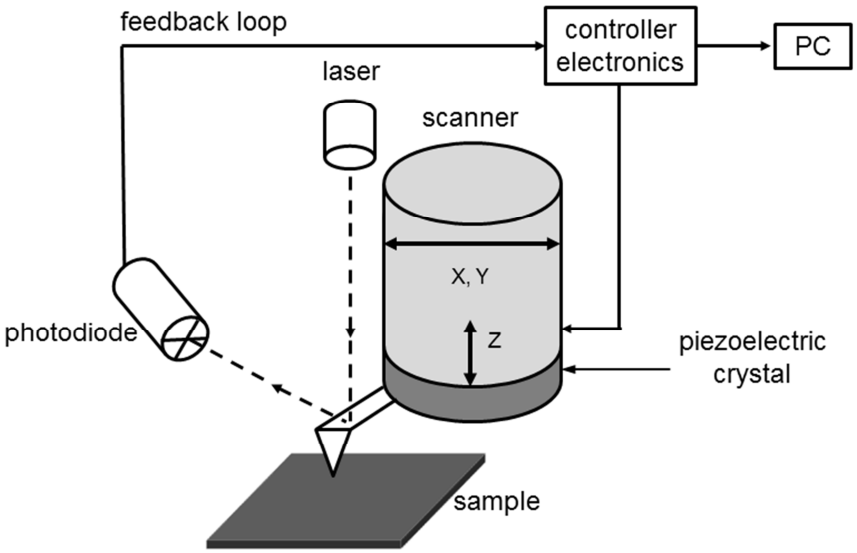

Figure 2.7. Schematic diagram of an atomic force microscopy and direct surface measurements – contact mode (based on a diagram in ref. 16).

The AFM can be operated in several modes for imaging such as a tapping mode, a non-contact mode and a contact mode - the latter was used in this study. In the contact mode, a tip and the surface of a sample remain in close contact as the scanning proceeds (‘contact’ means the repulsive regime of the intermolecular force curve, **Figure 2.8**). The cantilever deflection is maintained constant by the position adjustment of the scanner, thus the force between the tip and the sample is constant and a topographic image of the surface is produced.

The forces associated with AFM at short probe-sample distance are van der Waals interactions, while significant long-range interactions, further away from the surface, can be capillary, hydrophobic, electrostatic forces. In the contact mode, the probe predominately experiences repulsive forces. The relation between the force and distance is shown in **Figure 2.8**.

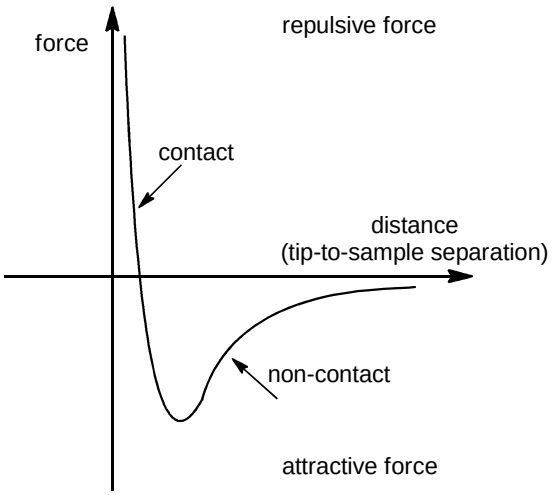

Figure 2.8. Interatomic force versus distance curve.

In the non-contact region, the cantilever is held on the order of tens to hundreds of angstroms from the sample surface, and the interatomic force between the cantilever and the sample is attractive. In the contact region, the cantilever is held less than a few angstroms from the sample surface, and the interatomic force between the cantilever and the sample is repulsive.[17]

2.4.1. Details of AFM

The atomic force microscope used in this study was a PicoSPM II (Molecular Imaging, AZ, USA) with an interchangeable nose scanner. The nominal spring constant of the cantilevers used was 0.06-0.12 N/m (Veeco, CA, USA). Images were recorded in ambient in contact mode at a scanning speed of ~0.8 lines/s and with a nominal constant force on the order of 10 nN.

2.5. Literature

1. D. Samanta and A. Sarkar, *Chem. Soc. Rev.*, 2011, **40**, 2567-2592.
2. C. R. Brundle, J. C. A. Evans and S. Wilson, *Encyclopedia of Materials Characterization*, Manning Publications Co., Greenwich, 1992.
3. J. F. Watts and J. Wolstenholme, *An Introduction to Surface Analysis by XPS and AES*, John Wiley & Sons Ltd, Chichester, West Sussex, 2003.
4. N. Fairley, *CasaXPS Manual 2.3.15 XPS AES ToF-MS SNMS Dynamic-SIMS*, Casa Software Ltd., Devon, 2009.
5. R. Forch, H. Schonherr and A. T. A. Jenkins, *Surface Design: Applications in Bioscience and Nanotechnology*, Wiley-VCH, Weinheim, 2009.
6. A. Ulman, *An Introduction to Ultrathin Organic Films from Langmuir-Blodgett to Self-Assembly*, Academic Press, San Diego, 1991.
7. S. Wang and L. Jiang, *Adv. Mater.*, 2007, **19**, 3423-3424.
8. R. M. A. Azzam and N. M. Bashara, *Ellipsometry and Polarized Light*, North-Holland Publishing Co., Amsterdam, 1977.
9. H. G. Tompkins and E. A. Irene, *Handbook of ellipsometry*, William Andrew Publishing, Norwich, 2005.
10. C. Herzinger and B. Joghs, *Guide to Using WVASE 32*, J. A. Woollam Co., Inc., 1996.
11. N. Tillman, A. Ulman, J. S. Schildkraut and T. L. Penner, *J. Am. Chem. Soc.*, 1988, **110**, 6136-6144.
12. D. L. Angst and G. W. Simmons, *Langmuir*, 1991, **7**, 2236-2242.
13. G. Binnig, C. F. Quate and C. Gerber, *Phys. Rev. Lett.*, 1986, **56**, 930-933.
14. C. J. Chen, *Introduction to Scanning Tunneling Microscopy*, Oxford University Press, Inc., New York, 1993.
15. F. J. Giessibl, *Rev. Mod. Phys.*, 2003, **75**, 949-983.
16. *Scanning Probe Microscopy Training Notebook (Version 3.0)*, Digital Instruments, Veeco Metrology Group, 2000.
17. P. W. Atkins and J. De Paula, *Physical Chemistry*, 9 edn., W. H. Freeman, New York, 2010.

3. Synthesis of Vinyl-Terminated Self-Assembling Molecules

Long chain alkyl organosilane compounds are widely used to modify the properties of inorganic material surfaces. They can form very stable films, thus are commonly used in semiconductor technology, for example in micro-electromechanical systems (MEMS) and nano-electromechanical systems (NEMS).[1-5] Silane-based precursor molecules can contain one (R_3SiX), two (R_2SiX_2) or three ($RSiX_3$) good leaving groups. Although all three silanes are used in the modification of hydroxylated surfaces, only trifunctional ones are able to form closely packed monolayers, because of their ability to form cross-linking bonds between two adjacent head groups,[6] as discussed in Chapter 1. SAMs formed from mono- and di-functional self-assembling molecules are less dense due to steric repulsion between the 'R' groups of adjacent silane head groups.[7-9] Precursor molecules with three reactive sites are usually functionalised with either halogen or alkoxy groups ($Si\text{-}X_3$ where X = Cl, $(OCH_3)_3$ or $(OCH_2CH_3)_3$), and chlorosilanes are preferred over alkoxysilanes as they are more reactive.[9, 10] However, the high reactivity and the water sensitivity of the chlorosilane head group limits the range of terminal functional groups that can be introduced onto the silane precursors.[11] If the terminal functional group reacts with the trichlorosilane group, this leads to the formation of polymeric aggregates in solution, which subsequently react with the surface, resulting in an inhomogeneous films.

3.1. Self-Assembling Molecules

In this project a series of vinyl-terminated SAMs were required. The target molecules were vinyl-terminated trichlorosilanes with alkyl chain lengths of ten (9-decenyltrichlorosilane **1a** (CH_2=CH-$(CH_2)_8$-$SiCl_3$)), eleven (10-undecenyltrichlorosilane **1b** (CH_2=CH-$(CH_2)_9$-$SiCl_3$)), and fifteen (14-pentadecenyltrichlorosilane **1c** (CH_2=CH-$(CH_2)_{13}$-$SiCl_3$)) carbon atoms (**Figure 3.1**).

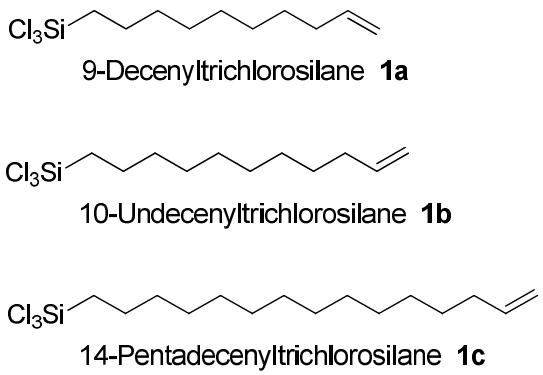

Figure 3.1. Synthetic targets for the formation of SAMs on silicon substrates.

Two different synthetic approaches for preparing the trichlorosilane precursors **1a**-**1c** are described in the literature.[12-18] The routes are summarised in **Scheme 3.1** and **Scheme 3.2**.

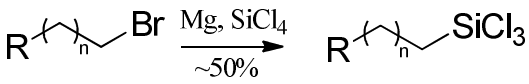

Scheme 3.1. First synthetic route to obtain trichlorosilane self-assembling molecules.[12, 13]

Wasserman *et al.*,[12] prepared long chain alkyl trichlorosilanes *via* a Grignard reaction using a bromide precursor following the procedure described by Whitmore *et al.*,[13] as illustrated in **Scheme 3.1**. In a similar manner, Maoz and Sagiv synthesised *trans*-13-docosentyltrichlorosilane ($CH_3(CH_2)_7CH=CH(CH_2)_{12}SiCl_3$) by transforming the alcohol into the bromide derivative, which was then converted into the trichlorosilane *via* addition of its Grignard reagent and excess of tetrachlorosilane.[14, 15] According to the literature the synthesis of trichlorosilanes have yields of ~50%. In the second method, trichlorosilane ($HSiCl_3$) was reacted with a vinyl-terminated alkene in the presence of a platinum catalyst[12, 16, 17] as shown in **Scheme 3.2**. The yield of this reaction was reported to be around 70%.

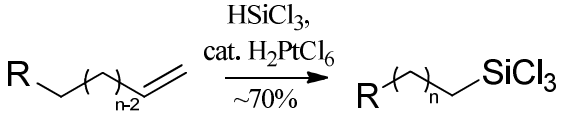

Scheme 3.2. Second synthetic route to obtain trichlorosilane self-assembling molecules.

Our aim was to prepare molecules with double bonds as terminal functional groups, thus we selected the Wasserman procedure. The method in **Scheme 3.2** would require a starting alkene with two terminal double bonds ($CH_2=CH-(CH_2)_n-CH=CH_2$) and would require a selectivity that is not obvious to achieve.

3.1.1. The synthetic route of 9-decenyl- and 10-undecenyl- trichlorosilane

The synthetic route developed for the preparation of 9-decenyltrichlorosilane (**1a**) and 10-undecenyltrichlorosilane (**1b**) is illustrated in **Scheme 3.3**.

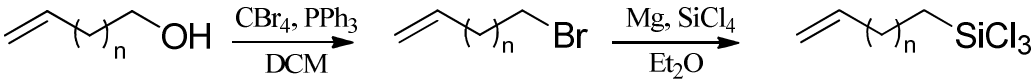

4a, n = 7
4b, n = 8

5a, n = 7, 92%
5b, n = 8, 77%

1a, n = 7, 29%
1b, n = 8, 37%

Scheme 3.3. Synthesis of 9-decenyl- and 10-undecenyl- trichlorosilane.

In the first step, commercially available 9-decen-1-ol (**4a**) and 10-undecen-1-ol (**4b**), were treated with carbon tetrabromide and triphenylphosphine in dichloromethane, as precursors to the bromides **5a** and **5b**. The reaction proceeded quickly and the starting material was consumed in less than three hours. The compounds **5a** and **5b** were purified by distillation under reduced pressure and obtained in good yields of 92% and 77%, respectively. The resultant trichlorosilanes **1a** and **1b** were then obtained by the reaction of tetrachlorosilane ($SiCl_4$) with the Grignard reagents prepared from **5a** and **5b**. The products **1a** and **1b** are very sensitive to water, and the work-up had to be carried out under dry conditions. In the first work up step, dry hexane was added to the reaction mixture and stirred for a few minutes. This allowed the product to be extracted from the reaction residue. After sedimentation of inorganic side products, the clear solution of trichlorosilanes **1a** or **1b** in hexane was transferred to a different flask *via* cannula under an inert atmosphere. The hexane was evaporated on the Schlenk line, and then the product was purified by distillation. The trichlorosilanes **1a** and **1b** were obtained in moderate yields (29% and 37%, respectively). Complete NMR (^{29}Si, ^{1}H, ^{13}C) characterisation of 9-decenyltrichlorosilane (**1a**) is shown as an example in **Figure 3.2**.

(a) ^{29}Si NMR

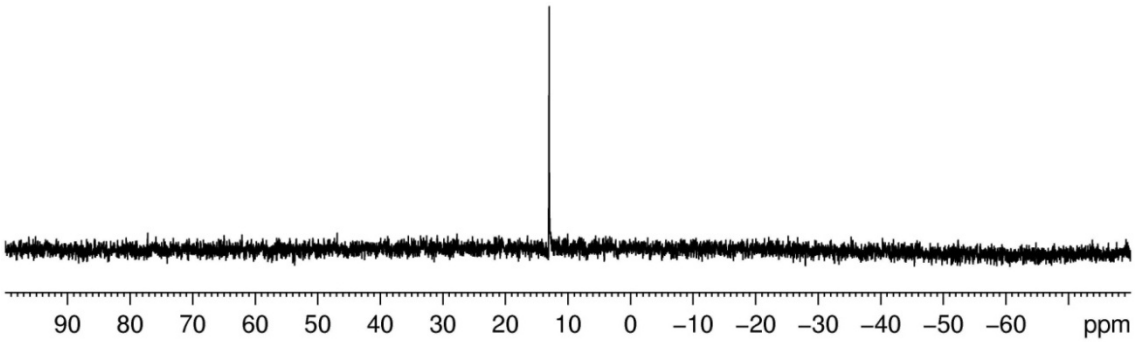

(b) ^{1}H NMR

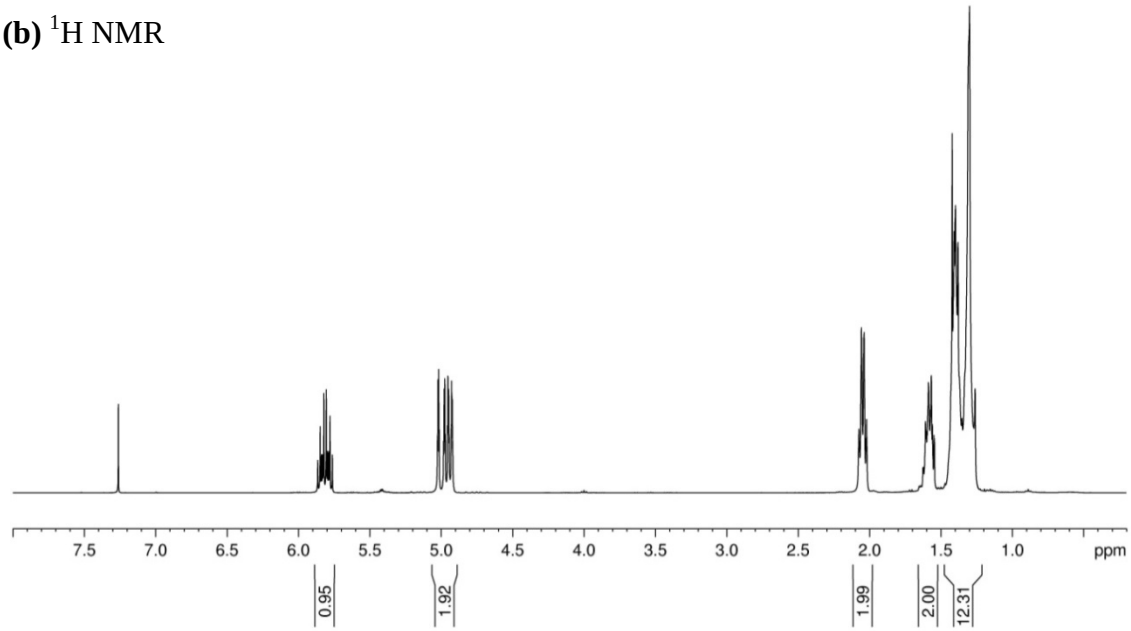

(c) ^{13}C NMR

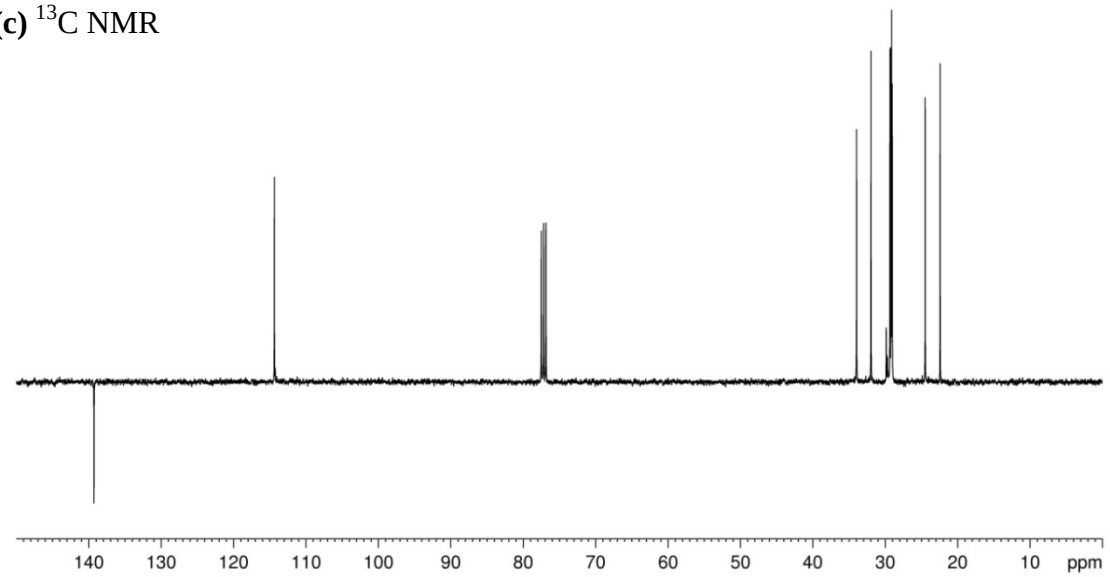

Figure 3.2. (a) ^{29}Si NMR, (b) ^{1}H NMR and (c) ^{13}C NMR (400 MHz, $CDCl_3$) of 9-decenyltrichlorosilane **1a**.

3.1.2. The synthetic route of 14-pentadecenyltrichlorosilane 1c

The synthetic route used for the preparation of the longest chain precursor **1c** is illustrated in **Scheme 3.4**.

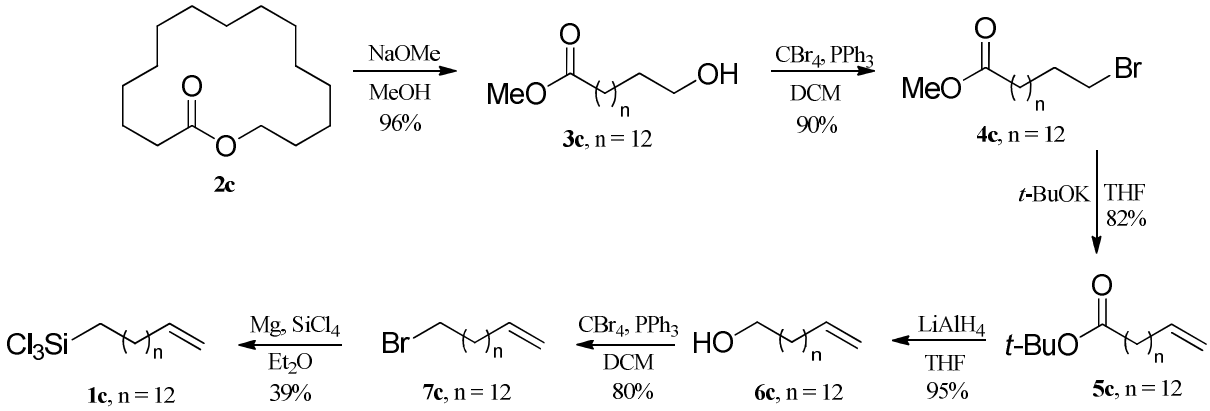

Scheme 3.4. Synthetic route of 14-pentadecenyltrichlorosilane **1c**.

In the first step of the reaction sequence, commercially available ω-pentadecalactone **2c** was used as a starting material. Following a procedure described by *Hostetler et al,*[19] nucleophilic ring opening of lactone **2c** with sodium methoxide afforded ω-hydroxy methyl ester **3c**. The product was then purified by column chromatography and isolated in very good yield (96%). Conversion of the ω-hydroxy methyl ester **3c** to ω-bromo ester **4c** was achieved as before by an Appel reaction using triphenylphosphine and carbon tetrabromide in dichloromethane.[20] Purification of compound **4c** was easily achieved by chromatography and obtained also in a good yield (90%). The ω-bromo methyl ester **4c** was then treated with an excess of *t*-BuOK resulting in two reactions occurring simultaneously at both ends of the molecule. First, HBr elimination provided the expected terminal alkene, but also a transesterification of the methyl ester into the corresponding *tert*-butyl ester occurred. Purification of the ω-unsaturated *tert*-butyl ester **5c** was achieved by column chromatography and this product could be isolated in 82% yield.[19] Reduction of ester **5c** with lithium aluminium hydride ($LiAlH_4$) resulted in its conversion to the ω-unsaturated alcohol **6c**.[21] The product was purified by chromatography in 95% yield. Alcohol **6c** was again brominated under Appel reaction conditions and was purified by column chromatography resulting in 80% yield of bromide **7c**. The ω-unsaturated alkenyl bromide **7c** was then used to prepare the corresponding Grignard

reagent and was reacted with tetrachlorosilane.[22] Both the reaction and work-up had to be performed under an inert atmosphere (nitrogen) using oven-dried glassware. 14-Pentadecenyltrichlorosilane (**1c**) was isolated by Kugelrohr distillation with moderate yield of 39%. The trichlorosilane products are very moisture sensitive, and must be stored in an inert atmosphere in a cool, dark place.

3.2. Experimental

3.2.1. General Information

Materials. Chemicals were obtained from commercial sources (Sigma-Aldrich, Alfa Aesar, Acros, and Fisher Scientific) and were used as received. All reactions were performed under an inert atmosphere using oven-dried glassware.

Commercially available n-type, one-side polished silicon (100) wafers (Wacker, Munich, Germany) were used as substrates.

Instrumentation. ^{1}H NMR spectra were recorded on Bruker Avance 300 (300 MHz); Bruker Avance II 400 (400 MHz). All spectra were acquired in deuterochloroform. The multiplicity of each signal is indicated by: s (singlet); bs (broad singlet); d (doublet); t (triplet); dd (doublet of doublets); dddd (doublet of doublet of doublet of doublets); q (quartet); m (multiplet). The number of protons (n) for a given resonance signal is indicated by nH. Coupling constants (J) are quoted in Hz and are recorded to the nearest 0.1 Hz. Identical proton coupling constants are averaged in each spectrum and reported to the nearest 0.1 Hz. The coupling constants were determined by analysis using Bruker TopSpin software.

^{13}C NMR spectra were recorded on a Bruker Avance 300 (75 MHz) or on a Bruker Avance II 400 (101 MHz) spectrometer.

^{29}Si NMR spectra were recorded on a Bruker Avance II 400 (79.5 MHz). The chemical shift data for each signal are given as δ in units of parts per million (ppm) relative to tetramethylsilane (TMS) where δ_{Si} (TMS) = 0.00 ppm.

^{19}F NMR spectra were recorded on a Bruker Avance 300 (282 MHz) or on a Bruker Avance II 400 (376 MHz). The chemical shift data for each signal are given as δ in units of parts per million (ppm). Coupling constants (J) are quoted in Hz and are recorded to the nearest 0.1 Hz.

Mass spectrometry spectra were obtained on Waters Micromass GCT Time of Flight Mass Spectrometer using electron impact or chemical ionisation techniques. Chemical ionisation spectra were obtained using methane as the ionising gas. Electrospray ionisation spectra were obtained on Waters Micromass LCT Time of Flight Mass Spectrometer coupled to a Waters 2975 HPLC, operating in positive or negative mode, from solutions of acetonitrile; *m/z* values are reported in Daltons. Samples sent to the EPSRC mass spectrometry service in Swansea were analysed on a Thermofisher LTQ Orbitrap XL mass spectrometer using either atmospheric pressure chemical ionisation (APCI) or electrospray ionisation (ESI).

Melting points were measured using an Electrothermal 9100 or Gallenkamp Griffin MPA350 melting point apparatus, and are uncorrected.

Analytical thin layer chromatography (TLC) was carried out on Merck silica gel 60 F_{254} aluminium-supported thin layer chromatography sheets. Visualisation was by thermal development after dipping in an ethanolic solution of phosphomolybdic acid (PMA).

Flash Column chromatography was carried out on Merck Geduran silica gel 60 (400-630 mesh), eluting with solvents as supplied under a positive pressure of compressed air.

Anhydrous solvents (diethyl ether, hexane, dichloromethane, tetrahydrofuran) were obtained using a MBRAUN GmbH MB SPS-800 solvent purification system.

In vacuo refers to the use of a diaphragm vacuum pump to remove solvent under reduced pressure on a Büchi Rotavapor at 40 °C.

3.2.2. Synthesis of self-assembling molecules

3.2.2.1. Methyl 15-hydroxypentadecanoate - 3c[19]

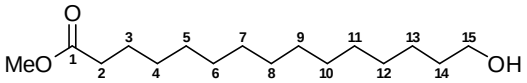

Sodium methoxide was generated by the addition of sodium metal (2.4 g, 104 mmol, 5.0 eq) to dry MeOH (130 mL) at 0 °C. The mixture was warmed to rt and stirred until all of the sodium was consumed. ω-Pentadecalactone **2c** (5.0 g, 21 mmol, 1.0 eq) was added in a single portion and the solution was warmed to 80 °C and stirred for 3 h. The reaction was cooled to rt and quenched with HCl solution (1 M, 175 mL) and diluted with water (175 mL). The aqueous layer was extracted into diethyl ether (3 × 100 mL), and the combined organic layers were washed with water (150 mL), brine (150 mL), and dried over $MgSO_4$ and the solvent removed *in vacuo*. The product was purified by silica gel chromatography (2:1 hexane:EtOAc), to afford methyl 15-hydroxypentadecanoate **3c** (5.43 g, 96%) as a colourless solid: mp 46-48 °C [Lit.[19] 47-48 °C]; ^{1}H NMR (400 MHz, $CDCl_3$) δ_H 3.65 (3H, s, OC$\underline{H_3}$), 3.63 (2H, t, *J* 6.6 Hz, C$\underline{H_2}$OH), 2.29 (2H, t, *J* 7.0 Hz, C$\underline{H_2}$COOCH$_3$), 1.62-1.54 (4H, m, C$\underline{H_2}$CH$_2$OH and C$\underline{H_2}$CH$_2$COOCH$_3$), 1.31-1.23 (20H, m, C$\underline{H_2}$: C4-C13); ^{13}C NMR (101 MHz, $CDCl_3$) δ_C 174.4 (<u>C</u>=O), 63.2 (<u>C</u>H$_2$OH), 51.5 (O<u>C</u>H$_3$), 34.2 (<u>C</u>H$_2$COOCH$_3$), 32.8, 29.6, 29.5, 29.4, 29.2, 29.1, 25.7, 24.9 (<u>C</u>H$_2$: C3-C14); *m/z* (ESI): $C_{16}H_{31}NaO_3$ $[M+Na]^+$ 294.97.

3.2.2.2. Methyl 15-bromopentadecanoate - 4c[20]

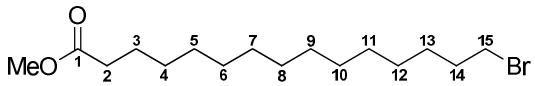

Triphenylphosphine (4.3 g, 17.1 mmol, 1.1 eq) was added to a solution of methyl 15-hydroxypentadecanoate **3c** (4.2 g, 15.6 mmol, 1.0 eq) and carbon tetrabromide (5.7 g, 17.1 mmol, 1.1 eq) in dichloromethane (15 mL) at 0 °C in portions over 30 min, with vigorous stirring. The colourless solution turned a pale brown colour upon addition of the phosphine and was stirred for additional 2 h at rt. The reaction was concentrated *in vacuo*

to a brown oil, hexane (200 mL) was added and the mixture was stirred for 15 min. The resulting white precipitate was removed by filtration, and the filtrate was concentrated *in vacuo*. The product was purified over silica gel (20:1 hexane:EtOAc), to afford methyl 15-bromopentadecanoate **4c** (4.6 g, 90%) as a colourless solid: mp 38-40 °C [Lit.[19] 38-39 °C]; ^{1}H NMR (400 MHz, $CDCl_3$) δ_H 3.65 (3H, s, OC$\underline{H}_3$), 3.39 (2H, t, *J* 6.9 Hz, C$\underline{H}_2$Br), 2.29 (2H, t, *J* 7.5 Hz, C$\underline{H}_2$COOCH$_3$), 1.87-1.80 (2H, m, C$\underline{H}_2$CH$_2$Br), 1.64-1.56 (2H, m, C$\underline{H}_2$CH$_2$COOCH$_3$), 1.44-1.36 (2H, m, C$\underline{H}_2$CH$_2$CH$_2$Br), 1.31-1.21 (18H, m, C$\underline{H}_2$: C4-C12); ^{13}C NMR (101 MHz, $CDCl_3$) δ_C 51.6 (O$\underline{C}$H$_3$), 34.2, 33.0, 29.9, 29.7, 29.6, 29.5, 29.4, 29.3, 28.9, 28.3, 25.1 ($\underline{C}$H$_2$: C2-C15); *HRMS m/z* (CI): calculated for $C_{16}H_{32}O_2{}^{79}Br_1$ $[M+H]^+$ 335.1586, found 335.1595.

3.2.2.3. *tert*-Butyl 14-pentadecanoate - 5c[19]

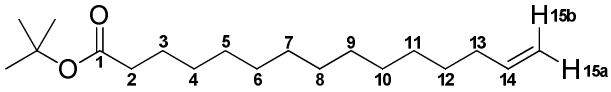

Methyl 15-bromopentadecanoate **4c** (4.0 g, 11.9 mmol, 1.0 eq) was added to a solution of *t*BuOK in THF (1 M, 60 mL) and the reaction mixture was stirred at rt for 1 h. The reaction was then quenched with HCl solution (1 M, 150 mL). The aqueous layer was extracted into diethyl ether (3 × 100 mL), and the combined organic layers were washed with water (150 mL), brine (150 mL), dried over $MgSO_4$ and the solvent was removed *in vacuo*. The product was purified over silica gel (100:1 hexane:EtOAc), to afford *tert*-butyl 14-pentadecanoate **5c** (2.89 g, 82%) as a colourless oil; ^{1}H NMR (300 MHz, $CDCl_3$) δ_H 5.80 (1H, dddd, *J* 17.2, 10.2, 6.8, 6.8 Hz, C$\underline{H}$=CH$_2$), 4.96 (1H, dddd, *J* 17.2, 3.5, 1.5, 1.5 Hz, CH=C$\underline{H}_2$ 15b), 4.90 (1H, dddd, *J* 10.2, 3.5, 1.5, 1.5 Hz, CH=C$\underline{H}_2$ 15a), 2.19 (2H, t, *J* 7.4 Hz, C$\underline{H}_2$COOC(CH$_3$)$_3$), 2.07-1.99 (2H, m, C$\underline{H}_2$CH=CH$_2$), 1.61-1.51 (2H, m, C$\underline{H}_2$CH$_2$COOC(CH$_3$)$_3$), 1.44 (9H, s, OC(C$\underline{H}_3$)$_3$), 1.31-1.22 (18H, bs, C$\underline{H}_2$: C4-C12); ^{13}C NMR (75 MHz, $CDCl_3$) δ_C 173.5 ($\underline{C}$=O), 139.4 ($\underline{C}$H=CH$_2$), 114.2 (CH=$\underline{C}$H$_2$), 80.0 ($\underline{C}$(CH$_3$)$_3$), 35.8 ($\underline{C}$H$_2$COOC(CH$_3$)$_3$), 33.9 ($\underline{C}$H$_2$CH=CH$_2$), 29.7, 29.6, 29.4, 29.3, 29.2, 29.2, 29.1 ($\underline{C}$H$_2$: C4-C12), 28.3 (C($\underline{C}$H$_3$)$_3$), 25.3 ($\underline{C}$H$_2$CH$_2$COOC(CH$_3$)$_3$); *HRMS m/z* (CI): calculated for $C_{19}H_{37}O_2$ $[M+H]^+$ 297.2794, found 297.2800.

3.2.2.4. 14-Pentadecen-1-ol - 6c[23]

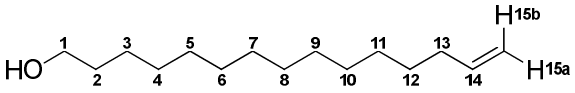

t-Butyl 14-pentadecanoate **5c** (2.4 g, 8 mmol, 1.0 eq) was added *via* cannula in portions over 30 min to a solution of lithium aluminium hydride (0.5 g, 12 mmol, 1.5 eq) in dry THF (15 mL) cooled to 10 °C. After the addition was complete, the reaction mixture was warmed to rt and then heated under reflux for 16 h. The reaction mixture was then cooled again to 10 °C and diluted with diethyl ether (15 mL). The reaction was quenched by dropwise addition of water (1 mL), aqueous sodium hydroxide solution (15%, 1 mL) and water (2 mL) over 30 min. The solution was stirred for 30 min and the resultant white precipitate was removed by filtration. The residue was washed with diethyl ether (3 × 10 mL) and the organic filtrates were combined, dried over anhydrous Na_2SO_4, and the solvent was removed *in vacuo*. The product was purified over silica gel (3:1 hexane:EtOAc), affording 14-pentadecen-1-ol **6c** (1.74 g, 95%) as a colourless oil; ^{1}H NMR (400 MHz, $CDCl_3$) δ_H 5.80 (1H, dddd, *J* 17.1, 10.3, 6.8, 6.8 Hz, C*H*=CH_2), 5.02-4.95 (1H, m, CH=C*H*$_2$ 15b), 4.94-4.89 (1H, m, CH=C*H*$_2$ 15a), 3.63 (2H, t, *J* 6.7 Hz, C*H*$_2$OH), 2.07-1.99 (2H, m, C*H*$_2$CH=CH_2), 1.68 (1H, s, O*H*), 1.60-1.50 (2H, m, C*H*$_2$$CH_2$OH), 1.41-1.22 (20H, m, C*H*$_2$: C3-C12); ^{13}C NMR (101 MHz, $CDCl_3$) δ_C 139.4 (*C*H=CH_2), 114.2 (CH=*C*H_2), 63.3 (*C*H_2OH), 33.9 (*C*H_2CH=CH_2), 32.8 (*C*$H_2$$CH_2$OH), 29.8, 29.7, 29.6, 29.5, 29.3, 29.1 (*C*H_2: C4-C12), 25.8 (*C*$H_2$$CH_2$$CH_2$OH); *HRMS m/z* (CI): calculated for $C_{15}H_{31}O_1$ $[M+H]^+$ 227.2375, found 227.2371.

3.2.2.5. 15-Bromo-1-pentadecene - 7c[20, 24, 25]

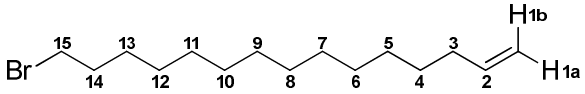

Triphenylphosphine (1.9 g, 7.2 mmol, 1.1 eq) was added in portions over 30 min with vigorous stirring to a solution of 14-pentadecen-1-ol **6c** (1.5 g, 6.5 mmol, 1.0 eq) and carbon tetrabromide (2.4 g, 7.2 mmol, 1.1 eq) in dichloromethane (15 mL) cooled to 0 °C. The colourless solution turned a pale brown colour upon addition of the phosphine and was

stirred for additional 2 h at rt. The mixture was concentrated *in vacuo* to give a brown oil. Hexane (150 mL) was added and the mixture was stirred for 15 min. The resultant colourless precipitate was removed by filtration, and the filtrate was concentrated *in vacuo*. This oil was purified over silica gel (hexane), affording 14-bromo-1-pentadecene **7c** (1.52 g, 80%) as a colourless oil; ^{1}H NMR (400 MHz, $CDCl_3$) δ_H 5.80 (1H, dddd, *J* 17.1, 10.2, 6.7, 6.7 Hz, C*H*=CH_2), 4.99 (1H, dddd, *J* 17.1, 3.6, 1.4, 1.4 Hz, CH=C*H*$_2$ 1b), 4.92 (1H, dddd, *J* 10.2, 3.6, 1.4, 1.4 Hz, CH=C*H*$_2$ 1a), 3.40 (2H, t, *J* 6.7 Hz, C*H*$_2$Br), 2.07-1.99 (2H, m, C*H*$_2$CH=CH_2), 1.89-1.80 (2H, m, C*H*$_2$$CH_2$Br), 1.46-1.22 (20H, m, C*H*$_2$: C4-C13); ^{13}C NMR (101 MHz, $CDCl_3$) δ_C 139.5 (*C*H=CH_2), 114.3 (CH=*C*H_2), 34.2 (*C*H_2Br), 34.0 (*C*H_2CH=CH_2), 32.9 (*C*$H_2$$CH_2$Br), 29.7, 29.6, 29.6, 29.5, 29.3, 29.1, 28.9 (*C*H_2: C4-C12), 28.3 (*C*$H_2$$CH_2$$CH_2$Br); *m/z* (CI): $C_{15}H_{29}{}^{81}Br_1$ [M^+] 290.15.

3.2.2.6. 14-Pentadecenyltrichlorosilane - 1c[22, 26]

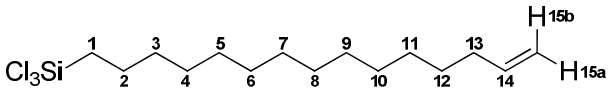

$SiCl_4$ (6.0 g, 4.1 mL, 4.4 eq) was added *via* cannula to a suspension of magnesium (0.9 g, 35.9 mmol, 4.5 eq) in diethyl ether (10 mL). A solution of 14-bromo-1-pentadecene **6c** (2.3 g, 8.0 mmol, 1.0 eq) in diethyl ether (5 mL) was then introduced *via* cannula in small portions over 3 h, and then stirred for a further 16 h at rt. The product was extracted from the resulting solids with hexane (4 × 70 mL). After filtration, the hexane was evaporated and distillation of the residues yielded 15-pentadecenyltrichlorosilane **1c** (1.06 g, 39%) as a colourless oil: bp 145-150 °C/ 4 mbar; ^{1}H NMR (400 MHz, $CDCl_3$) δ_H 5.81 (1H, dddd, *J* 17.0, 10.2, 6.7, 6.7 Hz, C*H*=CH_2), 4.99 (1H, dddd, *J* 17.0, 1.6, 1.3, 1.3 Hz, CH=C*H*$_2$ 15b), 4.92 (1H, dddd, *J* 10.2, 1.6, 1.3, 1.3 Hz, CH=C*H*$_2$ 15a), 2.09-1.98 (2H, m, C*H*$_2$CH=CH_2), 1.65-1.51 (2H, m, C*H*$_2$), 1.41-1.14 (22H, m, C*H*$_2$); ^{13}C NMR (101 MHz, $CDCl_3$) δ_C 139.4 (*C*H=CH_2), 114.2 (CH=*C*H_2), 33.9 (*C*H_2CH=CH_2), 31.9, 29.8, 29.7, 29.7, 29.6, 29.5, 29.3, 29.1, 29.1, 24.5, 22.4 (*C*H_2: C1-C12); ^{29}Si NMR (80 MHz, $CDCl_3$) δ_{Si} 13.3; *HRMS m/z* (CI): calculated for $C_{20}H_{30}{}^{35}Cl_3Si_1$ $[M+H]^+$ 343.1182, found 343.1176.

3.2.2.7. 10-Bromo-1-decene - 5a[20, 27-30]

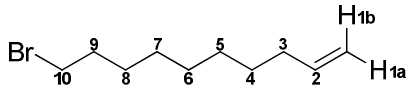

Following the procedure **3.2.2.5**, and starting from 9-decen-1-ol **4a** (5.0 g, 32.0 mmol), this reaction furnished 10-bromo-1-decene **5a** (7.01 g, 92%) as a colourless oil: bp 85-86 °C/ 2 mbar; ^{1}H NMR (400 MHz, $CDCl_3$) δ_H 5.80 (1H, dddd, *J* 17.2, 10.2, 6.7, 6.7 Hz, C*H*=CH_2), 4.98 (1H, dddd, *J* 17.2, 2.1, 1.5, 1.5 Hz, CH=C*H*$_2$ 1b), 4.92 (1H, dddd, *J* 10.2, 2.1, 1.5, 1.5 Hz, CH=C*H*$_2$ 1a), 3.40 (2H, t, *J* 6.8 Hz, C*H*$_2$Br), 2.03-2.11 (2H, m, C*H*$_2$CH=CH_2), 1.92-1.84 (2H, m, C*H*$_2$$CH_2$Br), 1.48-1.31 (10H, m, C*H*$_2$:C4-C8); ^{13}C NMR (101 MHz, $CDCl_3$) δ_C 139.3 (*C*H=CH_2), 114.3 (CH=*C*H_2), 34.2 (*C*H_2Br), 33.9 (*C*H_2CH=CH_2), 32.9 (*C*$H_2$$CH_2$Br), 29.4, 29.1, 29.0, 28.8, 28.3 (*C*H_2: C4-C8); *HRMS m/z* (CI): calculated for $C_{10}H_{20}{}^{79}Br_1$ $[M+H]^+$ 219.0743, found 219.0745.

3.2.2.8. 11-Bromo-1-undecene - 5b[20, 31, 32]

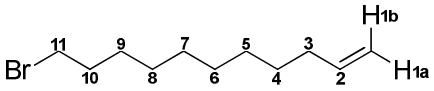

Following the procedure **3.2.2.5**, and starting from 10-undecen-1-ol **4b** (5.0 g, 29.4 mmol), this reaction furnished 11-bromo-1-undecene **5b** (5.22 g, 77%) as a colourless oil: bp 105-106 °C/ 4 mbar; ^{1}H NMR (400 MHz, $CDCl_3$) δ_H 5.87 (1H, dddd, *J* 17.0, 10.3, 6.7, 6.7 Hz, C*H*=CH_2), 5.05 (1H, dddd, *J* 17.0, 2.0, 1.4, 1.4 Hz, CH=C*H*$_2$ 1b), 4.99 (1H, dddd, *J* 10.3, 2.0, 1.4, 1.4 Hz, CH=C*H*$_2$ 1a), 3.69 (2H, t, *J* 6.7 Hz, C*H*$_2$Br), 2.14-2.07 (2H, m, C*H*$_2$CH=CH_2), 1.67-1.58 (2H, m, C*H*$_2$$CH_2$Br), 1.49-1.31 (12H, m, C*H*$_2$: C4-C9); ^{13}C NMR (101 MHz, $CDCl_3$) δ_C 139.3 (*C*H=CH_2), 114.3 (CH=*C*H_2), 34.2 (*C*H_2Br), 33.9 (*C*H_2CH=CH_2), 32.9 (*C*$H_2$$CH_2$Br), 29.65, 29.2, 29.0, 28.9, 28.3 (*C*H_2: C4-C9); *HRMS m/z* (CI): calculated for $C_{11}H_{22}{}^{79}Br_1$ $[M+H]^+$ 233.0899, found 233.0896.

3.2.2.9. 9-Decenyltrichlorosilane - 1a[22]

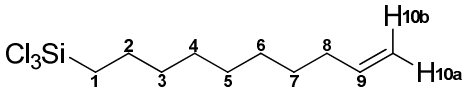

Following the procedure **3.2.2.6**, and starting from 10-bromo-1-decene **5a** (7.0 g, 31.9 mmol), this reaction furnished 9-decenyltrichlorosilane **1a** (2.5 g, 29%) as a colourless oil: bp 102-105 °C/ 2 mbar; ^{1}H NMR (400 MHz, $CDCl_3$) δ_H 5.81 (1H, dddd, *J* 17.0, 10.3, 6.7, 6.7 Hz, C*H*=CH_2), 4.99 (1H, dddd, *J* 17.0, 1.9, 1.3, 1.3 Hz, CH=C*H*$_2$ 10b), 4.93 (1H, dddd, *J* 10.2, 1.9, 1.3, 1.3 Hz, CH=C*H*$_2$ 10a), 2.09-2.01 (2H, m, C*H*$_2$CH=CH_2), 1.64-1.53 (2H, m, C*H*$_2$), 1.39-1.13 (12H, m, C*H*$_2$); ^{13}C NMR (101 MHz, $CDCl_3$) δ_C 139.3 (*C*H=CH_2), 114.4 (CH=*C*H_2), 34.0 (*C*H_2CH=CH_2), 31.6, 29.3, 29.2, 29.1, 29.0, 24.5, 22.4 (*C*H_2: C1-C7); ^{29}Si NMR (80 MHz, $CDCl_3$) δ_{Si} 13.9; *HRMS m/z* (ESI): calculated for $C_{10}H_{20}{}^{35}Cl_3Si_1$ $[M+H]^+$ 273.0394, found 273.0391.

3.2.2.10. 10-Undecenyltrichlorosilane - 1b[12, 22]

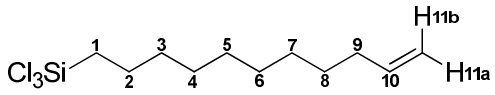

Following the procedure **3.2.2.6**, and starting from 11-bromo-1-undecene **5b** (5.0 g, 21.5 mmol), this reaction furnished 10-undecenyltrichlorosilane **1b** (2.5 g, 37%) as a colourless oil: bp 110-113 °C/ 2 mbar; ^{1}H NMR (400 MHz, $CDCl_3$) δ_H 5.74 (1H, dddd, *J* 17.2, 10.2, 6.7, 6.7 Hz, C*H*=CH_2), 4.92 (1H, dddd, *J* 17.2, 2.1, 1.5, 1.5 Hz, CH=C*H*$_2$ 11b), 4.86 (1H, dddd, *J* 10.2, 2.1, 1.5, 1.5 Hz, CH=C*H*$_2$ 11a), 2.01-1.93 (2H, m, C*H*$_2$CH=CH_2), 1.55-1.45 (2H, m, C*H*$_2$), 1.37-1.17 (14H, m, C*H*$_2$); ^{13}C NMR (101 MHz, $CDCl_3$) δ_C 139.4 (*C*H=CH_2), 114.3 (CH=*C*H_2), 34.0 (*C*H_2CH=CH_2), 31.9, 29.5, 29.4, 29.2, 29.1, 29.1, 24.5, 22.4 (*C*H_2: C1-C8); ^{29}Si NMR (80 MHz, $CDCl_3$) δ_{Si} 13.5; *m/z* (CI): $C_{11}H_{21}{}^{35}Cl_3Si_1$ $[M+H]^+$ 287.0203.

3.3. Literature

1. J. J. Gooding, F. Mearns, W. R. Yang and J. Q. Liu, *Electroanalysis*, 2003, **15**, 81-96.
2. A. Ulman, *Chem. Rev.*, 1996, **96**, 1533-1554.
3. D. Samanta and A. Sarkar, *Chem. Soc. Rev.*, 2011, **40**, 2567-2592.
4. R. Maboudian, W. R. Ashurst and C. Carraro, *Sens. Actuator A-Phys.*, 2000, **82**, 219-223.
5. R. Maboudian, *Surf. Sci. Rep.*, 1998, **30**, 209-268.
6. Y. X. Zhuang, O. Hansen, T. Knieling, C. Wang, P. Rombach, W. Lang, W. Benecke, M. Kehlenbeck and J. Koblitz, *J. Microelectromech. Syst.*, 2007, **16**, 1451-1460.
7. R. R. Rye, G. C. Nelson and M. T. Dugger, *Langmuir*, 1997, **13**, 2965-2972.
8. M. J. Stevens, *Langmuir*, 1999, **15**, 2773-2778.
9. A. Y. Fadeev and T. J. McCarthy, *Langmuir*, 2000, **16**, 7268-7274.
10. Y. X. Zhuang, O. Hansen, T. Knieling, C. Wang, P. Rombach, W. Lang, W. Benecke, M. Kehlenbeck and J. Koblitz, *J. Micromech. Microeng.*, 2006, **16**, 2259-2264.
11. N. Herzer, S. Hoeppener and U. S. Schubert, *Chem. Commun.*, 2010, **46**, 5634-5652.
12. S. R. Wasserman, Y. T. Tao and G. M. Whitesides, *Langmuir*, 1989, **5**, 1074-1087.
13. F. C. Whitmore, L. H. Sommer, P. A. D. Giorgio, W. A. Strong, R. E. v. Strien, D. L. Bailey, H. K. Hall, E. W. Pietrusza and G. T. Kerr, *J. Am. Chem. Soc.*, 1946, **68**, 475-481.
14. R. Maoz and J. Sagiv, *Langmuir*, 1987, **3**, 1034-1044.
15. R. Maoz and J. Sagiv, *Langmuir*, 1987, **3**, 1045-1051.
16. K. Yamamoto, T. Hayashi and M. Kumada, *J. Organomet. Chem.*, 1971, **28**, 37-38.
17. N. Balachander and C. N. Sukenik, *Langmuir*, 1990, **6**, 1621-1627.
18. P. Silberzan, L. Leger, D. Ausserre and J. J. Benattar, *Langmuir*, 1991, **7**, 1647-1651.
19. E. D. Hostetler, S. Fallis, T. J. McCarthy, M. J. Welch and J. A. Katzenellenbogen, *J. Org. Chem.*, 1998, **63**, 1348-1351.
20. T. W. Baughman, J. C. Sworen and K. B. Wagener, *Tetrahedron*, 2004, **60**, 10943-10948.
21. A. I. Meyers, D. A. Dickman and T. R. Bailey, *J. Am. Chem. Soc.*, 1985, **107**, 7974-7978.
22. S. B. Amin and T. J. Marks, *J. Am. Chem. Soc.*, 2007, **129**, 2938-2953.
23. Y. S. Hon, Y. C. Wong, C. P. Chang and C. H. Hsieh, *Tetrahedron*, 2007, **63**, 11325-11340.
24. W. C. Qu, K. Ploessl, H. Truong, M. P. Kung and H. F. Kung, *Bioorg. Med. Chem. Lett.*, 2009, **19**, 3382-3385.
25. J. Christoffers and H. Oertling, *Tetrahedron*, 2000, **56**, 1339-1344.
26. Y. L. Wang, T. J. Su, R. Green, Y. Q. Tang, D. Styrkas, T. N. Danks, R. Bolton and J. R. Liu, *Chem. Commun.*, 2000, 587-588.
27. M. C. Roux, R. Paugam and G. Rousseau, *J. Org. Chem.*, 2001, **66**, 4304-4310.
28. M. L. Hunnicutt, J. M. Harris and C. H. Lochmuller, *J. Phys. Chem.*, 1985, **89**, 5246-5250.
29. E. B. Bauer, F. Hampel and J. A. Gladysz, *Organometallics*, 2003, **22**, 5567-5580.
30. Y. Kobayashi and H. Okui, *J. Org. Chem.*, 2000, **65**, 612-615.

31. Z. H. Shen, M. C. Huang, C. D. Xiao, Y. Zhang, X. Q. Zeng and P. G. Wang, *Anal. Chem.*, 2007, **79**, 2312-2319.
32. M. Bartra and J. Vilarrasa, *J. Org. Chem.*, 1991, **56**, 5132-5138.

4. Deposition of Self-Assembled Monolayers

Parts of this Chapter have been published in: M. Adamkiewicz, T. O'Hara, D. O'Hagan, G. Hähner, *Thin Solid Films*, 2012, **520**, 6719-6723.

In the last few decades, the interest in silane coatings has greatly increased due to their stability and possibility for further chemical modification.[1] These characteristics have made SAMs very attractive candidates for the surface functionalisation of micro-electromechanical systems (MEMS) and their smaller equivalents nano-electromechanical systems (NEMS).[2, 3] Self-assembled monolayer films can be produced either in a liquid phase or in a gas phase process. However, the solution phase process is less suitable particularly for manufacturing purposes. Liquid phase deposition is cumbersome because the SAM solution has to be freshly prepared and used immediately to coat the surface of a substrate. If this solution is not handled with sufficient care, the surfactant molecules will polymerise, because of their sensitivity to water. The quality of solution formed films is often good and if the same procedure is followed each time, the results are reproducible. However, problems arise when it is necessary to scale up the process and modify a larger wafer or multi-wafer cassettes.[4] In the liquid phase deposition process a large amount of solvent is used increasing the costs.[5, 6] All of these factors make liquid phase deposition an inconvenient and unpredictable methodology for the manufacture of coatings on an industrial scale.[2] Vapour phase deposition can eliminate some of the problems encountered in wet chemistry[5] and it has been found that the method can provide higher quality monolayers on silicon substrates,[2, 7-9] because polymeric organosilane aggregates do not vaporise and deposit on the surface. Furthermore, vapour phase processes are generally reproducible[8, 10] and can be easily adapted to industrial requirements.[8]

Vinyl-terminated SAMs possess functionality for further chemical modification, for example *via* oxidation,[11] a Heck-type coupling reaction,[12] addition reactions,[13] or metathesis.[14, 15] Vinyl-terminated SAMs also offer the potential as a starting point to tailor functionalisation of silicon microstructures, such as MEMS, with a variety of chemical functional groups. This kind of chemical functionalisation is only possible if high quality monolayer films can be prepared from the vapour phase. This Chapter describes the

preparation of quality films prepared from vinyl-trichlorosilane precursor molecules onto a silicon substrate in both the solution and gas phase processes. Methyl-terminated films were also prepared as references. All of the SAMs were independently characterised by four techniques: X-ray photoelectron spectroscopy (XPS), atomic force microscopy (AFM), contact angle goniometry and ellipsometry.

4.1. Surfactants

The self-assembling molecules shown in **Figure 4.1** were used for the formation of SAMs in the solution and vapour phase processes. The synthesised surfactants were vinyl-terminated trichlorosilanes with alkyl chain lengths of ten (9-decenyltrichlorosilane (CH_2=CH-(CH_2)$_8$-$SiCl_3$), **1a**), eleven (10-undecenyltrichlorosilane (CH_2=CH-(CH_2)$_9$-$SiCl_3$), **1b**), and fifteen carbon atoms (14-pentadecenyltrichlorosilane (CH_2=CH-(CH_2)$_{13}$-$SiCl_3$), **1c**). The commercially available methyl-terminated molecules with ten and eighteen carbons in an alkyl chain, decyltrichlorosilane **1d** (CH_3-(CH_2)$_9$-$SiCl_3$) and octadecanetrichlorosilane **1e** (CH_3-(CH_2)$_{18}$-$SiCl_3$), were used as non-vinyl reference SAMs (**Figure 4.1**).

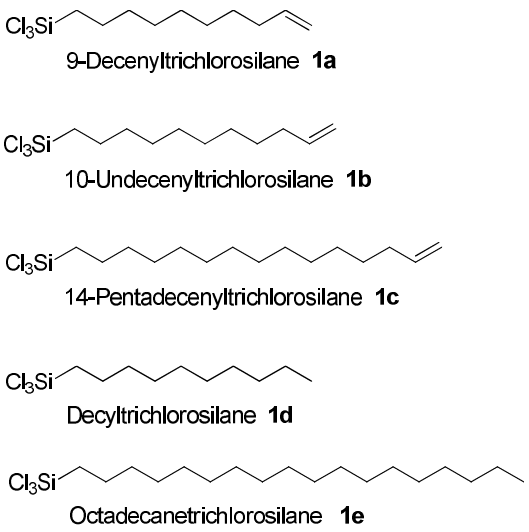

Figure 4.1. Trichlorosilanes used for the formation of SAMs on a silicon substrate.

4.2. Pre-treatment of the silicon substrates

The thickness of the monolayer is determined by the length of a single self-assembling molecule and is usually within several nanometers, thus the uniformity and homogeneity of the SAM could be easily disturbed by the presence of contamination on the substrate. Particles and other contaminants, present on a surface during the deposition process, may lead to the formation of cracks, pinholes and defects in the final film. Therefore, the selection of an appropriate cleaning procedure was crucial to obtain a high quality film with high reproducibility.[16]

Ideally, a silicon wafer should have a clean silicon oxide layer with a high density of hydroxyl groups on the surface. The cleaning procedure can be divided into two types of method: dry and wet. The most widely employed dry methods used to clean silicon wafers are: reactive plasma-assisted cleaning (oxygen-based plasma),[17] photochemical cleaning (UV irradiation in an oxygen atmosphere)[17, 18] and ozone cleaning.[19, 20] All of these techniques oxidise organic impurities on the surface into gases or water-soluble species.[18] Unfortunately, these methods are not suitable for inorganic impurities, such as metals. Liquid phase cleaning processes always employ hot acidic and alkali solutions.[21] However, the order of the reagents, dipping time and temperature of the solution may vary.[21, 22] First, the wafers are immersed in a mixture of sulfuric acid (H_2SO_4) and hydrogen peroxide (H_2O_2), known as 'Piranha Solution'.[23] This solution removes only the organic contaminants from the surface, but does not remove inorganic species.[24] In the second step, a mixture of water (H_2O), hydrogen peroxide (H_2O_2) and ammonium hydroxide (NH_4OH), also known as 'Ammonia/Peroxide Mixture' (APM or SC-1 solution) is used to remove inorganic contaminants (heavy metal complexes – group I B and II B metals such as Au, Ag, Cu, Zn, Cd, and several other metals, including Ni, Co, Cr) as well as any unwanted particulates (dust, silica, silicon) and any remaining organic contaminations.[16, 24] In the last step, a mixture of water (H_2O), hydrogen peroxide (H_2O_2) and hydrochloric acid (HCl), also known as 'Hydrochloric/Peroxide Mixture' (HPM or SC-2 solution) is used to dissolve and remove alkali residues and any residual trace metals such as Au, as well as metal hydroxides including $Al(OH)_3$, $Fe(OH)_3$ and $Mg(OH)_2$.[16] Each step is followed by rinsing with water. This cleaning process generates a clean silicon substrate with a thin hydrophilic oxide layer.[16]

4.2.1. Results and Discussion

A combination of dry and wet cleaning method was used in this work to obtain a clean silicon substrate. The quality of the cleaning procedure was monitored independently by three different analytical techniques: X-ray photoelectron spectroscopy, contact angle goniometry and ellipsometry.

4.2.1.1. X-ray Photoelectron Spectroscopy

Freshly cut silicon wafers were exposed to an ozone atmosphere for fixed periods of time: 5, 10, 20, and 30 min, respectively. All wafers were then transferred to the XPS chamber. During this transfer wafers were exposed to the ambient atmosphere for only a few seconds. The XPS survey spectra, taken from treated wafers after the various exposure times, are shown in **Figure 4.2**.

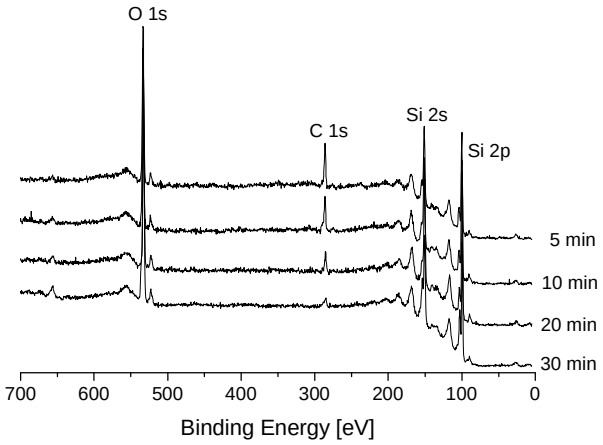

Figure 4.2. The XPS survey scans of cleaned silicon wafers, taken after ozone treatment.

All surfaces exhibit the presence of silicon (2s 150.4 eV, 2p 99.2 eV), carbon (1s 284.6 eV) and oxygen (1s 533.0 eV). The spectra distinguish between the bulk Si (2s 150.4 eV, 2p 99.2 eV) and the silicon oxide (2s 154.3 eV, 2p 102.8 eV). High resolution scans of Si 2p, C 1s and O 1s regions taken from the sample exposed to the ozone atmosphere for 10 min are presented in **Figure 4.3**.

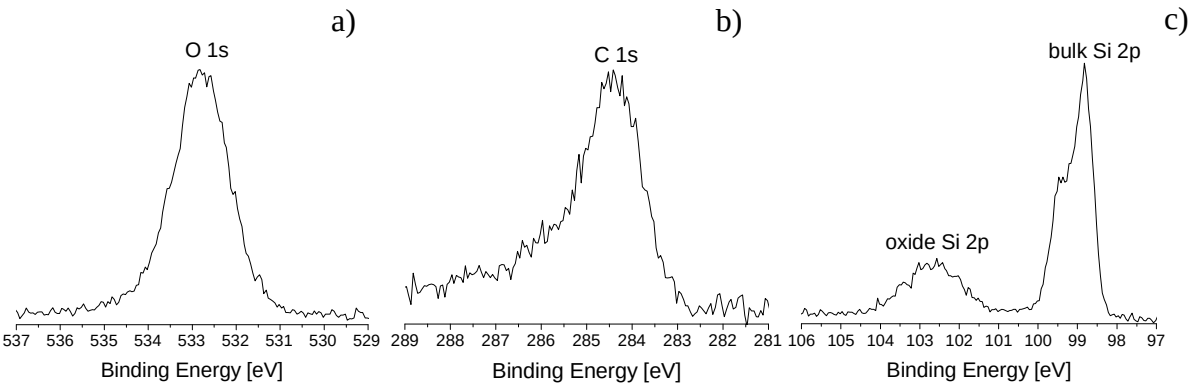

Figure 4.3. High resolution scans of O 1s (a), C 1s (b) and Si 2p (c) regions taken from a silicon wafer exposed to an ozone atmosphere for 10 min.

The most intense carbon signal, which correspond to organic contaminants was observed in the sample exposed to ozone for 5 min. This signal gradually decreased when the exposure time was increased. After 30 min of treatment, almost no C signal was observed. The small impurity observed can be explained by the fact that the sample was contaminated during transfer to the XPS chamber.

The results obtained from XPS analysis confirmed that in order to remove organic contaminants from the surface, the sample should be exposed to an ozone atmosphere for a minimum of 30 min. However, this method is not sufficient to remove inorganic particles. For this reason additional cleaning (wet method) must be applied, to improve the purity of a substrate.

4.2.1.2. Contact angle

Before exposure to an ozone atmosphere, all silicon substrates were inspected under an optical microscope. The water contact angle of each sample was also measured. Untreated silicon wafers exhibited a water contact angle of 35°, which was high compared to the CA values of clean silicon substrate.[25, 26] It was clear that the substrate surfaces were covered with some particles and dust, which were apparent under the microscope. These results confirmed that the silicon surfaces were contaminated and cleaning was required.

The water contact angle measured after sample exposure to an ozone atmosphere for 5, 10, 20 and 30 min were 30°, 25°, 20° and 15°, respectively (**Figure 4.4**). The results obtained from contact angle measurements were consistent with the XPS data. The lowest C 1s signal, observed on XPS for the samples also produced the lowest water contact angles, as expected.

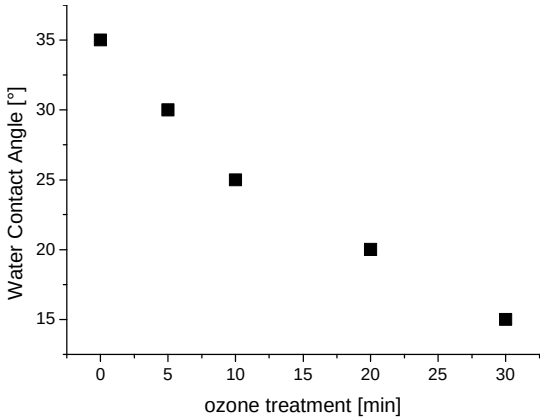

Figure 4.4. Water contact angle versus exposure time to the ozone treatment of silicon wafers.

Additionally, a solution cleaning procedure was applied after the ozone cleaning. The samples were immersed in 'Piranha Solution', ammonium hydroxide solution and then hydrochloric acid solution, in order to remove the inorganic contaminants.

The combined methods of ozone treatment and immersing the wafers in three oxidising solutions resulted in clean and hydrophilic surfaces with a contact angle (CA) of ~5°, which was in good agreement with the results reported in the literature.[25, 26]

4.2.1.3. Ellipsometry

The thickness of the silicon oxide layer on freshly cleaned silicon wafers was measured by ellipsometry and an average value of 16 ± 1 Å was recorded.[27] This value was used for the ellipsometry thickness calculations of all prepared films.

4.2.2. Cleaning procedure

From the presented results it was concluded that a clean silicon substrate (cut into 1.5 cm × 1.5 cm pieces) can be obtained when the following cleaning procedure is applied:

1. Exposure the wafers to an ozone atmosphere for 30 min;
2. Wash the wafers in a solution of concentrated H_2SO_4 and 30% H_2O_2 (2:1) at 70 °C for 15 min *(Caution: "piranha" solution reacts violently with many organic materials and should be handled with care)*; Rinse with deionised water (DI);
3. Wash in a solution of concentrated NH_4OH, DI water, 30% H_2O_2 (1:5:1) at 70 °C for 15 min; Rinse with DI water;
4. Wash in a solution of concentrated HCl, DI water, and 30% H_2O_2 (1:6:1) at 70 °C for 15 min; Rinse with DI water.

All cleaning mixtures were freshly prepared before use to give the best results. Elevated temperature (above 70 °C) was avoided due to the high sensitivity and easy decomposition of hydrogen peroxide.[16] After the last cleaning step, the substrates were rinsed with DI water, dried under a nitrogen atmosphere, and used immediately for the SAMs preparation, as the clean wafers can become re-contaminated very easily.[16] Identical cleaning procedures were always applied to the silicon wafers prior to the preparation of the SAMs.

4.3. Preparation of alkyl- and alkenyl- trichlorosilanes monolayers from the liquid phase

Solution phase deposition is the most common method of preparing self-assembled monolayers on a small scale.[28] However, reproduction of silane films with the same quality is difficult, because SAM formation is sensitive to the reaction conditions and factors such as the length of the surfactant molecule, water volume,[29-32] age and concentration of the solution,[10, 33] deposition time, temperature[29, 32, 34, 35] and the type of solvent.[36] These aspects were discussed in Chapter 1.

4.3.1. Solution deposition process

SAMs were prepared from the trichlorosilane self-assembling molecules **1a-1e** (**Figure 4.1**). Freshly cleaned silicon wafers were placed in glass vials and 5 mL of a solution (1 mM) of the trichlorosilane precursor in toluene was added. Before immersion, the silicon wafers were carefully dried under a flow of nitrogen, as the water used for the final rinsing step tended to trap on the edges of the wafers. This water is responsible for polymerisation of surfactants, which transforms the clear solutions into cloudy solutions in reaction vessels. The substrates remained in the solutions for 16-24 h at room temperature. The experimental set-up is illustrated in **Figure 4.5**.

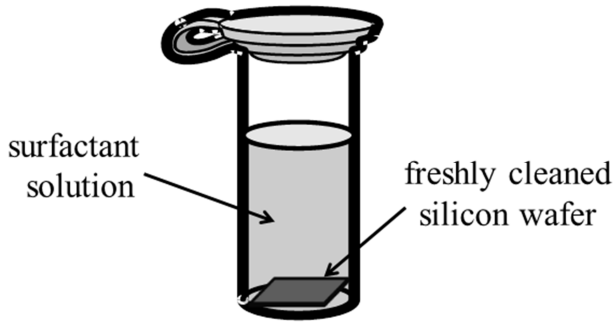

Figure 4.5. The experimental set-up of the reaction vessel used to deposit SAMs from solution on clean silicon wafer.

After this time, samples were withdrawn from the solutions, rinsed with toluene, dichloromethane and DI water, and placed in a desiccator. In order to remove larger polymerised aggregates that were physically adsorbed on the substrates, the samples were sonicated sequentially in toluene, dichloromethane and DI water for 15 min each.

It should be noted that solutions of surfactant precursors had to be freshly prepared. If they were not clear and transparent or some white flakes were observed, they were not used for the deposition process. Precipitation or even a haziness are good indicators that there is too much water in the environment. Silanes start to polymerise, and using such solutions would result in the formation of a nonhomogeneous film.

4.3.2. Results and Discussion

In this study five SAM coatings on silicon/silicon oxide substrate were successfully prepared from the liquid phase. The self-assembling molecules contained two different terminal groups: methyl group (-CH_3) **1d** and **1e**, and vinyl group (-$CH{=}CH_2$) **1a**, **1b** and **1c**, four different spacer lengths [ten (**1a**, **1d**), eleven (**1b**), fifteen (**1c**) and eighteen (**1e**) carbons in alkyl chain], and one active head group (-$SiCl_3$). **Figure 4.6** summarises the surfactants used for the formation of SAMs.

n = 7 **1a**, n = 8 **1b**, n = 12 **1c** n = 7 **1d**, n = 15 **1e**

Figure 4.6. Self-assembling molecules used in the deposition process.

4.3.2.1. Ellipsometry

The results of the ellipsometry measurements, together with the calculated thickness values of the analogues of the saturated trichlorosilanes[11] **1a**-**1e** are listed in **Table 4.1**.

Surfactant	Film Thickness [Å]				
	C_{10}-vinyl 1a	**C_{11}-vinyl 1b**	**C_{15}-vinyl 1c**	**C_{10}-methyl 1d**	**C_{18}-methyl 1e**
Theoretical[11]	16.1	17.4	22.4	16.1	26.2
Experimental	13.9±0.4	15.1±0.2	18.6±0.1	14.9±0.3	25.9±0.1

Table 4.1. Calculated thicknesses of the saturated trichlorosilane analogues and measured thickness values from ellipsometry.

The theoretical lengths of saturated trichlorosilane molecules were calculated according to **Equation 4.1** proposed by Wasserman *et al.*[11]

$$L = 1.26n + 4.78 \qquad \textbf{Equation 4.1.}$$

where L is the length (Å) of a methyl-terminated monolayer containing n methylene units.

As a model, that study[11] used a saturated hydrocarbon monolayer oriented nearly perpendicular to the surface with a *n*-alkyl chain in all-*trans* conformation. The coefficient 1.26 represents the C-C bond length in the *trans* projection to the surface normal, while the value of 4.78 includes projections of a C-Si bond, Si-O bond and a methyl terminal group.

All film thicknesses obtained with ellipsometry are consistent with monolayer films and are in a good agreement with the literature.[11] The experimental thicknesses measured for methyl-terminated surfactants **1d** and **1e** are close to both theoretical and experimental values reported.[37] The measured thicknesses of the vinyl-terminated films are slightly lower than the theoretical values for saturated films. A small difference in thickness might be due to differences in the conformation of the vinyl- and methyl- terminal group, which might influence the overall packing density in the films.[19]

4.3.2.2. X-ray Photoelectron Spectroscopy

The XPS spectra of all of the samples prepared in this study showed the presence of Si (2s 150.4 eV, 2p 99.2 eV), C (1s 284.6 eV) and O (1s 533.0 eV) as expected. Typical examples of SAMs prepared from vinyl-terminated silanes **1a-1c** are shown in **Figure 4.7**.

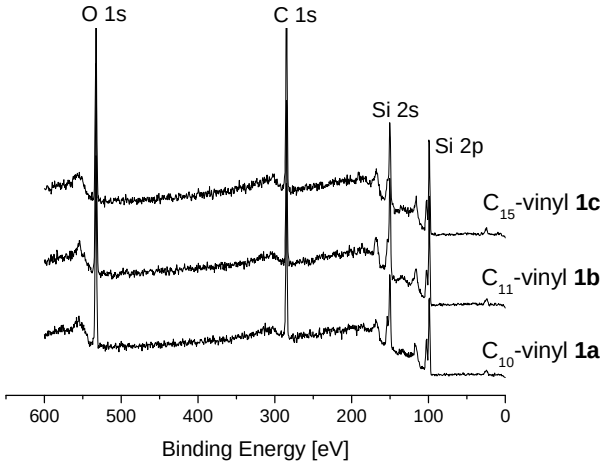

Figure 4.7. The XPS survey scans of vinyl-terminated SAMs (**1a-1c**) prepared by liquid phase deposition.

There were no unexpected elements detected in the films or any sign of unreacted silane (no Cl signal was observed). The C 1s peak intensity increased with increasing alkyl chain length, as expected. There is a possibility of small amounts of hydrocarbon

contamination. The signal of such species would contribute to the aliphatic carbon peak. The data obtained from XPS analysis was consistent with monolayer films.

The elemental composition of each film was taken from high resolution scans. Examples of single region scans of the C 1s peak of one vinyl- and one methyl- terminated film are compared in **Figure 4.8**.

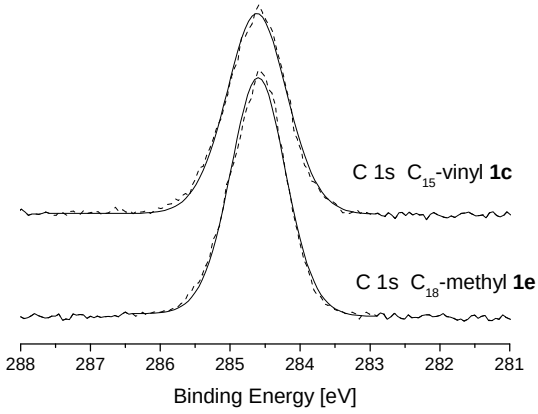

Figure 4.8. XPS C 1s elemental scans of a methyl-terminated (bottom) and vinyl-terminated (top) SAMs of **1c** and **1e**. Dash lines are experimental data, solid lines are fitted curves.

There was no obvious difference in the aliphatic C 1s region between the CH_3- and CH_2=CH- terminal SAMs. In a few cases, the peaks of vinyl-terminated films showed a slight asymmetry towards higher binding energies, which might be explained by the presence of a C=C double bond. According to the literature,[38] the energy difference between the methyl and vinyl C 1s signal should be very small, *i.e.* ~0.4 eV. However, in our films there was only one double bond per self-assembling molecule, for this reason the signal assigned to the double bond was not expected to be detected. The observed asymmetry was very small, therefore no attempt was made to fit the C 1s signal with two peaks. Instead, in such cases, the C 1s signal of the vinyl-terminated films was fitted with a single, broader peak.[19]

The film thickness/density of molecules **1a**, **1b** and **1c** was evaluated from the measured ratio of the C 1s signal to the Si 2p (oxide/bulk) signal based on the film thicknesses of well-known methyl-terminated monolayer films of decyltrichlorosilane (C_{10}) and octadecanetrichlorosilane (C_{18}).[11, 39] The oxide layer was assumed to be identical for all samples studied. Following the procedure described by Herrwerth and co-workers,[40] the C1s/Si2p ratio was measured for SAMs prepared from **1d** and **1e** molecules, and it was

found to be 0.67 and 1.52, respectively.[41] The dependence of C1s/Si2p on the effective molecular chain length can be represented by **Equation 4.2**:[40]

$$\ln\left(\frac{C1s}{Si2p}\right) = 0.081 \times (\textit{effective molecular chain length}) - 1.702 \qquad \textbf{Equation 4.2.}$$

This equation was then used to determine the effective molecular length values of the synthesised molecules. **Table 4.2** summarises all of the results. The thicknesses obtained from ellipsometry are shown for comparison.

Surfactant	**C_{10}-vinyl 1a**	**C_{11}-vinyl 1b**	**C_{15}-vinyl 1c**
C1s/Si2p ratio	0.54	0.68	1.05
Effective molecular length [Å]	13.4	16.3	21.6
Film thickness [Å] (ellipsometry)	13.9±0.4	15.1±0.2	18.6±0.1

Table 4.2. XPS atomic ratios of C1s/Si2p, experimentally determined effective molecular lengths and thicknesses measured by ellipsometry of SAMs derived from **1a-1c**.

The values of thicknesses obtained from XPS are similar to those determined by ellipsometry. All of the results indicate monolayer films. The values based on XPS have an uncertainty of ~2 Å. This is partially due to the low number of available methyl-terminated reference samples of different lengths used for the determination of the thickness depending on the ratio of the C 1s to the Si 2p signal[11] and the large error in the calibration of the thickness associated with it. There is also a small error in the peak areas that is based on the XPS fits. However, the thickness values determined from XPS are within a couple of Angstroms of the values obtained with ellipsometry and support monolayer films.[19]

4.3.2.3. Contact angle

The vinyl-terminated SAMs derived from **1a**, **1b**, and **1c** showed water contact angles of 101°, 101° and 103°, respectively. The measured values for the methyl-terminated SAMs of **1d** and **1e** were 107° and 109°, respectively. The experimental and literature values are shown in **Table 4.3**. It should be noted that the reported contact angles were measured directly after placing drops of water onto modified silicon samples.

Surfactant	**Water Contact Angle[°]**				
	C_{10}-vinyl 1a	**C_{11}-vinyl 1b**	**C_{15}-vinyl 1c**	**C_{10}-methyl 1d**	**C_{18}-methyl 1e**
Liquid phase deposition	101±1	101 ±1	103±1	107±1	109±1
Literature	101[a]	101[42]	105[b]	106[43]	109[44, 45]

Table 4.3. The experimental and theoretical water contact angle values obtained from the liquid phase process. [a]The water contact angle of 10-undecenyltrichlorosilane[42] and [b] the water contact angle of 15-hexadecenyltrichlorosilane[46] are used as reference because there are no literature values for **1a** and **1c**.

The water contact angle values of methyl-terminated films prepared as a reference from toluene were consistent with well-defined and ordered films. Literature values for such films prepared from solution are around 110°.[23, 43, 47, 48] The values measured for the vinyl-terminated films were lower than those for the methyl-terminated SAMs. This was expected because of the slightly more polar terminal -CH=CH_2 group instead of a -CH_3 group. The results are consistent with values of ~100° reported for similar films.[25, 47, 49]

4.3.2.4. Atomic Force Microscopy

Atomic Force Microscopy was used to determine the quality of the deposited coatings, *i.e.* to determine if aggregations were present on the coated surfaces. A typical AFM result of a SAM derived from CH_2=CH-$(CH_2)_8$-$SiCl_3$ **1a** prepared from solution is shown in **Figure 4.9**.

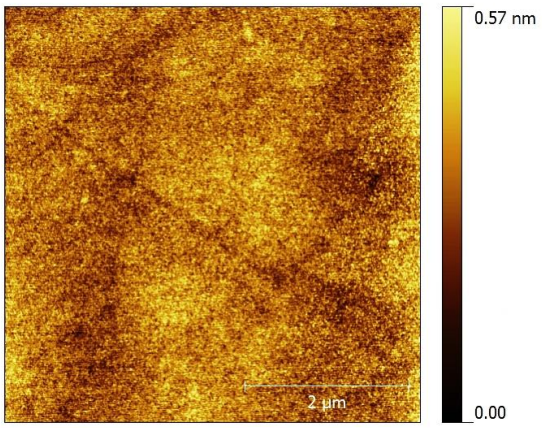

Figure 4.9. AFM images of 5 µm × 5 µm area of C_{10}-vinyl **1a** SAM, RMS 53 pm.

This AFM image (**Figure 4.9**) shows a very smooth surface with a root mean square (RMS) value of ~53 pm averaged over an area of 5 µm × 5 µm for the solution phase deposited film of **1a**. All recorded AFM images showed similarly smooth surfaces with roughness RMS values in the range of 53-99 pm for all films studied. For comparison, clean SiO_x substrates typically displayed RMS values of ~70 pm. Similar values were reported in the literature.[50] The contact angle results, in connection with the results obtained by the other surface analytical techniques, underline the presence of similarly densely packed and homogeneous monolayer films.

4.4. Preparation of alkyl- and alkenyl- trichlorosilanes monolayers in the vapour phase

Vapour phase deposition of self-assembled monolayers is not a common method of preparing SAMs on a small scale. However, on a larger industrial scale, this process is convenient because it eliminates many of the quality control problems encountered in solution deposition process.[51]

4.4.1. Deposition process

The freshly cleaned silicon wafers were placed in a Schott Duran^{TM} bottle (100 mL capacity) containing a small glass vessel. The deposition process was performed by placing ~0.1 mL of the trichlorosilane precursor in the open vessel (**Figure 4.10**). There was no direct contact between the liquid surfactant and the substrate during preparation. The liquid was still present in the vessel after the reaction.

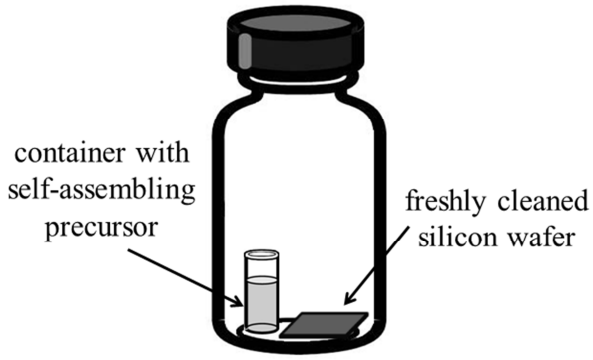

Figure 4.10. The experimental set-up of the reaction vessel used to deposit SAMs on a clean silicon wafer from the vapour phase under atmospheric pressure.

The SAM formation process was performed in one of two ways: 1) the air from the flask was evacuated using a vacuum pump for a few seconds (the pressure measured directly at the vacuum pump inlet was ~4 mbar) before the reaction had begun, 2) at atmospheric pressure (with air inside). Each of the reactions was left for 4 days at 60 °C in the case of the shorter molecules **1a**, **1b**, and **1d**, and for 3 days at 70 °C in the case of the longer molecules **1c** and **1e**. After the deposition process, the substrates were treated identically to those prepared from solution.

4.4.2. Results and Discussion

The trichlorosilane self-assembling molecules used in the deposition process are shown in **Figure 4.1**. The commercially available methyl-terminated surfactants **1d** and **1e**, were used as standards to optimise the deposition conditions. Some of the tested parameters as well as averaged results are shown in **Table 4.4**. Each film was prepared at least twice under each of the preparation conditions.

Surfactant Molecule	Deposition Temperature	Deposition Time	Film Thickness [Å]		Film Contact Angle [°]	
			Reduced Pressure	Atmospheric Pressure	Reduced Pressure	Atmospheric Pressure
C_{18}-methyl **1e**	70 °C	1 day	<10	<10	~55	~55
C_{10}-methyl **1d**	70 °C	1 day	<10	<10	~55	~55
C_{10}-methyl **1d**	70 °C	2 days	10.1±0.2	11.3±0.2	73±1	74±1
C_{10}-vinyl **1a**	70 °C	2 days	12.2±0.2	9.5±0.3	93±1	69±1
C_{11}-vinyl **1b**	70 °C	2 days	11.6±0.1	10.4±0.1	89±1	71±1
C_{15}-vinyl **1c**	70 °C	2 days	14.3±0.1	15.7±0.2	74±1	93±1
C_{18}-methyl **1e**	70 °C	2 days	17.4±0.1	18.6±0.1	95±1	95±1
C_{18}-methyl **1e**	60 °C	3 days	22.2±0.1	21.0±0.1	104±1	104±1
C_{15}-vinyl **1c**	60 °C	3 days	16.3±0.1	15.2±0.2	97±1	97±1
C_{18}-methyl **1e**	70 °C	3 days	26.4±0.1	26.9±0.1	109±1	109±1
C_{15}-vinyl **1c**	70 °C	3 days	19.3±0.1	17.8±0.1	103±1	103±1
C_{10}-vinyl **1a**	70 °C	3 days	19.1±0.3	22.7± 0.3	101±1	101±1
C_{11}-vinyl **1b**	70 °C	3 days	20.5±0.2	19.2±0.1	101±1	101±1
C_{10}-methyl **1d**	70 °C	3 days	20.7±0.1	21.3±0.1	107±1	107±1
C_{10}-vinyl **1a**	60 °C	4 days	13.1±0.2	14.5±0.3	101±1	101±1
C_{11}-vinyl **1b**	60 °C	4 days	14.7±0.1	15.3±0.2	101±1	101±1
C_{10}-methyl **1d**	60 °C	4 days	15.6±0.3	13.5±0.3	107±1	107±1
C_{18}-methyl **1e**	60 °C	3 days	20.1±0.1	19.1±0.1	106±1	106±1
C_{15}-vinyl **1c**	60 °C	3 days	16.2±0.2	17.4±0.3	100±1	100±1
C_{10}-vinyl **1a**	50 °C	4 days	9.1±0.4	11.3±0.2	98±1	99±1
C_{11}-vinyl **1b**	50 °C	4 days	12.4±0.2	10.2±0.2	100±1	99±1
C_{10}-methyl **1d**	50 °C	4 days	10.2±0.1	11.1±0.1	102±1	102±1
C_{18}-methyl **1e**	50 °C	4 days	16.6±0.1	15.6±0.1	96±1	95±1
C_{15}-vinyl **1c**	50 °C	4 days	14.8±0.2	13.6±0.3	93±1	93±1
C_{18}-methyl **1e**	70 °C	4 days	35.7±0.2	38.4±0.4	109±1	109±1
C_{18}-methyl **1e**	70 °C	6 days	>50	>50	109±1	109±1
C_{10}-methyl **1d**	60 °C	5 days	20.1±0.2	22.3±0.1	107±1	107±1
C_{10}-methyl **1d**	60 °C	6 days	26.4±0.4	27.8±0.3	107±1	107±1

Table 4.4. Examples of tested parameters used for preparation SAMs from the vapour phase.

4.4.2.1. Ellipsometry

The best results obtained for the SAMs prepared from **1a**-**1e**, are shown in **Table 4.5**. The thicknesses obtained from liquid phase deposition are also shown, for comparison.

Surfactant	Film Thickness [Å]				
	C_{10}-vinyl **1a**	C_{11}-vinyl **1b**	C_{15}-vinyl **1c**	C_{10}-methyl **1d**	C_{18}-methyl **1e**
Vapour phase (reduced pressure)	13.1±0.2	14.7±0.1	19.3±0.1	15.6±0.3	26.4±0.1
Vapour phase (atmospheric pressure)	14.5±0.3	15.3±0.2	17.8±0.2	13.5±0.2	26.9±0.1
Liquid phase	13.9±0.4	15.1±0.2	18.6±0.1	14.9±0.3	25.9±0.1

Table 4.5. Ellipsometry values obtained for liquid and vapour phase deposition under reduced and atmospheric pressure.

The thickness values obtained by the vapour phase process are consistent with monolayer films and are close to the values obtained by liquid phase deposition. The film thickness depends on the deposition conditions: temperature and reaction time. The deposition procedure described by Fadeev and co-workers[43] was used as a starting point in our research. The vapour phase reactions of surfactants **1a**-**1e** were performed for 3 days at 70 °C. This procedure gave thin and homogenous films formed from the longer molecules **1c** and **1e**. Under these conditions, SAMs prepared from shorter surfactants **1a**, **1b** and **1d** showed polymeric aggregates, which were observed as a cloudiness on the surface of silicon. These aggregates were still present even after rinsing and sonication, resulting in thick films (more than a monolayer). This was confirmed by higher values obtained from ellipsometry measurements (~20 Å). Lowering the temperature to 60 °C and increasing the reaction time to 4 days produced films of the reported thicknesses (**Table 4.5**). The depositions were also carried out at lower temperatures *e.g.* 50 °C for 4 days (**Table 4.4**). The measured thicknesses were around ~10 Å (in case of shorter surfactants) and ~15 Å (in case of longer surfactants), suggesting the formation of incomplete films. The vapour phase deposition process was not tested at temperatures above 70 °C, because optimal films had been achieved.

The same tendency was observed when the reaction was performed for different time periods, *i.e.* the thicknesses obtained from samples prepared for less than 3 days (**Table 4.4**) were lower than a monolayer film (suggesting that the molecules were disordered due to low packing density). The values of thicknesses obtained for molecules **1a**, **1b** and **1d** were ~10 Å. In case of a longer molecule, **1c**, it was ~15 Å, and **1e** was ~18 Å. Films prepared for longer than 4 days, exhibited thicknesses greater than a monolayer. For example the deposition of **1e** for 4 days resulted in a film thickness of ~35 Å. This value did not change even when additional cleaning was applied.

4.4.2.2. X-ray Photoelectron Spectroscopy

The results obtained from X-ray photoelectron spectroscopy of samples prepared in the vapour phase showed the presence of silicon, carbon and oxygen as expected. The chemical composition, positions of peaks as well as the absence of Cl 2p signal, were consistent with those results obtained from films prepared by liquid deposition.

The density/thickness of the films was determined in the same manner as described in section 4.3.2.2. All of the samples were measured under the same conditions, therefore the results obtained from the methyl-terminated reference samples in the liquid phase were used as standards to determine the density of films prepared in the vapour phase. The values obtained according to **Equation 4.2**, are shown in **Table 4.6**. The thicknesses obtained from ellipsometry are shown for comparison.

	Vapour phase deposition (atmospheric pressure)			Vapour phase deposition (reduced pressure)		
Surfactant	**C_{10}-vinyl 1a**	**C_{11}-vinyl 1b**	**C_{15}-vinyl 1c**	**C_{10}-vinyl 1a**	**C_{11}-vinyl 1b**	**C_{15}-vinyl 1c**
C1s/Si2p ratio	0.70	0.76	0.93	0.63	0.69	0.88
Effective molecular length [Å]	16.6	17.6	20.1	15.3	16.4	19.4
Film thickness [Å] (ellipsometry)	14.5±0.3	15.3±0.2	17.8±0.1	13.1±0.2	14.7±0.1	19.3±0.1

Table 4.6. XPS atomic ratios of C1s/Si2p, experimentally determined effective molecular lengths of the films prepared in the vapour phase under reduced and atmospheric pressure, and thickness (measured by ellipsometry) of surfactants molecules **1a-1c**.

The thickness values obtained from XPS are in good agreement with results obtained from ellipsometry measurements. All results indicate monolayer films, but the values based on XPS are slightly higher than those from ellipsometry. This tendency was also observed in the case of the liquid phase results. The higher density can be explained by a small amount of organic contamination on the surface during the measurements. All of the XPS results were obtained either at the University of Edinburgh or at the University of Newcastle (NEXUS at nanoLAB), thus it is difficult to define the exact time for which the samples were exposed to air before the actual measurements were carried out. This may explain the small variations in film thicknesses.

4.4.2.3. Contact angle

The water contact angle values obtained from the vinyl- and methyl- terminated SAMs prepared by both the vapour phase process under atmospheric and reduced pressure are summarised in **Table 4.7**. The contact angle values measured after liquid phase deposition are shown for comparison.

Surfactant	**Water Contact Angle [°]**				
	C_{10}-vinyl 1a	**C_{11}-vinyl 1b**	**C_{15}-vinyl 1c**	**C_{10}-methyl 1d**	**C_{18}-methyl 1e**
Vapour phase (reduced pressure)	101±1	101±1	103±1	107±1	109±1
Vapour phase (atmospheric pressure)	101±1	101±1	103±1	107±1	109±1
Liquid phase	101±1	101±1	103±1	107±1	109±1

Table 4.7. The water contact angle obtained from SAMs prepared in the liquid phase process and the vapour phase process under reduced and atmospheric pressure.

The water contact angle values are independent of the preparation method, *i.e.* samples prepared from solution or vapour phase and under different pressures gave identical values for films from the same surfactant. These results indicate the formation of uniform and hydrophobic films.

The water contact angle measurements were extensively used to monitor the progress of monolayer formation. Contact angle values were recorded for all films

deposited under different conditions. The results were used to find the best deposition parameters. Contact angle values in the range of 55-95° were obtained for reaction periods of less than 3 days (**Table 4.4**). Lower contact angles were also observed when the deposition was performed at 50 °C for 4 days. These values were too low for densely packed films and it was concluded that incomplete coatings were produced. These results are consistent with the ellipsometry data. However, the water contact angle values cannot be used to determine the difference between mono- and multi-layer films, because the observed values will also be influenced by the methyl- and vinyl- groups on the surface, independent of the film thickness.

4.4.2.4. Atomic Force Microscopy

Atomic Force Microscopy was used to define the homogeneity and smoothness of the deposited coatings. The AFM image of a SAM derived from C_{10}-vinyl **1a**, and prepared by vapour phase deposition, is shown in **Figure 4.11**.

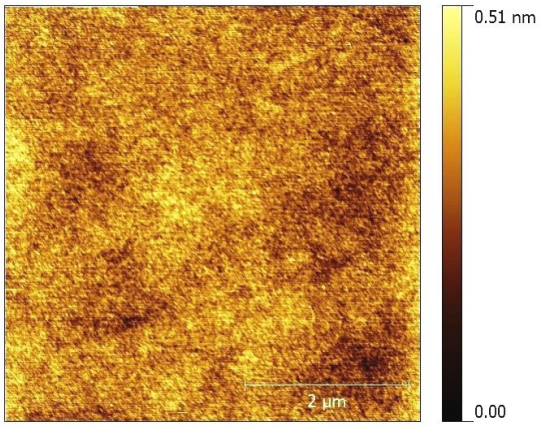

Figure 4.11. AFM images of 5 µm × 5 µm area of C_{10}-vinyl **1a** SAM, RMS 62 pm.

The results obtained from AFM analysis of all surfactants deposited from the vapour phase were consistent with the image in **Figure 4.11**. Also similar AFM data were obtained from samples prepared by liquid phase deposition. There were no aggregations or defects observed by AFM on all of the SAM coatings. The resultant films show very smooth and homogenous surfaces with root mean square (RMS) values not higher than 100 pm. The RMS values of the monolayer films were similar to those found for clean SiO_x substrates indicating that the monolayers produce extremely smooth surfaces. The measured RMS values of the methyl-terminated layers are in good agreement with

those reported for similar films,[39, 52] supporting densely packed monolayers for both preparation methods. However, wafers with many aggregations were also produced when different deposition parameters were tested, which is consistent with data obtained from ellipsometry measurements. An example of an AFM image taken from a thick film, formed from C_{18}-methyl **1e** is shown in **Figure 4.12**. The measured RMS value of 580 pm in the case of this film is much higher than reported values of smooth and homogenous films. Many defects and excess material are clearly observed. Similar results were obtained in case of all trichlorosilane molecules tested. This quality of film is not sufficient for our work, because the SAMs should be used in the next step for a chemical modification. Defects can potentially reduce the reactivity of the terminal functional groups of SAMs by changing *e.g.* conformation or packing of molecules in the film, resulting in a lower availability of these groups for chemical reaction.

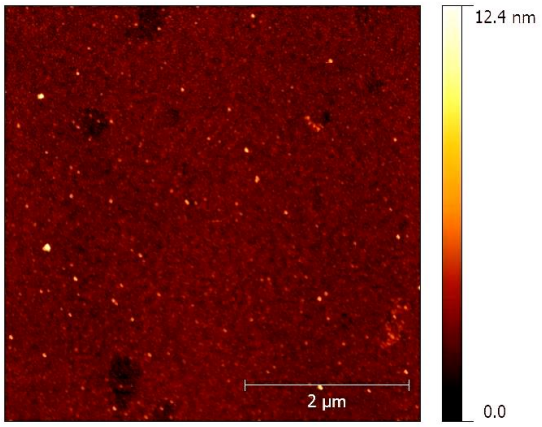

Figure 4.12. AFM images of 5 µm × 5 µm area of C_{18}-methyl **1e** SAM prepared in the vapour phase under atmospheric pressure, RMS 580 pm.

It should be noted that the overall quality of the vapour phase derived films depends on the preparation conditions. It is necessary to limit the amount of water present in the system to avoid the formation of polymeric aggregates on the surface.[31, 39] However, the surface of the silicon/silicon dioxide substrate cannot be completely anhydrous, and a thin film of surface-condensed water may in fact be beneficial for the formation of the monolayer as suggested previously.[31, 53] Reactions in the gas phase between surfactant molecules and the substrate are more likely to occur under higher temperature. The amount of water present in the gas phase is almost independent of the temperature since the experiments were performed in a sealed container with no water reservoir. This is supported by the fact that the films obtained under atmospheric and reduced pressure

conditions were of identical quality at the same temperatures.[19] A similar observation has been reported for methyl-terminated trichlorosilanes of different alkane chain lengths deposited from the vapour phase.[43] In that study films of saturated trichorosilanes were prepared under identical conditions. This resulted in films of a monolayer for the longer self-assembling molecules but more than a monolayer for shorter surfactants.[43]

High quality monolayers were only obtained from the vapour phase if the reaction was left running for a sufficiently long time. The formation of films was not completed when the deposition was shorter than 3 days. The samples showed low contact angles (55-95°) as well as low thicknesses. The thicknesses were smaller than the length of a single surfactant molecule indicating that SAM formation was not finished. However, when the reaction was run for longer than 3 or 4 days (depending on the surfactant used), the silicon surface was covered with an excess of material. This was shown by white spots and a cloudiness across the whole modified surface. Therefore, it was concluded that shorter reaction time was optimal.

4.5. Conclusions

From this work we can conclude that there are a few crucial steps required to obtain high quality ultrathin films on SiO_x/Si substrate. Firstly, a silicon wafer cannot be used in the deposition process without strict purification. Untreated wafers showed a significant amount of contamination, which was confirmed by the water contact angle and X-ray photoelectron spectroscopy analysis. The combination of strongly oxidising solutions, as well as an ozone atmosphere, allowed substrates to be obtained with satisfactory purity. Secondly, to reproduce a high quality SAM, the preparation procedure needs to be optimised. In this study silicon wafers were successfully modified with vinyl- and methyl-terminated trichlorosilanes from both liquid and vapour phases. All films prepared as described in this Chapter looked smooth by eye inspection. The AFM results confirmed smooth and homogeneous surfaces. The thickness values of the prepared SAMs obtained from ellipsometry measurements indicated formation of monolayer films. Only three elements were observed by X-ray photoelectron spectroscopy: silicon, carbon and oxygen. The XPS analysis allowed the thicknesses of the SAMs to be calculated, using methyl-terminated films as references. These results were in good agreement with the ellipsometry data, supporting the formation of monolayer films. Finally, water contact angle

measurements indicated hydrophobic films in all cases. All of measured values were in the range of 101-109°.

The combined results of the different surface analytical characterisation techniques clearly indicate that densely packed, smooth and homogeneous monolayer films were achieved for all of the surfactants studied. Since the hydrophobicity, homogeneity, film thickness, and density of the films prepared from the vapour phase were similar to those obtained for films prepared from solution, it is concluded that the number of vinyl groups exposed and the surface chemistry of the films was also similar. The films prepared from the vapour phase therefore have potential for further modification and could be of interest in connection with silicon oxide microstructures where the preparation of such SAMs from solution is not an option.

4.6. Literature

1. S. Onclin, B. J. Ravoo and D. N. Reinhoudt, *Angew. Chem., Int. Ed.*, 2005, **44**, 6282-6304.
2. W. R. Ashurst, C. Carraro and R. Maboudian, *IEEE Trans. Device Mater. Reliab.*, 2003, **3**, 173-178.
3. W. M. Van Spengen, R. Puers and I. De Wolf, *J. Adhesion Sci. Technol.*, 2003, **17**, 563-582.
4. R. Maboudian, W. R. Ashurst and C. Carraro, *Tribol. Lett.*, 2002, **12**, 95-100.
5. Y. X. Zhuang, O. Hansen, T. Knieling, C. Wang, P. Rombach, W. Lang, W. Benecke, M. Kehlenbeck and J. Koblitz, *J. Micromech. Microeng.*, 2006, **16**, 2259-2264.
6. B. Dorvel, B. Reddy, I. Block, P. Mathias, S. E. Clare, B. Cunningham, D. E. Bergstrom and R. Bashir, *Adv. Funct. Mater.*, 2010, **20**, 87-95.
7. T. Koga, M. Morita, H. Ishida, H. Yakabe, S. Sasaki, O. Sakata, H. Otsuka and A. Takahara, *Langmuir*, 2005, **21**, 905-910.
8. Y. X. Zhuang, O. Hansen, T. Knieling, C. Wang, P. Rombach, W. Lang, W. Benecke, M. Kehlenbeck and J. Koblitz, *J. Microelectromech. Syst.*, 2007, **16**, 1451-1460.
9. T. M. Mayer, M. P. de Boer, N. D. Shinn, P. J. Clews and T. A. Michalske, *J. Vac. Sci. Technol. B*, 2000, **18**, 2433-2440.
10. Y. Ito, A. A. Virkar, S. Mannsfeld, J. H. Oh, M. Toney, J. Locklin and Z. A. Bao, *J. Am. Chem. Soc.*, 2009, **131**, 9396-9404.
11. S. R. Wasserman, Y. T. Tao and G. M. Whitesides, *Langmuir*, 1989, **5**, 1074-1087.
12. D. J. Macquarrie and S. E. Fairfield, *J. Mater. Chem.*, 1997, **7**, 2201-2204.
13. N. Herzer, S. Hoeppener and U. S. Schubert, *Chem. Commun.*, 2010, **46**, 5634-5652.
14. J. K. Lee, K. B. Lee, D. J. Kim and I. S. Choi, *Langmuir*, 2003, **19**, 8141-8143.
15. S. Dutta, M. Perring, S. Barrett, M. Mitchell, P. J. A. Kenis and N. B. Bowden, *Langmuir*, 2006, **22**, 2146-2155.
16. W. Kern, *J. Electrochem. Soc.*, 1990, **137**, 1887-1892.
17. D. A. Hook, J. A. Olhausen, J. Krim and M. T. Dugger, *Microelectromechanical Systems, Journal of*, 2010, **19**, 1292-1298.
18. J. B. Brzoska, I. Benazouz and F. Rondelez, *Langmuir*, 1994, **10**, 4367-4373.
19. M. Adamkiewicz, T. O'Hara, D. O'Hagan and G. Hähner, *Thin Solid Films*, 2012, **520**, 6719-6723.
20. A. Ermolieff, S. Marthon, X. Rochet, D. Rouchon, O. Renault, A. Michallet and F. Tardif, *Surf. Interface Anal.*, 2002, **33**, 433-436.
21. D. K. Aswal, S. Lenfant, D. Guerin, J. V. Yakhmi and D. Vuillaume, *Anal. Chim. Acta*, 2006, **568**, 84-108.
22. S. Petitdidier, V. Bertagna, N. Rochat, D. Rouchon, P. Besson, R. Erre and M. Chemla, *Thin Solid Films*, 2005, **476**, 51-58.
23. B. D. Booth, S. G. Vilt, C. McCabe and G. K. Jennings, *Langmuir*, 2009, **25**, 9995-10001.
24. K. Choi, S. Ghosh, J. Lim and C. M. Lee, *Appl. Surf. Sci.*, 2003, **206**, 355-364.
25. D. Janssen, R. De Palma, S. Verlaak, P. Heremans and W. Dehaen, *Thin Solid Films*, 2006, **515**, 1433-1438.
26. R. Maboudian, *Surf. Sci. Rep.*, 1998, **30**, 209-268.
27. J. M. Delarios, C. R. Helms, D. B. Kao and B. E. Deal, *Appl. Surf. Sci.*, 1987, **30**, 17-24.

28. D. K. Schwartz, *Annu. Rev. Phys. Chem.*, 2001, **52**, 107-137.
29. P. Silberzan, L. Leger, D. Ausserre and J. J. Benattar, *Langmuir*, 1991, **7**, 1647-1651.
30. C. P. Tripp and M. L. Hair, *Langmuir*, 1992, **8**, 1120-1126.
31. D. L. Angst and G. W. Simmons, *Langmuir*, 1991, **7**, 2236-2242.
32. J. B. Brzoska, N. Shahidzadeh and F. Rondelez, *Nature*, 1992, **360**, 719-721.
33. T. Vallant, H. Brunner, U. Mayer, H. Hoffmann, T. Leitner, R. Resch and G. Friedbacher, *J. Phys. Chem. B*, 1998, **102**, 7190-7197.
34. A. N. Parikh, D. L. Allara, I. B. Azouz and F. Rondelez, *J. Phys. Chem.*, 1994, **98**, 7577-7590.
35. C. Carraro, O. W. Yauw, M. M. Sung and R. Maboudian, *J. Phys. Chem. B*, 1998, **102**, 4441-4445.
36. Y.-a. Cheng, B. Zheng, P.-h. Chuang and S. Hsieh, *Langmuir*, 2010, **26**, 8256-8261.
37. N. Tillman, A. Ulman, J. S. Schildkraut and T. L. Penner, *J. Am. Chem. Soc.*, 1988, **110**, 6136-6144.
38. F. Bournel, F. Jolly, F. Rochet, G. Dufour, F. Sirotti and P. Torelli, *Phys. Rev. B*, 2000, **62**, 7645-7653.
39. Y. L. Wang and M. Lieberman, *Langmuir*, 2003, **19**, 1159-1167.
40. S. Herrwerth, W. Eck, S. Reinhardt and M. Grunze, *J. Am. Chem. Soc.*, 2003, **125**, 9359-9366.
41. P. Harder, M. Grunze, R. Dahint, G. M. Whitesides and P. E. Laibinis, *J. Phys. Chem. B*, 1998, **102**, 426-436.
42. G. S. Ferguson, M. K. Chaudhury, H. A. Biebuyck and G. M. Whitesides, *Macromolecules*, 1993, **26**, 5870-5875.
43. A. Y. Fadeev and T. J. McCarthy, *Langmuir*, 2000, **16**, 7268-7274.
44. W. R. Ashurst, C. Yau, C. Carraro, C. Lee, G. J. Kluth, R. T. Howe and R. Maboudian, *Sens. Actuator A-Phys.*, 2001, **91**, 239-248.
45. S. A. Kulkarni, S. A. Mirji, A. B. Mandale and K. P. Vijayamohanan, *Thin Solid Films*, 2006, **496**, 420-425.
46. L. Netzer and J. Sagiv, *J. Am. Chem. Soc.*, 1983, **105**, 674-676.
47. N. Balachander and C. N. Sukenik, *Langmuir*, 1990, **6**, 1621-1627.
48. S. C. Clear and P. F. Nealey, *J. Colloid Interface Sci.*, 1999, **213**, 238-250.
49. J. P. Dong, A. F. Wang, K. Y. S. Ng and G. Z. Mao, *Thin Solid Films*, 2006, **515**, 2116-2122.
50. A. Crossley, C. J. Sofield, J. P. Goff, A. C. I. Lake, M. T. Hutchings and A. Menelle, *J. Non-Cryst. Solids*, 1995, **187**, 221-226.
51. C. A. E. Hamlett, K. Critchley, M. Gorzny, S. D. Evans, P. D. Prewett and J. A. Preece, *Surf. Sci.*, 2008, **602**, 2724-2733.
52. Y. A. Cheng, B. Zheng, P. H. Chuang and S. C. Hsieh, *Langmuir*, 2010, **26**, 8256-8261.
53. D. L. Allara, A. N. Parikh and F. Rondelez, *Langmuir*, 1995, **11**, 2357-2360.

5. Chemical Surface Modification *via* Carbene Chemistry in the Liquid Phase

Solid substrates can be functionalised by the adsorption of self-assembled monolayers, generated from appropriate organic molecules.[1] This method offers the possibility of tuning surface properties in a controllable fashion. This can be achieved in two ways. The direct approach allows pre-functionalised molecules to coat the substrate, either from the liquid phase or vapour phase. However, the reactivity of a terminal functional group, *e.g.* $RSiCl_3$ in the case of SiO_x/Si substrate, limits the introduction of some reactive end groups *e.g.* alcohols.[1, 2] The second approach can overcome this problem by performing a chemical reaction on a pre-coated surface. The latter offers a great flexibility for expanding the range of functionality on the surface.

The aim of this Chapter is to present a novel chemical reaction which was developed to functionalise vinyl-terminated SAMs. The SAM modification was examined by X-ray photoelectron spectroscopy, contact angle goniometry, atomic force microscopy and ellipsometry.

5.1. Proof of concept

In order to develop chemistry for the modification of vinyl-terminated SAMs, it was necessary to determine if the double bonds, present in the film, are accessible enough to undergo chemical reactions. A good method to verify the presence of double bonds is to modify SAMs by bromination.[3] Such a reaction has already been reported by Wasserman *et al.*,[4] and this became a control reaction in this study.

Bromination reaction on SAMs

Vinyl-terminated SAMs were soaked in a Br_2 solution (2 mM) in dichloromethane (3 mL), at room temperature for 2 h. After the reaction, the wafers were washed with toluene, dichloromethane and DI water. The reaction progress was monitored by XPS analysis, water contact angle measurements and ellipsometry.

The XPS survey scan and high resolution scan of the Br 3d region obtained after the bromination reaction are presented in **Figure 5.1**.

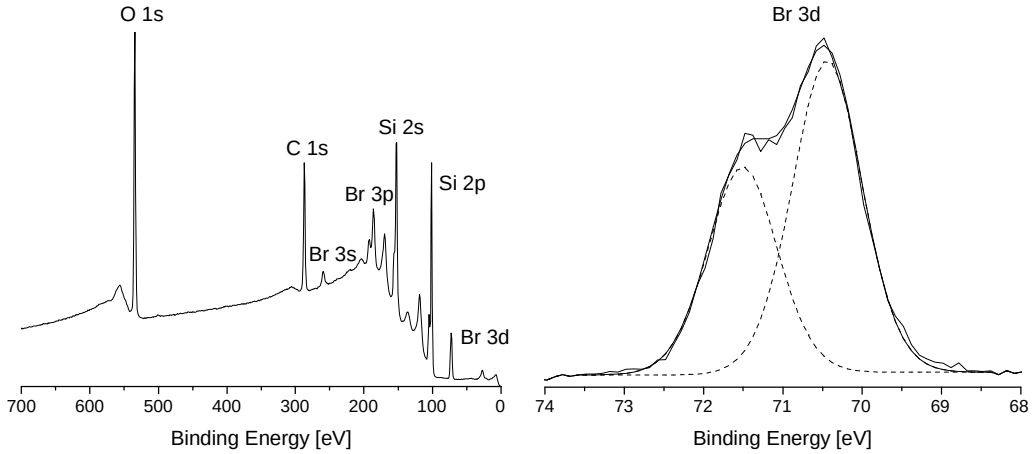

Figure 5.1. The XPS survey scan and Br 3d elemental scan of C_{11}-vinyl **1b** SAM film after the reaction with Br_2.

The XPS spectrum of the functionalised monolayer revealed three peaks, in addition to the expected Si, C and O signals. A strong peak at 71 eV was assigned to Br 3d and peaks at 190 eV and 258 eV were assigned to Br 3p and Br 3s, respectively.[5, 6] Moreover, an additional signal appeared in the C 1s region (**Figure 5.2,** fitting details are provided in Chapter 2, paragraph 2.1.1).

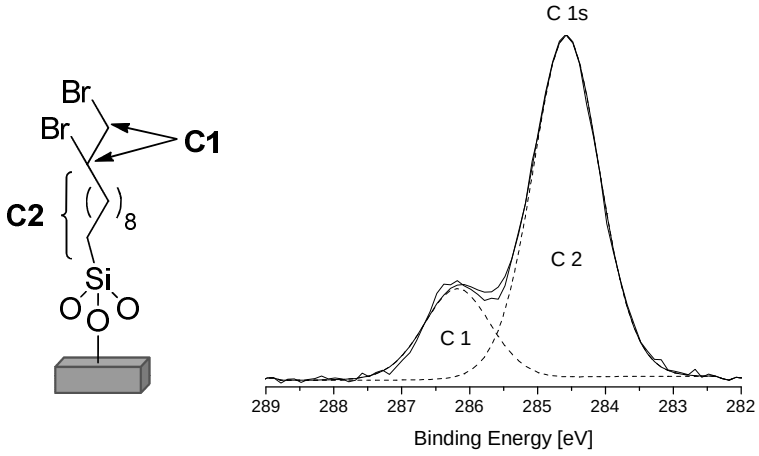

Figure 5.2. The C 1s high resolution scan obtained after the bromination reaction.

In the carbon region, two signals can be clearly distinguished. The less intensive peak, which is shifted towards higher binding energies was assigned as carbon C1 (286.3 eV),[7] which corresponds to carbons bonded directly to bromine. The more intensive peak C2, at a binding energy of 284.6 eV was assigned to the CH_2 carbons from the alkyl chains.[8, 9]

XPS analysis allows an approximate value of the conversion by comparing the intensities of the Br 3d and the C 1s signals. The measured experimental intensity (I_m) of

the C 1s signal is lower than the total C 1s intensity (*I*) based on the number of carbon atoms present, due to attenuation: the C 1s electrons created close to the substrate surface have to travel through the entire hydrocarbon film. Many of electrons lose energy due to collisions with neighbouring atoms and appear at apparently higher binding energies in the background signal, and do not contribute to the C 1s signal. This has to be taken into account when quantifying the amount of carbon that is present.

Without attenuation the C 1s intensity *I* would be simply proportional to the film thickness, *d*:

$$I = I_0 \cdot d \qquad \textbf{Equation 5.1}$$

where *I* is the C 1s intensity emitted from all atoms of the layer of thickness *d*, while I_0 is the intensity obtained from a film of unit thickness.

In order to include the attenuation, the Beer-Lambert law[10] needs to be taken into account (**Equation 5.2**):

$$I_e = I_0 \exp(-x/\lambda) \qquad \textbf{Equation 5.2}$$

where I_e is the intensity of electrons emitted from a single layer of carbon atoms at depth *x* detected normal to the surface, and λ is the mean free path of the electrons.[10] The electrons travelling from different depths experience different attenuations, therefore the total intensity emitted from a film of thickness *d* (and hence detected by the instrument) can be calculated by integrating eq. 5.2:

$$I_m = \int_0^d I_0 \exp\left(\frac{-x}{\lambda}\right) dx = I_0 \lambda \left[1 - \exp\left(\frac{-d}{\lambda}\right)\right] \qquad \textbf{Equation 5.3}$$

The measured intensity I_m has therefore to be corrected by the factor

$$\frac{d}{\lambda\left[1-\exp\left(\frac{-d}{\lambda}\right)\right]}$$

Based on the intensity of the Br 3d signal and the sum of the intensities of the C 1s signals without correction the bromination reaction yield is ~68%. Taking the attenuation

factor into account and assuming that the mean free path λ of the electrons of the film is λ = 3.5 nm,[11] the reaction yield of the C_{11}-vinyl **1b** film is ~59%.

The water contact angle of the starting vinyl-terminated film was 101°. After the bromination reaction, this value decreased to 80°, which is consistent with the literature.[4-6, 12] The film thickness measured before and after SAM exposure to Br_2 solution remained the same at ~15 Å.

The results obtained from these three independent techniques, clearly indicate formation of a Br-terminated monolayer without film degradation, which is in good agreement with data obtained by Wasserman *et al.*[4] The bromination reaction confirmed that films with terminal double bonds can be successfully modified and could be subject to different chemical reactions.

5.2. Carbene precursors

A carbene is a reactive intermediate with the chemical formula of $:CR_2$.[3] Carbene chemistry is a promising route to modify pre-coated silicon wafers. The reaction *via* a carbene intermediate leads to the formation of a new C-C bond and could be used to modify the surface of SAMs. However, such an application has never been reported, thus the reaction conditions, selectivity and SAMs stability require investigation.

In this work, three commercially available chemicals (chloroform $CHCl_3$, bromoform $CHBr_3$ and Ruppert-Prakash reagent $CF_3Si(CH_3)_2$) were used as carbene sources for chemical surface modification. From these molecules dichloro-, dibromo- and difluoro-carbenes ($:CCl_2$, $:CBr_2$, $:CF_2$, respectively) were generated in solution (**Scheme 5.1**). Halogenated carbenes were selected because they can introduce new elements, other than carbon onto the surface. These can be easily monitored *e.g.* by X-ray photoelectron spectroscopy providing information on the progress of conversion. Our experimental work also provided insight into the possible products formed during the reaction with carbenes.

In every experiment described in this Chapter, two vinyl-terminated SAM films (C_{11}-vinyl **1b** and C_{15}-vinyl **1c**) were reacted with carbenes and the methyl-terminated SAM (C_{18}-methyl **1e**) was used as reactive controls (**Scheme 5.1**).

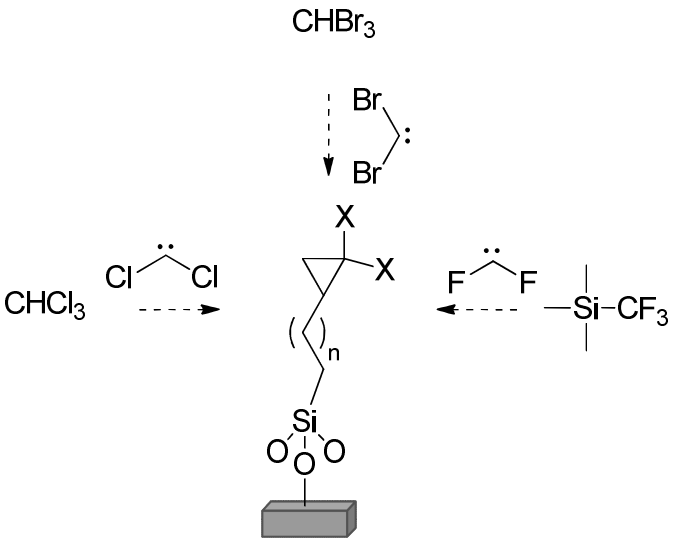

Scheme 5.1. Carbene precursors and possible products formed by reacting :CR_2 with vinyl-terminated SAMs in the liquid phase.

5.3. Chemistry on SAMs involving dichloro- and dibromo- carbene

In this reaction, chloroform was used to generate dichlorocarbene :CCl_2, while bromoform was used to generate dibromocarbene :CBr_2 (**Scheme 5.2**).[13]

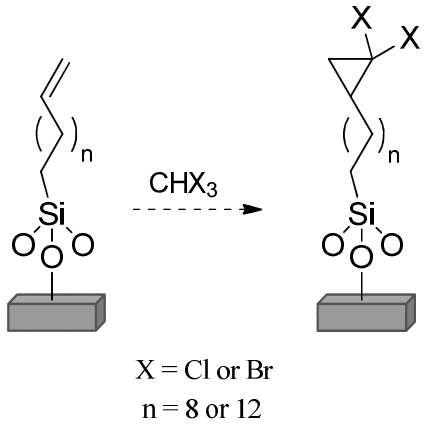

Scheme 5.2. Dichloro- and dibromo- carbene reaction on C_{11} **1b** and C_{15} **1c** vinyl-terminated SAMs. The expect product is a cyclopropane.

5.3.1. Chemistry and sources of :CCl_2 and :CBr_2

In 1954, Doering and Hoffmann[14] demonstrated the first addition of dichlorocarbene to olefins. They generated the carbene intermediate from chloroform using potassium *t*-butoxide in the presence of cyclohexene. The cyclopropane product, 7,7-dichlorobicyclo[4.1.0]heptane (**5.1**), was isolated in 59% yield. A similar reaction was performed with bromoform to give 7,7-dibromobicyclo[4.1.0]heptane (**5.2**) in 75% yield (**Scheme 5.3**).[14]

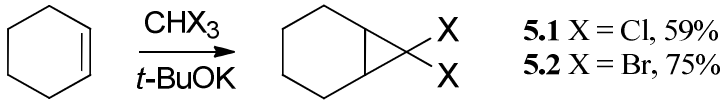

Scheme 5.3. Synthesis of 7,7-dichlorobicyclo[4.1.0]heptane (**5.1**) and 7,7-dibromobicyclo-[4.1.0]heptane (**5.2**).[14]

Parham and Schweizer[15] generated dichlorocarbene from ethyl trichloroacetate using sodium methoxide, sodium ethoxide or potassium *t*-butylate as a base, in either the presence or absence of solvent. Dichlorocyclopropanes were obtained in very good yields (72-88%) with all bases. Hexachloroacetone (**5.3**) can also be used as a source of dichlorocarbene.[16, 17] Moreover, from one mole of the reagent (**5.3**) two equivalents of :CCl_2 are formed (**Scheme 5.4**).

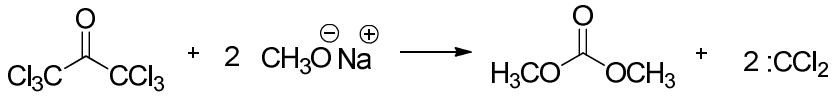

5.3

Scheme 5.4. Generation of dichlorocarbene from hexachloroacetone (**5.3**).[16, 17]

In 1962, Schollkopf and Hilbert[18] generated :CCl_2 from methyl trichloromethanesulfinate (**5.4**) in the presence of either potassium *t*-butoxide or sodium methoxide (**Scheme 5.5**). The highest yield, 48%, of 7,7-dichlorobicyclo[4.1.0]heptane (**5.1**) was obtained when the reaction was performed at 82 °C.

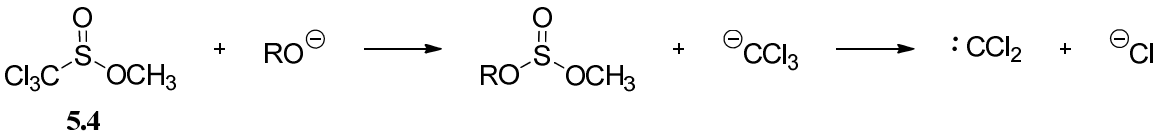

5.4

Scheme 5.5. Generation of :CCl_2 from methyl trichloromethanesulfinate (**5.4**) in the presence of strong base.[18]

In 1965, Seyferth *et al.*,[19] synthesised *gem*-dihalocyclopropanes (**5.6**) from phenyl(trihalomethyl)mercury (**5.5**) and an excess of cyclohexene in very good yields (**Scheme 5.6**). The report claimed an advantage in using phenyl(trihalomethyl)mercury reagent (**5.5**) is its ability to react with poor nucleophiles, *e.g.* ethylene or tetrachloroethylene, as well as with olefins which contain base-sensitive substituents, *e.g.* vinyl acetate.[19] However, disadvantages of this procedure are the high cost and toxic nature of the mercuric reagent.

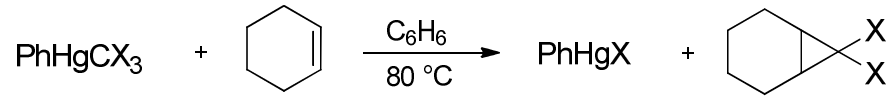

5.5
X = Cl or Br

5.6
X = Cl, 89%
X = Br, 88%

Scheme 5.6. Synthesis of 7,7-dihalononcarane (**5.6**) from phenyl(trihalomethyl)mercury (**5.5**).[19]

In 1970, Kobrich *et al.*,[20] investigated whether trichloromethyllithium (**5.7**, TML) reacts *via* a carbene intermediate in electrophilic reactions. They reacted TML with a mixture of cyclohexene and another olefin, *e.g.* 1-heptene. The reaction is shown in **Scheme 5.7**.

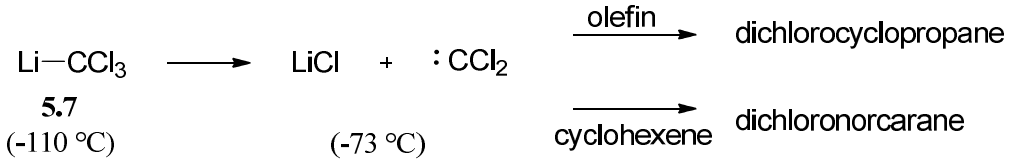

5.7
(-110 °C)

(-73 °C)

Scheme 5.7. Preparation of dichlorocyclopropanes from TML (**5.7**).[20]

Makosza[21] and Starks[22] discussed the use of phase-transfer catalysts in heterogeneous reactions. Although generation of :CCl_2 under basic conditions requires an anhydrous environment due to rapid degradation of the CCl_3^- anion,[23] Makosza and Starks managed to prepare dichlorocyclopropanes (in 60% yield) from olefins, chloroform and

25% NaOH solution in the presence of a phase-transfer catalyst (*e.g.* quaternary ammonium or phosphonium salts).

In 1977, Julia and Ginebreda[24] published a new method of dichlorocarbene generation by means of solid-liquid phase-transfer catalysis.[25] The reaction was performed in $CHCl_3$ using powdered NaOH as a base.[26, 27] The authors claimed that their method was simple, used readily available reagents and the reaction time was short.

In 2003, Lin *et al.*,[28] reported a procedure of $:CCl_2$ generation from carbon tetrachloride using ultrasonic irradiation (**Scheme 5.8**). They obtained a range of *gem*-dichlorocyclopropane derivatives in good yields (40-93%).

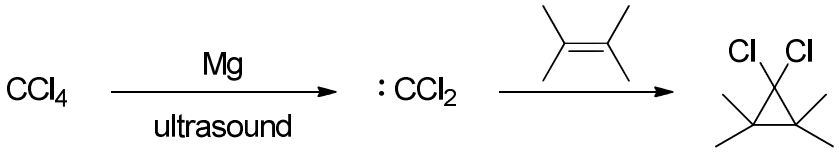

Scheme 5.8. Generation of dichlorocarbene by the reaction of carbon tetrachloride with magnesium at room temperature.[28]

The authors claimed that the main advantage of the method was a short reaction time as well as a base-free environment, which allowed side reactions to be avoided.

Wang *et al.*,[29-31] reported a kinetic study of a dichlorocyclopropanation reaction. One of the reactions they investigated was the $:CCl_2$ addition to allyl phenyl ether (**5.8**) in the presence of a phase-transfer catalyst, benzyltriethylammonium bromide, BTEAB, (**Scheme 5.9**).

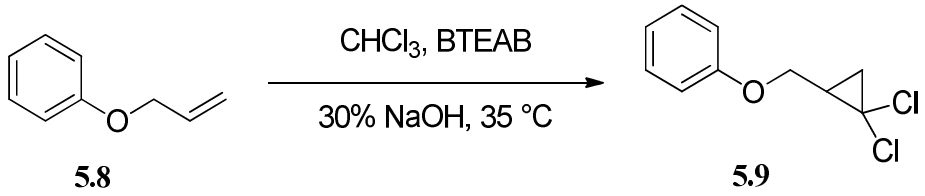

5.8 **5.9**

Scheme 5.9. Formation of (2,2-dichlorocyclopropylmethoxy)benzene (**5.9**) from allyl phenyl ether (**5.8**).[30]

The authors investigated which factors (*e.g.* stirring speed, concentration of different catalysts, NaOH concentration, volume of chloroform and substrate and temperature) affected the overall reaction rate.

5.3.2. Procedure for the reaction of $CHCl_3$ and $CHBr_3$ with SAMs

In this research the procedure of Ziyat *et al*.,[32] has been used as a starting point to produce dichloro- and dibromo- cyclopropane terminated SAMs. The procedure involved stirring a solution of NaOH (100 mg, 200 mg, 300 mg, 400 mg or 500 mg), $CHCl_3$ or $CHBr_3$ (1 mL) and benzyltriethylammonium chloride (BTEAC, 0.1 mmol) in dichloromethane (1 mL) for 10 min at 0 °C. The silicon wafers (1 cm × 1.5 cm), pre-coated with vinyl-terminated SAMs, were immersed in the reaction mixture and the liquids were stirred at room temperature for fixed periods of time (30 min, 1 h, 2 h, 3 h, 4 h, 5 h). The experimental set-up is shown in **Figure 5.3**.

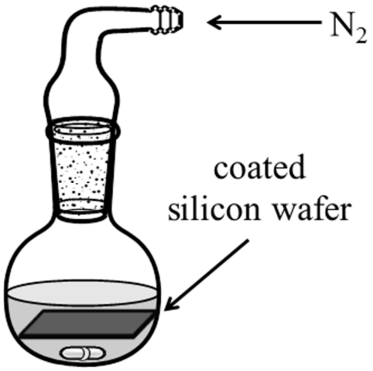

Figure 5.3. The experimental set-up for the carbene reactions performed on vinyl-terminated SAMs.

It has to be noted that the stirring bar did not touch the surface of the wafers throughout all of the reaction. After the reactions, wafers were washed repeatedly with distilled water followed by sonication in dichloromethane, toluene and DI water. This ensured that the surfaces were clean for subsequent analysis (Appendix 1).

5.3.3. Results and Discussion

The reaction conversion, as well as SAM stability under the applied conditions, was monitored by four different analytical techniques. X-ray photoelectron spectroscopy was used to determine the chemical composition of the new films and to calculate the reaction conversion. Water contact angle measurements were recorded to observe changes in wetting properties, while ellipsometry was used to measure the thickness of the SAMs in order to determine the degradation onset. Finally, AFM was used to monitor the homogeneity and smoothness of the film after modification.

5.3.3.1. X-ray Photoelectron Spectroscopy

Optimisation of the reaction conditions is crucial in surface chemistry, because the goal is to achieve the highest conversion with minimum film degradation. SAMs on silicon oxide substrates are considered to be very stable films.[1] However, the stability of SAMs can be disturbed when subjecting the modified surface to chemicals. Wasserman *et al.*,[4] reported an experiment in which methyl-terminated SAMs on SiO_x/Si were immersed in HCl (0.1 M) or NaOH (0.1 M) solution. They observed that the monolayers were stable in acid at room temperature. However, when the wafers were exposed to basic solution at room temperature, 50% of the monolayer was removed after 80 min of immersion. Moreover, they noted that after 160 min under these conditions, the surface of the substrate was visibly etched,[4] caused by the Si-O bond hydrolysis.[33, 34] For this reason, NaOH concentration in particular and the reaction time, needed to be optimised. The reaction temperature was kept constant (around 25 °C) to minimise SAM degradation under the basic conditions. Moreover, due to the possibility of degradation, a solid-liquid phase-transfer catalyst was chosen to generate the $:CX_2$ carbenes.

Optimisation of the NaOH concentration

The first experiment was designed to find the minimum NaOH concentration required to generate a $:CX_2$ carbene from CHX_3 (where X = Cl or Br). The reactions were carried out on C_{11}-vinyl **1b** and C_{15}-vinyl **1c** SAMs at room temperature for 30 min using CHX_3 (1 mL), BTEAC (0.1 mmol) and NaOH (100 mg, 200 mg, 300 mg, 400 mg, 500 mg). The XPS survey spectra taken from each sample, after the reaction with $CHCl_3$ and $CHBr_3$, are shown in **Figure 5.4**.

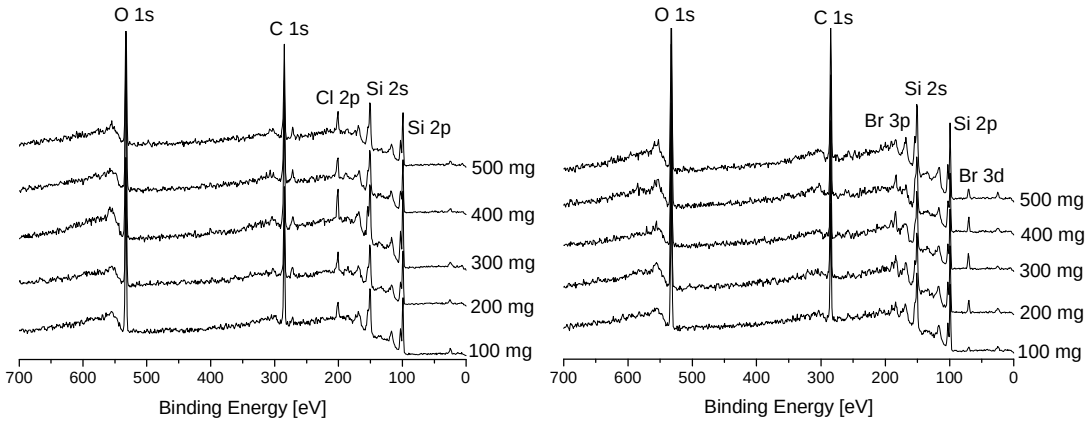

Figure 5.4. The XPS survey scans obtained after carbene chemistry on C_{11}-vinyl **1b** SAMs. Carbene generated from $CHCl_3$ (left spectrum) and $CHBr_3$ (right spectrum) using different amounts of NaOH (for details see text).

Elements such as silicon, carbon and oxygen are expected in all cases. The left hand spectra represent the surface after chemical modification with $:CCl_2$ generated from $CHCl_3$. In all cases, new signals at binding energies of 201 eV and 270 eV were detected. These were assigned to Cl 2p and Cl 2s, respectively. It can clearly be observed that the most intensive Cl 2p signal was measured when 300 mg NaOH was used. The right hand spectra (**Figure 5.4**) show the results obtained from SAMs after modification with $:CBr_2$ generated from $CHBr_3$. New peaks appeared at binding energies of 71 eV and 182 eV in all of the samples. These were assigned to Br 3d and Br 3p signals, respectively. The most intensive Br 3d signal was detected for the sample using 300 mg of NaOH. The XPS high resolution scans of Cl 2p and Br 3d region are shown in **Figure 5.5**.

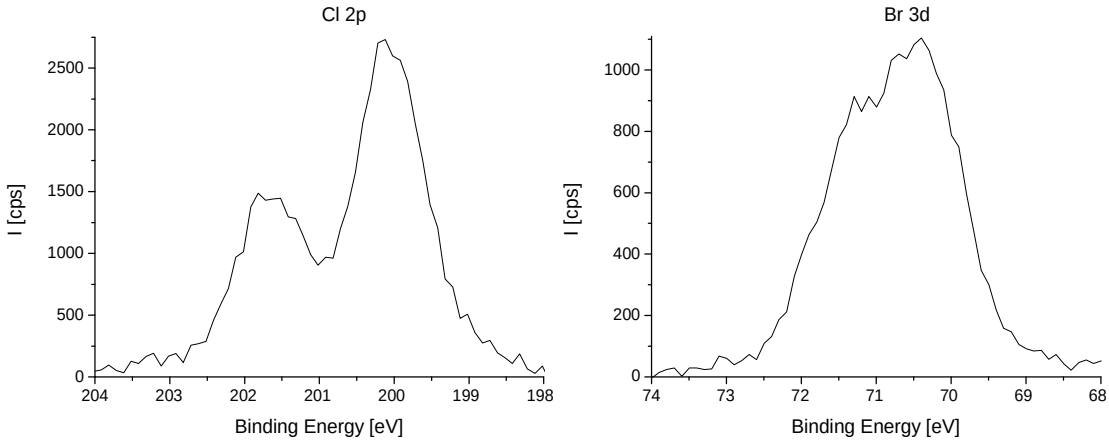

Figure 5.5. The high resolution scan of Cl 2p region (left spectrum) and Br 3d region (right spectrum), taken from the reaction with 300 mg of NaOH.

The highest conversions were observed under the same reaction conditions in each case. However, a comparison of the two samples reacted using 300 mg of NaOH and taking into account the relative sensitivity factor (R.S.F.) of both elements, shows that the Cl 2p signal is more intense than the Br 3d signal (**Figure 5.5**). This may be due to the different sizes of the halogen atom on the surface. Chlorine is smaller than bromine. The van der Waals radius of a chlorine (0.175 nm) and shorter C-Cl bond (0.175 nm) compared to the van der Waals radius of a bromine (0.185 nm) and C-Br bond (0.191 nm) suggest a lower steric input.[35] Thus, reaction with the smaller group appears to be more efficient.

Optimisation of reaction time

A second experiment was designed to explore how long SAMs can be subjected to the reaction with :CCl_2 and :CBr_2 carbene without being degraded. Accordingly C_{11}-vinyl **1b** and C_{15}-vinyl **1c** SAMs were treated with CHX_3 (1 mL), BTEAC (0.1 mmol) in dichloromethane and NaOH (300 mg) for fixed periods of time (30 min, 1 h, 2 h, 3 h, 4 h, 5 h) at room temperature. The XPS survey scans obtained at time intervals are shown in **Figure 5.6**.

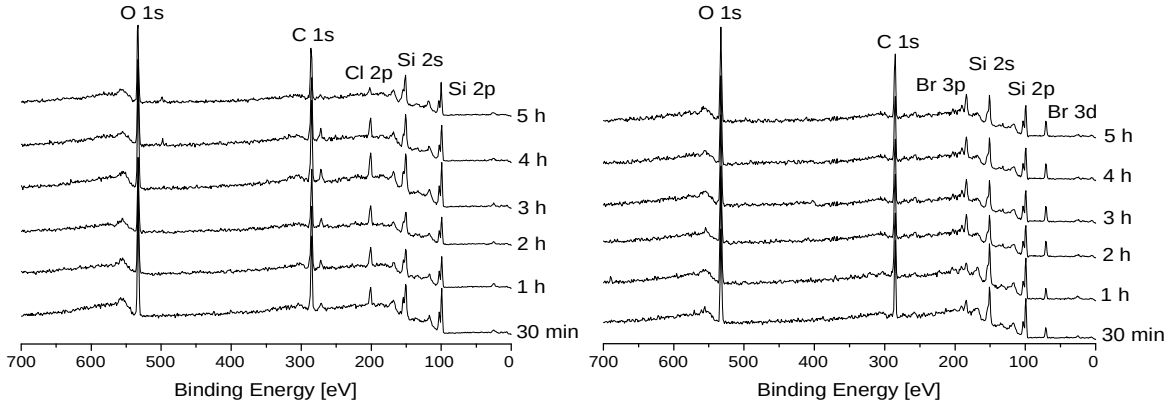

Figure 5.6. The XPS survey scans after reactions performed at fixed periods of time on C_{11}-vinyl **1b** SAMs. Carbene generated from $CHCl_3$ (left spectrum) and $CHBr_3$ (right spectrum).

From the XPS survey scans it is observed that the longer the reaction time between C_{11}-vinyl **1b** SAM and $CHCl_3$, the more intense the Cl 2p signal, but only up to 3 h of the reaction (**Figure 5.6**, left spectra). For reaction times longer than 3 h, the intensity of the Cl 2p signal started dropping gradually. Changes in the C 1s signal intensities were also observed. In the case of 4 h and 5 h reactions, the carbon signal decreased slightly, suggesting the beginning of SAM degradation on the surface.

A similar tendency was observed in the reaction between C11-vinyl **1b** SAM and $CHBr_3$ (**Figure 5.6**, right spectrum). However, the differences between the reactions are less pronounced than in the case of SAM modification with dichlorocarbene. The most intensive Br 3d signal was observed in the case of a 3 h reaction time. For reaction times longer than 3 h, the Br 3d signal started to decrease along with the decreasing intensity of the C 1s signal, suggesting film degradation. This was confirmed by other analytical techniques, which will be discussed later.

Exposure of methyl-terminated SAMs to $:CX_2$

In order to prove the selective reactivity of the $:CCl_2$ and $:CBr_2$ carbene with the terminal double bond functionality, a control reaction was carried out with C_{18}-methyl **1e** SAMs. The samples were subjected to similar reaction conditions, CHX_3 (1 mL), BTEAC (0.1 mmol), and NaOH (300 mg) for 3 h at room temperature. The XPS survey scans are shown in **Figure 5.7**.

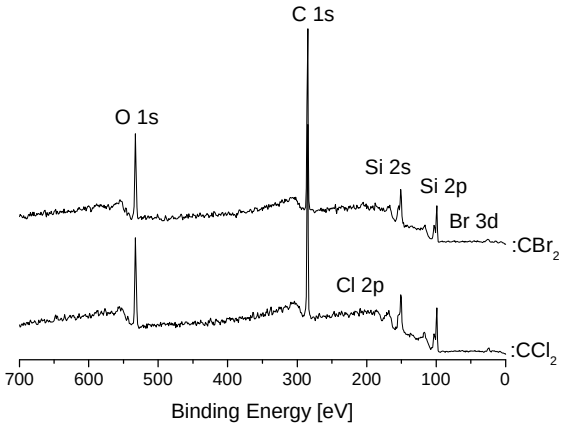

Figure 5.7. The XPS survey scans after the reaction between C_{18}-methyl **1e** SAMs with $:CBr_2$ (top) and $:CCl_2$ (bottom).

The XPS survey scans revealed as expected the presence of silicon, carbon and oxygen on the surface. Signals for Cl 2p and Br 3d were not observed. However, to explore if an insertion reaction of carbene into the aliphatic C-H bonds might occur at a low level, high resolution regions exploring of Cl and Br signals were carefully investigated. The high resolution elemental scans for Cl 2p and Br 3d are shown in **Figure 5.8**.

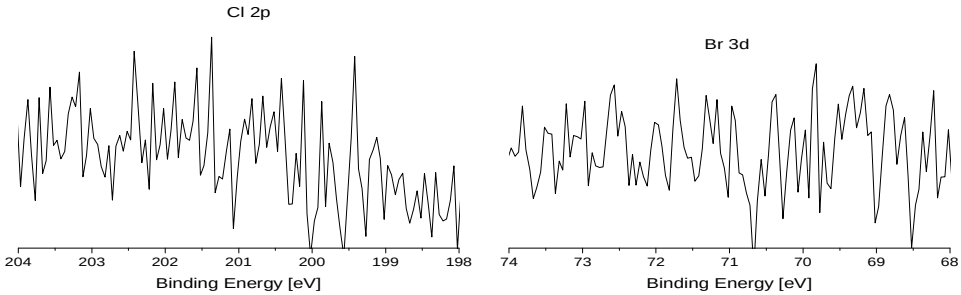

Figure 5.8. The high resolution XPS scans of Cl 2p and Br 3d region, after the reaction between C_{18}-vinyl **1e** SAMs and :CCl_2/:CBr_2.

The high resolution scans do not show any evidence for the presence of Cl or Br on the surface. These results clearly indicate that the methyl-terminated films are resistant to the reaction with carbenes. Moreover, it can be concluded that the modification of SAMs with carbenes is selective, because only films which contained the terminal C=C bonds, showed the presence of Cl and Br.

5.3.3.2. Water Contact Angle

The water contact angle measurements were recorded to investigate how the wettability of the surface changed after exposure of the SAMs to carbenes. The water contact angles of C_{11}-vinyl **1b** and C_{18}-methyl **1e** SAMs was 101° and 109°, respectively at the outset. The results obtained after a 30 min reaction between :CCl_2 or :CBr_2 and C_{11}-vinyl **1b** SAM with different amounts of NaOH are shown in **Figure 5.9**.

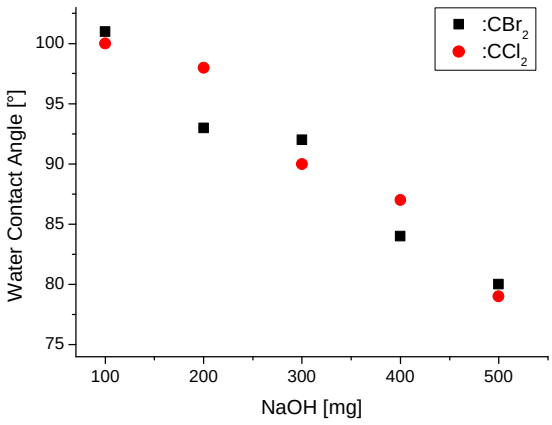

Figure 5.9. The water contact angles recorded after the reaction of C_{11}-vinyl **1b** SAMs with different amounts of NaOH used to generate carbene (:CCl_2, :CBr_2).

The results presented in **Figure 5.9** clearly show that after modification with carbenes the surface became more hydrophilic. The C_{11}-vinyl **1b** SAM exhibited a water contact angle of 101° before modification, while after the reaction, the recorded values were within the range of 100° to 79°. It is difficult to draw a conclusion on the extent of reaction from water contact angles, because film degradation, will also reduce the value. However, the water contact angle and the ellipsometry data, which will be discussed later, indicates that the best conversions resulted from 300 mg NaOH. The CA's were 90° for the $:CCl_2$ carbene and 92° for the $:CBr_2$ carbene. No changes in CA's were observed in the case of the methyl-terminated films, which remained at 109° before and after reaction (Appendix 2). The literature CA's for Cl-terminated films is reported at 85° and slightly less (80°) for Br-terminated SAMs.[4, 36]

The next experiment was performed with 300 mg NaOH for fixed periods of time (1 h, 2 h, 3 h, 4 h, 5 h) to obtain fully modified surfaces. The measured contact angles are presented in **Figure 5.10**.

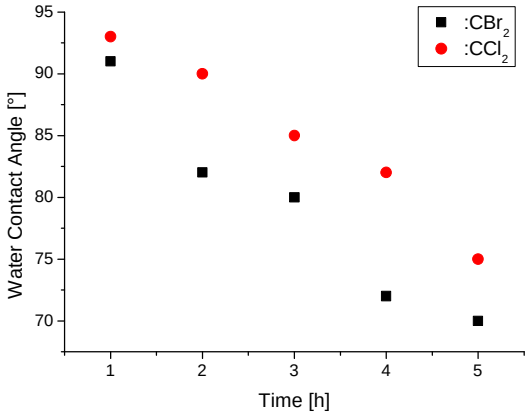

Figure 5.10. The water contact angle values recorded after carbene modification of C_{11}-vinyl **1b** SAM, performed for different periods of time.

The water contact angles of Cl and Br terminated surfaces were recorded for a reaction time of 3 h. In the case of $CHCl_3$ the water contact angle was 85° and that for $CHBr_3$ was 80°. This is in good agreement with the literature.[4, 36]

From these measurements it is concluded that the best film modification was obtained when the carbene reaction was performed for 3 h with 1 mL of $CHCl_3$/$CHBr_3$ and 300 mg NaOH. However, this technique does not provide enough information about film degradation, thus additional analysis was required to fully characterise the films.

5.3.3.3. Ellipsometry

Ellipsometry measurements were very useful for monitoring the onset of SAM's degradation under the reaction conditions.

The data revealed that the thicknesses of the C_{11}-vinyl **1b** SAMs did not change significantly for reactions with 100 mg, 200 mg and 300 mg of NaOH. However, lower thicknesses were observed in reaction with $CHBr_3$ at either 400 mg or 500 mg of NaOH. Values of 10.2 Å and 9.2 Å were recorded, respectively (~15 Å before modification). These thicknesses are too small for a modified monolayer film and suggest degradation. The same tendency was observed in the case of $CHCl_3$. Lower thicknesses were measured when 400 mg or 500 mg of NaOH was added to the reaction (Appendix 2). Significant difference in SAM thicknesses was observed when 400 mg of NaOH was used in the reaction. This is difficult to explain and might be caused by lower quality of SAM used in the reaction with $:CBr_2$. The ellipsometry results for the reaction with $CHCl_3$ and $CHBr_3$ are shown in **Figure 5.11**.

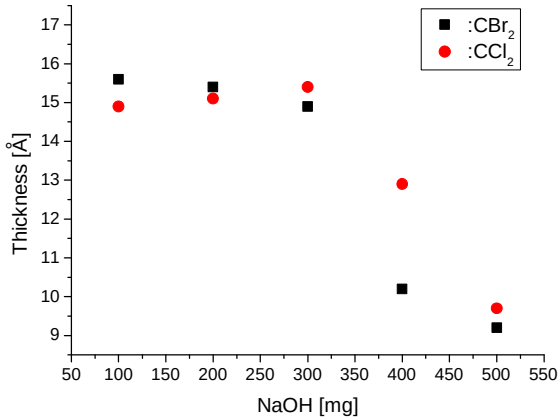

Figure 5.11. Ellipsometry results obtained after exposure C_{11}-vinyl **1b** SAMs to carbenes under different reaction conditions (for details see text).

The ellipsometry results taken with the water contact angles and XPS data, it is concluded that SAMs can be modified without observable degradation when 300 mg of NaOH was used in the reaction.

The ellipsometry measurements were also useful for investigating the minimum reaction time. SAM films were subjected to the carbene modification for 1 h, 2 h, 3 h, 4 h and 5 h. Film degradation was observed in the reaction time of 4 h and 5 h in the case of both carbenes. The recorded results were below 14 Å. A summary of these results is presented in Appendix 2.

5.3.3.4. Atomic Force Microscopy

AFM images were recorded for samples modified for 3 h at room temperature with 300 mg of NaOH, BTEAC and 1 mL of CHX_3. The AFM images obtained from C_{11}-vinyl **1b** SAM after modification with $:CCl_2$ and $:CBr_2$ carbene are shown in **Figure 5.12**.

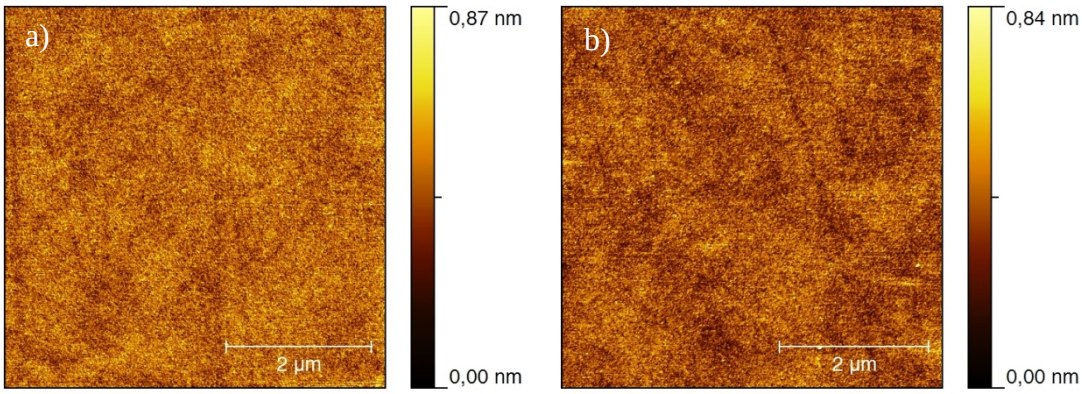

Figure 5.12. AFM images of 5 µm × 5 µm area of C_{11}-vinyl **1b** SAMs modified with a) $:CCl_2$ carbene, RMS 93 pm, and b) $:CBr_2$ carbene, RMS 101 pm.

Both images obtained after carbene modification in the liquid phase are very smooth and defect free. No excess of material was observed in the case of the reaction performed for 3 h with 300 mg NaOH. The RMS values in the case of both modified SAMs C_{11}-vinyl **1b** and C_{15}-vinyl **1c**, were small and never exceeded 150 pm.

5.3.4. Evidence for *gem*-dihalocyclopropane-terminated SAMs

Based on the results to date, the SAM films with the most halogen on the surface, were used for structure analysis and also to estimate the reaction conversion. From solution reaction of carbenes with olefins, it was anticipated that the *gem*-dichloro- and *gem*-dibromocyclopropane-terminated SAMs will be obtained (**Figure 5.13**). It was necessary to support this hypothesis with analytical data.

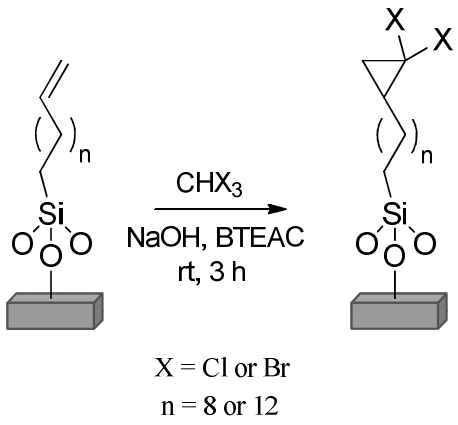

Figure 5.13. Putative formation of *gem*-dihalocyclopropane-terminated SAMs in the liquid phase.

XPS survey scans taken from methyl- and vinyl- terminated SAMs (based on **Figure 5.6** and **Figure 5.7**), after optimised carbene reactions, clearly reveal that only the latter SAMs reacted (**Figure 5.14**).

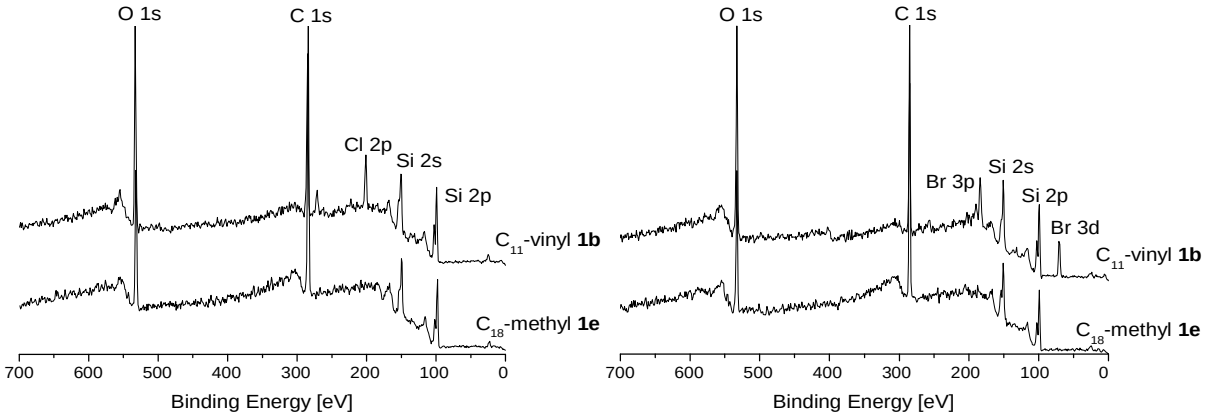

Figure 5.14. The XPS full scans after the exposure of methyl- **1e** and vinyl- **1b** terminated films to :CCl_2 (left spectrum) and :CBr_2 (right spectrum).

In the case of SAMs subjected to :CCl_2 carbene (**Figure 5.14**, left spectrum), a new Cl 2p signal can be clearly observed on reacted C_{11}-vinyl **1b** SAM (top spectrum). Otherwise, no changes were detected in the case of C_{18}-methyl **1e** SAM (bottom spectrum). The high resolution scans of the Cl 2p and C 1s regions taken from the reacted C_{11}-vinyl **1b** SAM are shown in **Figure 5.15** (fitting details are provided in Chapter 2, paragraph 2.1.1).

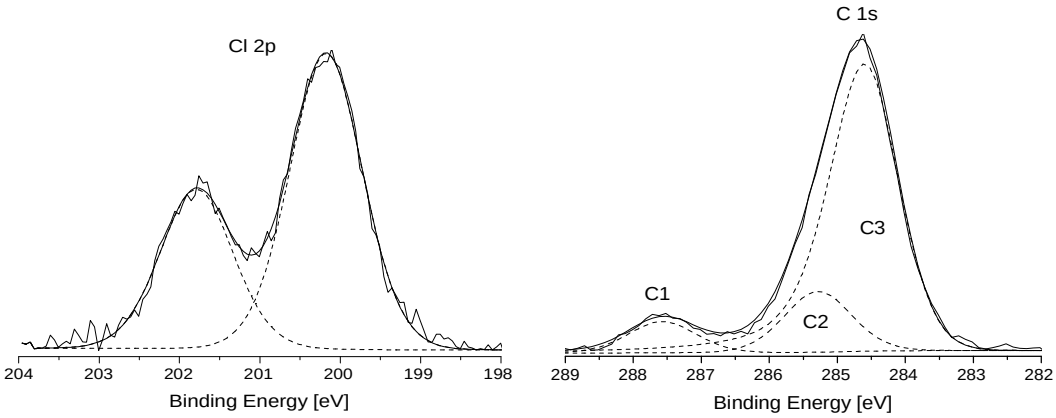

Figure 5.15. The XPS high resolution scans of the Cl 2p (left spectrum) and C 1s (right spectrum) regions of C_{11}-vinyl **1b** SAM after the reaction with :CCl_2.

The position of the signal at a binding energy of 201 eV suggests Cl 2p.[37] Moreover, in the carbon region, three signals were observed, two of which (assigned to C1 and C2) were not observed on the substrate. The most intense signal (C3) appearing at a binding energy of 284.6 eV, corresponding to the carbons from the alkyl chains.[9] Carbon C2 (285.3 eV) corresponds to the two formerly vinyl carbon atoms, which are now part of the cyclopropane ring. Finally, carbon C1 (287.7 eV) is assigned to the carbon atom from the :$\underline{C}Cl_2$ species (**Figure 5.17**).

In the case of SAMs subjected to :CBr_2 carbene, a new signal corresponding to Br, was detected on reacted C_{11}-vinyl **1b** SAM (**Figure 5.14**, right spectrum). No changes were observed for the C_{18}-methyl **1e** SAM (**Figure 5.14**, right spectrum), as in the case of reaction with dichlorocarbene. The high resolution scans of the Br 3d and C 1s region taken from the C_{11}-vinyl **1b** SAM are shown in **Figure 5.16**.

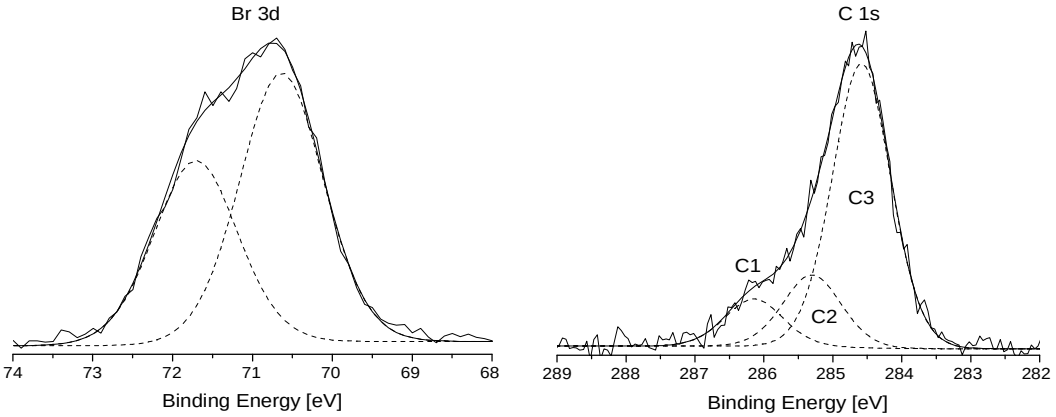

Figure 5.16. The XPS high resolution scans of the Br 3d (left spectrum) and C 1s (right spectrum) region of C_{11}-vinyl **1b** SAM after the reaction with :CBr_2.

After the reaction of vinyl-terminated SAMs with :CBr_2, a new XPS peak was detected at a binding energy of 71 eV, which can be assigned to Br.[4] In the C 1s region, three signals were observed. The C3 signal (284.6 eV) again comes from a $\underline{C}H_2$ carbons of the alkyl chain,[9] while C2 (285.3 eV) and C1 (286.2 eV) signals come from the cyclopropane ring. The higher binding energy of C1 suggests that this carbon atom is bonded to the two Br atoms (**Figure 5.17**).

Film modification was also confirmed by changes in the water contact angle. The vinyl-terminated SAMs before reaction with :CCl_2, exhibited a water contact angle of 101°, while after modification it decreased to 85°. The same trend was observed in the case of the :CBr_2 reaction. The water contact angle of :CBr_2 modified SAMs was 80°, identical to the value reported for a different Br-terminated film in the literature.[4] The ellipsometry measurements did not reveal any significant changes in thicknesses of the SAMs after the carbene modification. The measured thicknesses of the modified films were ~16 Å (~15 Å before modification), suggesting that decomposition did not occur.

The presence of *gem*-dihalocyclopropane groups on the surface is supported by the ratios of the C 1s to the Cl 2p and C 1s to the Br 3d signals (**Figure 5.17**).

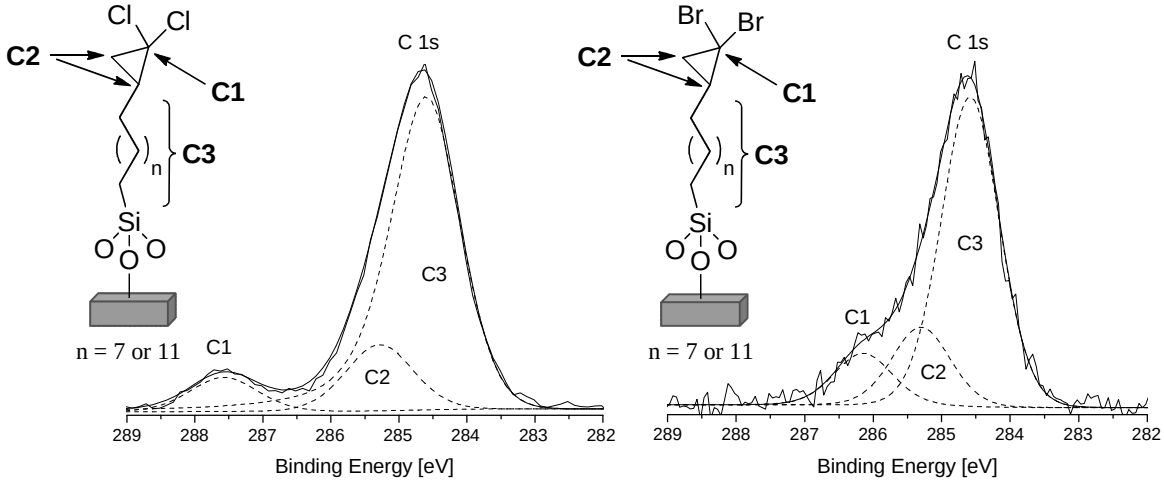

Figure 5.17. Assignment of the C 1s signals according to the possible structure formed on the surface.

The theoretical and experimental ratios between the carbon and halogen XPS signals are summarised in **Table 5.1**.

		Ratios		
		<u>*X*</u> : <u>*C*</u>1	<u>*X*</u> : <u>*C*</u>2	<u>*C*</u>1 : <u>*C*</u>2
Theor.	C_{11}-vinyl **1b**	2 : 1	1 : 1	1 : 2
	C_{15}-vinyl **1c**	2 : 1	1 : 1	1 : 2
Exp. :CBr_2	C_{11}-vinyl **1b**	2 : 1	1 : 1	1 : 2
	C_{15}-vinyl **1c**	2 : 1	1.1 : 1	1 : 1.8
Exp. :CCl_2	C_{11}-vinyl **1b**	2 : 1	1.1 : 1	1 : 1.8
	C_{15}-vinyl **1c**	2.1 : 1	1 : 1	1 : 2

Table 5.1. Theoretical and experimental ratios of the Br 3d to C 1s and Cl 2p to C 1s XPS signals of modified SAMs.

From the XPS data, the conversions of either the C_{11}-vinyl **1b** or C_{15}-vinyl **1c** SAMs with :CCl_2 or :CBr_2 can be estimated by taking into account the attenuation factor (paragraph 5.1). Based on the intensity of the Cl 2p signal and the sum of intensities of the C 1s signals, the dichlorocyclopropanation conversion is estimated at ~49% for the C_{11}-vinyl **1b** SAM and ~44% for the C_{15}-vinyl **1c** SAM. For the dibromocyclopropanation reaction the intensity of the Br 3d signal was used to estimate the reaction conversion at ~35% for the C_{11}-vinyl **1b** SAM and ~33% for the C_{15}-vinyl **1c** SAM.

The formation of a *gem*-dihalocyclopropane group on the surface, based on a working hypothesis, occurs through the solid-liquid phase transfer catalysis (PTC) mechanism[38] shown in **Scheme 5.10**.

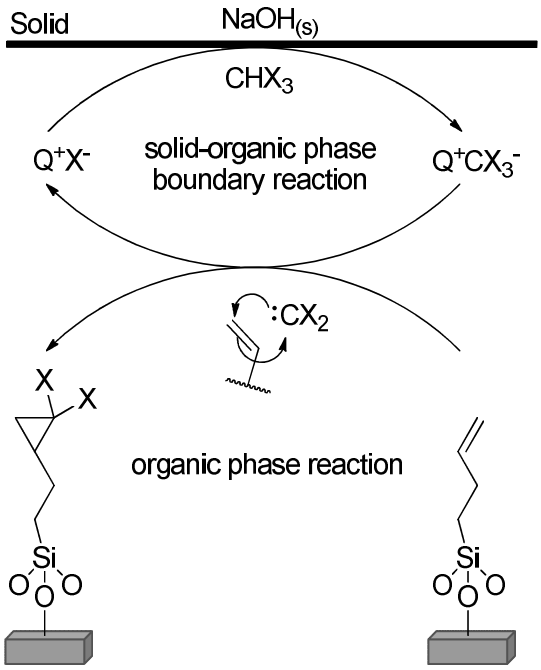

Scheme 5.10. Phase transfer relay for *gem*-dihalocyclopropanes on vinyl-terminated SAMs.

The reactions between the catalyst Q^+X^- (BTEAC, benzyltriethylammonium chloride, $Et_3N^+CH_2PhX^-$) and CHX_3 (X = Cl or Br) at the solid-liquid interface are shown in **Scheme 5.11**.

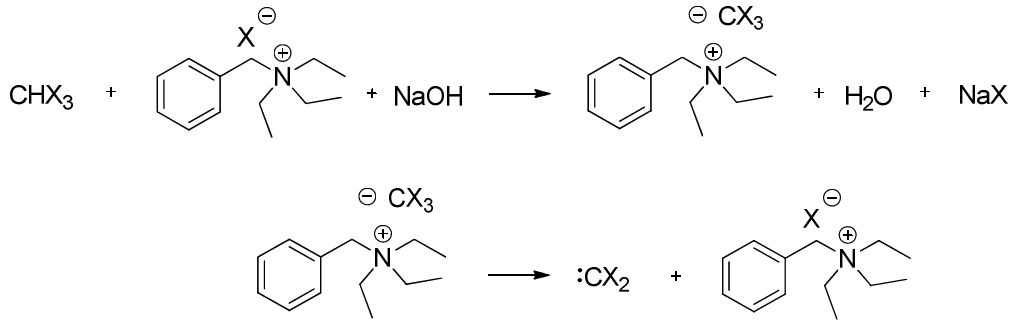

Scheme 5.11. Reactions at the solid-liquid interphase between organic reagent and catalyst-base species.

In the liquid-liquid phase transfer catalysis reaction, the quaternary ammonium salt (Q^+X^-) works as a carrier to transfer OH^- from the aqueous NaOH solution into the organic phase.[38] However, the Q^+OH^- species is insoluble in the organic medium, thus the reaction occurs at the aqueous-organic interphase.[21] In the case of solid-liquid phase transfer catalysis, the catalyst Q^+X^-, reacts with the solid at its surface. Then at the solid-organic interphase, the catalyst-base species reacts with CHX_3 to yield the quaternary ammonium

derivative of the trihalomethyl anion ($Et_3N^+CH_2Ph^-CX_3$), which is soluble in the organic phase. In the organic medium, the anion is transformed into a dihalocarbene :CX_2,[21] which then reacts with the double bonds to form a *gem*-dihalocyclopropane while the regenerated catalyst ($Et_3N^+CH_2PhX^-$, Q^+X^-) is recovered to the PTC cycle.

In order to confirm formation of a *gem*-dihalocyclopropane group during the reaction of vinyl-terminated SAM with dihalocarbene, a control reaction was carried out. Under exactly the same reaction conditions as the surface chemistry, dihalocarbene was generated and reacted with 1-decene. The reaction is shown in **Scheme 5.12**.

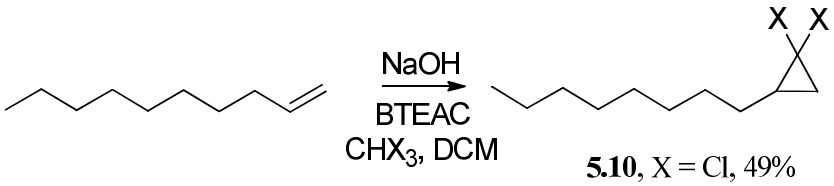

5.10, X = Cl, 49%
5.11, X = Br, 54%

Scheme 5.12. Synthesis of 1,1-dihalo-2-octylcyclopropane in the liquid phase.

Both cyclopropane products were obtained in moderate yields. 1,1-Dichloro-2-octylcyclopropane (**5.10**) was recovered in 49% yield and 1,1-dibromo-2-octylcyclopropane (**5.11**) in 54% yield (Appendices 3 and 4). These results show that formation of dihalocyclopropanation product is the major in solution and supports the hypothesis that they are generated on reaction with the vinyl-terminated SAMs. These products were fully characterised.

5.4. Chemistry on SAMs involving difluorocarbene

Difluorocyclopropanation was explored next. The reaction is shown in **Scheme 5.13.** Trifluoromethyltrimethylsilane ($TMSCF_3$) was used to generate difluorocarbene ($:CF_2$) in solution and reacted with the vinyl-terminated SAMs.

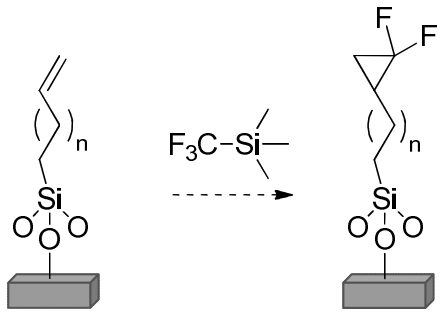

Scheme 5.13. Liquid-phase reaction between vinyl-terminated SAMs and $TMSCF_3$.

5.4.1. Chemistry and sources of $:CF_2$

In the 1960s, Seyferth *et al.*,[39, 40] reported a method of dihalocarbene generation from trihalomethyl-metal compounds. They synthesised *gem*-difluorocyclopropane **5.13** in a very good yield (73%) by generating $:CF_2$ carbene from trimethyl(trifluoromethyl)tin (**5.12**, Me_3SnCF_3) at 80 °C under neutral pH conditions (**Scheme 5.14**).

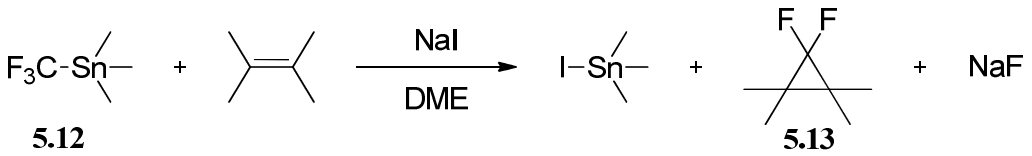

Scheme 5.14. Synthesis of *gem*-difluorocyclpropane (**5.13**) by generating the $:CF_2$ carbene from trimethyl(trifluoromethyl)tin (**5.12**).[39]

In the 1970s, the same research group[41, 42] investigated the use of organomercuric compounds as a source of $:CF_2$. They found that phenyl(trifluoromethyl)mercury ($PhHgCF_3$) is an excellent $:CF_2$ precursor. $PhHgCF_3$ was very stable under elevated temperatures and, unlike the trimethyl(trifluoromethyl)tin precursor (**5.12**), it could be used in solvent-free systems.

In 1973, Burton *et al.*,[43] presented a simple, one-step method of $:CF_2$ generation from bromodifluoromethylphosphonium salts. Moreover, the difluorocarbene precursors

could be generated *in situ* from commercially available phosphines (R_3P) and difluorodihalomethanes (CF_2X_2), in the presence of an olefin and fluoride salts (MF) (**Scheme 5.15**).

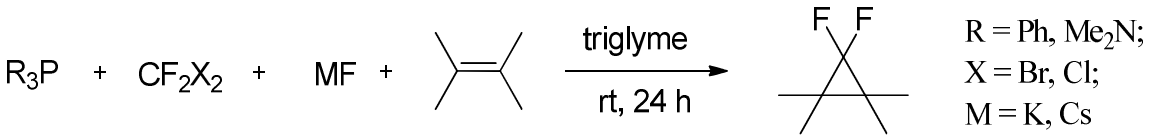

Scheme 5.15. Burton's generation of $:CF_2$ from synthesised *in situ* halodifluoromethylphosphonium salt.[43]

In 1990, Bessard *et al.*,[44] synthesised *gem*-difluorocyclopropanes using Burton's methodology.[43] They treated olefins with dibromodifluoromethane and triphenylphosphine in the presence of a catalytic amount of 18-crown-6. The advantages of Bessard's method are a shorter reaction time, replacement of expensive CsF by KF and the possibility of using mono- rather than tri-glyme as a solvent.

In the same year, Dolbier *et al.*,[45] presented a new zinc difluorocarbene reagent, which can be cheaply prepared and does not require anhydrous conditions. In this process CF_2Br_2 reacts with Zn in THF at room temperature in the presence of α-methylstyrene, yielding 71% of *gem*-difluorocyclopropane (**5.14**) (**Scheme 5.16**).

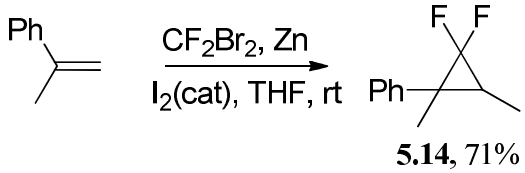

5.14, 71%

Scheme 5.16. Dolbier's *gem*-difluorocyclopropane (**5.14**) synthesis by reaction of an alkene with zinc difluorocarbene reagent.[45]

Babin[46] and Fujioka[47] generated $:CF_2$ carbene by thermolysis of sodium chlorodifluoroacetate ($ClCF_2COONa$). However, the process requires harsh conditions, (4 h at 160 °C[46] or 15 min at 180 °C)[47] and the corresponding *gem*-difluorocyclopropane compounds were obtained in 67% and 61% yield, respectively.

Trimethylsilyl 2,2-difluoro-2-(fluorosulfonyl)acetate ($FSO_2CF_2COOTMS$, TFDA) is also an efficient source of $:CF_2$.[48-51] The TFDA undergoes desilylation in the presence of a catalytic amount of F^- at temperatures above 100 °C (**Scheme 5.17**).[50]

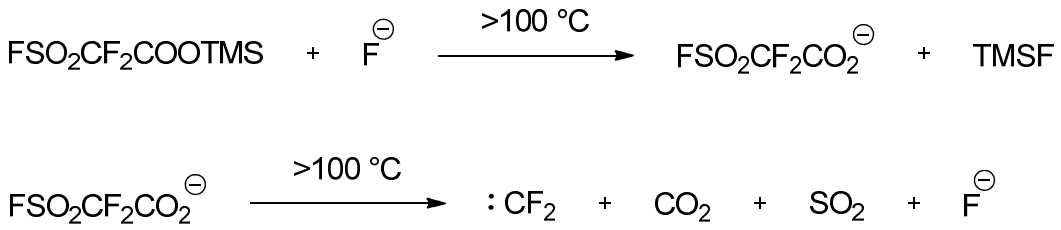

Scheme 5.17. Generation of :CF_2 from TFDA in the presence of F^-.[50]

Tian *et al.*,[48] used TFDA to perform the addition of :CF_2 to an electron deficient alkene, such as *n*-butyl acrylate **5.15**, in a yield of 73% (**Scheme 5.18**). Cai *et al.*,[49] synthesised 2,2-difluorocyclopropyl ethers by treating electron-rich aromatic ketones and *α,β*-unsaturated ketones with TFDA.

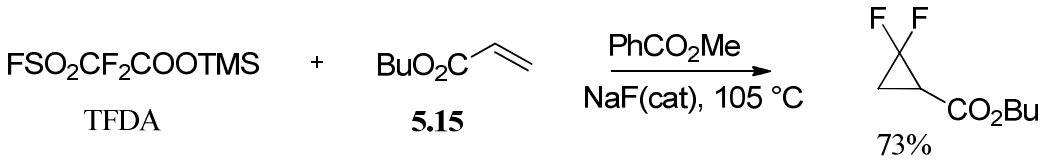

Scheme 5.18. Reaction of TFDA with *n*-butyl acrylate (**5.15**).[48]

In 2011, Wang *et al.*,[52] used commercially available trifluoromethyltrimethylsilane (Me_3SICF_3, $TMSCF_3$), also known as the Ruppert-Prakash reagent, as a source of :CF_2 carbene. The $TMSCF_3$ can be used under mild reaction conditions, enabling thermally unstable olefin substrates to undergo difluorocyclopropanation reaction. The cycloaddition reaction with $TMSCF_3$ under different conditions is shown in **Scheme 5.19**.

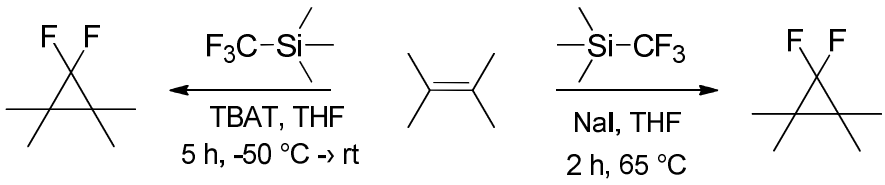

Scheme 5.19. [2+1] cycloaddition of difluorocarbene (generated from $TMSCF_3$) to an alkene with the Ruppert-Prakash reagent.[52]

Recently, Eusterwiemann *et al.*,[53] have reported that methyl 2,2-difluoro-2-(fluorosulfonyl)-acetate (MDFA) can act as a :CF_2 source if used in high concentration and elevated temperatures. The reactivity of MDFA is comparable to that of TFDA. MDFA is already known as a good precursor for the *in situ* generation of CF_3Cu (**Scheme 5.20**).[53-55]

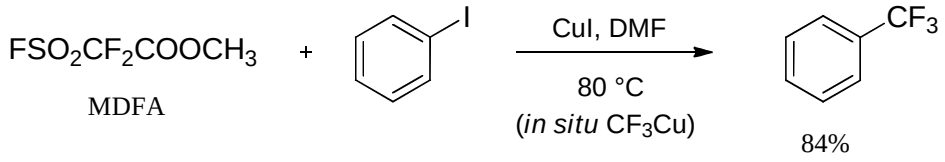

Scheme 5.20. Use of MDFA to prepare *in situ* CF_3Cu.[53]

Moreover, MDFA can be used as a $:CF_2$ source when the formation of trifluoromethyl anion is limited, by trapping the fluoride anion with trimethylsilyl chloride (TMSCl). A minimal mechanism for the generation of a difluorocarbene is shown in **Scheme 5.21**.[53]

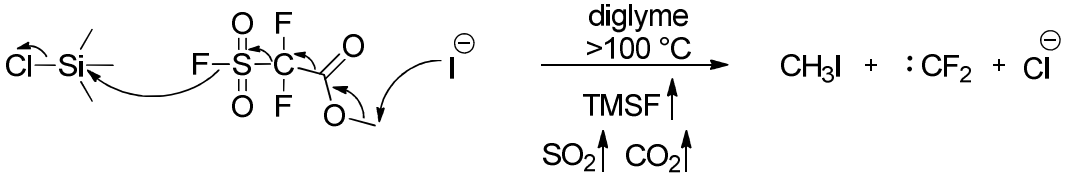

Scheme 5.21. Minimal mechanism for the formation of $:CF_2$ carbene from MDFA/TMSCl.[53]

5.4.2. Procedure for the reaction of $TMSCF_3$ with SAMs

The procedure described by Wang *et al.*,[52] using the Ruppert-Prakash reagent was used in this study to generate *gem*-difluorocyclopropane-terminated SAMs. The procedure involved stirring a solution of NaI (0.2 eq), $TMSCF_3$ (0.6 mM, 1.0 mM, 1.4 mM, 1.7 mM or 2.7 mM) in THF (2 mL). Next, the silicon wafers (1 cm × 1.5 cm), pre-coated with vinyl-terminated SAMs, were immersed in the reaction mixture and the solution was stirred at 65 °C for fixed periods of time (2 h, 3 h, 4 h, 5 h). After the reaction, the wafers were washed with distilled water and then sonicated in dichloromethane, toluene and DI water to clean the surfaces (Appendix 5).

5.4.3. Results and Discussion

The SAMs from the difluorocyclopropanation reactions were analysed by four techniques: X-ray photoelectron spectroscopy, contact angle goniometry, ellipsometry and atomic force microscopy.

In order to assess the best reaction conditions, two parameters were explored. The first focused on finding the optimal concentration of $TMSCF_3$ required for the reaction, while the second assessed the optimal reaction time.

5.4.3.1. X-ray Photoelectron Spectroscopy

Optimisation of $TMSCF_3$ concentration

A series of experiments were performed to investigate how the concentration of $TMSCF_3$ affects both the stability and conversion of the resultant SAMs. Different concentrations of $TMSCF_3$ (0.6 mM, 1.0 mM, 1.4 mM, 1.7 mM, 2.7 mM) were used in the reservoir to modify C_{11}-vinyl **1b** SAMs. The reaction was always performed in THF for 3 h at 65 °C in the presence of a catalytic amount of NaI. The XPS survey scans obtained after each reaction are shown in **Figure 5.18**.

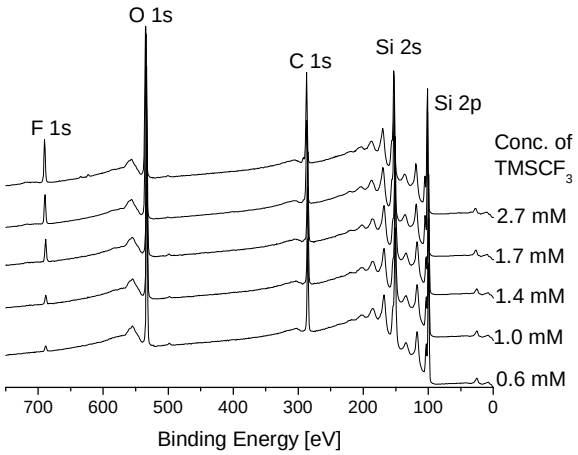

Figure 5.18. The XPS survey scans recorded after reactions of C_{11}-vinyl **1b** SAMs with $TMSCF_3$, at different concentrations.

The chemical composition of unmodified C_{11}-vinyl **1b** SAMs has already been discussed in Chapter 4. Elements such as Si, C and O were observed in all cases. The main focus was to investigate changes in F 1s region, consistent with formation of difluorocyclopropane rings. The XPS survey scans recorded after the reaction of SAMs with $TMSCF_3$, indicate a gradual increase in the F 1s peak with increasing concentration of $TMSCF_3$. Concentrations of the carbene precursor higher than 2.7 mM were not investigated due to significant film decomposition, as confirmed by CA and ellipsometry (see paragraph 5.4.3.2 and 5.4.3.3).

It is clear that the higher the concentration of $TMSCF_3$, the more fluorine was detected on the surface. The highest conversion with no detectable degradation of the SAMs was obtained at 1.7 mM of $TMSCF_3$ solution. The high resolution scan of the F 1s region showed a symmetrical fluorine signal, suggesting only one type of chemical

environment for the fluorine atoms. The F 1s signal appeared at a binding energy of 688.7 eV, which corresponds to fluorine in a CF_2 group[56] (**Figure 5.19**).

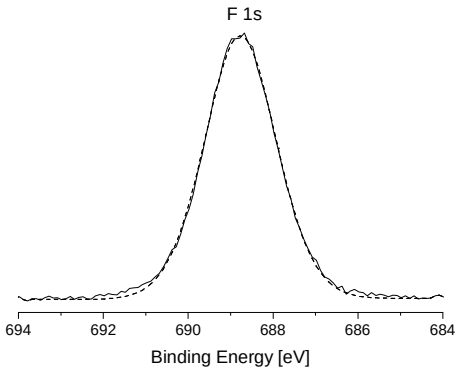

Figure 5.19. The XPS F 1s high resolution scan after the reaction of C_{11}-vinyl **1b** SAMs with :CF_2 at 65 °C.

Optimisation of the reaction time

A series of experiments was designed to explore how long the film could withstand the reaction conditions immersed in a solution of $TMSCF_3$. C_{11}-vinyl **1b** SAMs were treated with a 1.7 mM solution of $TMSCF_3$ (since this provided the best conversion) in THF for fixed periods of time (2 h, 3 h, 4 h or 5 h) at 65 °C. The XPS survey scans recorded after the reactions are shown in **Figure 5.20**.

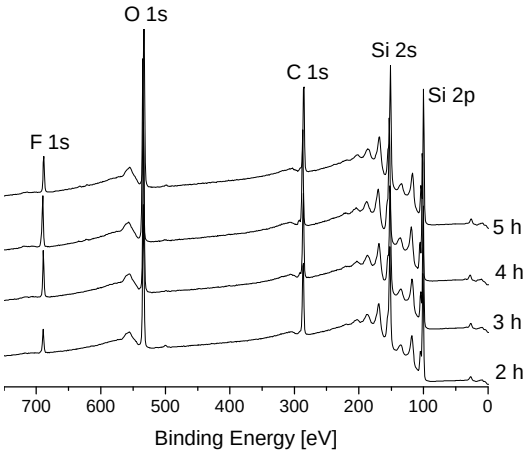

Figure 5.20. The XPS survey scans after the reaction of C_{11}-vinyl **1b** SAMs with $TMSCF_3$ (1.7 mM) for fixed periods of time.

The F 1s signal was observed by XPS for all of the samples. The F 1s signal increased from reactions at 2 h up to 4 h. In the case of a 5 h reaction a decrease in F 1s intensity was observed. Despite the fact that the most intense signal was detected at 4 h, suggests the highest conversion, the data obtained by other analytical techniques revealed

that SAM degradation was occurring at this stage. For these reasons, the optimum reaction time was set at 3 h.

Exposure of C_{18}-methyl 1e SAMs to $TMSCF_3$

A control reaction on the methyl-terminated SAMs was conducted with a C_{18}-methyl **1e** SAM using $TMSCF_3$ 1.7 mM solution for 3 h at 65 °C. The XPS results obtained after this experiment are shown in **Figure 5.21**.

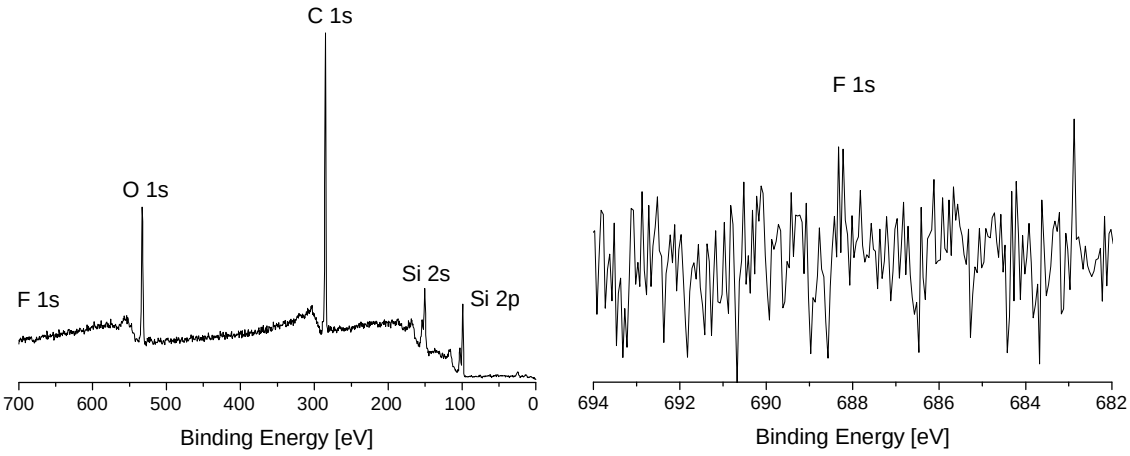

Figure 5.21. The XPS survey scan (left) and F 1s region (right) after exposure of C_{18}-methyl **1e** SAM to $TMSCF_3$.

From the full scan (**Figure 5.21**, left spectrum) obtained after exposure of methyl-terminated SAM to the $:CF_2$, only three elements (silicon, carbon and oxygen) were detected. Clearly if the SAM had reacted with the carbene, the F 1s signal would be apparent. This signal could not be observed even in a high resolution scan of the fluorine region (**Figure 5.21**, right spectrum).

This observation clearly indicates the resistance of C_{18}-methyl **1e** SAM to difluorocarbene reaction.

5.4.3.2. Water contact angle

The water contact angles were measured for all modified samples. The results obtained after reaction of C_{11}-vinyl **1b** SAMs with different amounts of $TMSCF_3$ are shown in **Figure 5.22**.

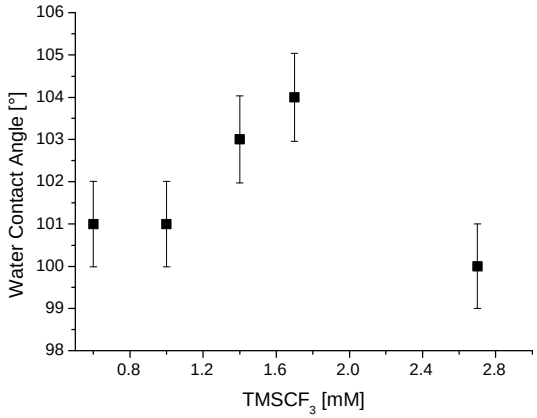

Figure 5.22. The water contact angles measured after reaction between C_{11}-vinyl **1b** SAMs with different concentrations of $TMSCF_3$.

The water contact angle of the unmodified vinyl-terminated film was 101°. The presence of fluorine on the surface was anticipated to increase film's hydrophobicity, however, the change was not expected to be significant. Fluorinated SAMs have been reported to exhibit higher water contact angles than their hydrocarbons.[57, 58] In the case of the reactions performed using 0.6 mM and 1.0 mM of $TMSCF_3$, no change in the water contact angle was observed. After the reaction at 1.4 mM $TMSCF_3$, the water contact angle increased to 103°. The highest value, 104°, was obtained when 1.7 mM solution of $TMSCF_3$ was used as a reagent. Moreover, when a higher concentration of the carbene precursor (2.7 mM) was used in the reaction mixture, the lowest water contact angle of 100° was recorded (**Figure 5.22**).

The same tendency was observed in the case of different reaction times (Appendix 6). The highest contact angle value (CA 104°) was obtained for the reaction performed for 3 h (the same value was previously recorded for the SAMs containing CF_2 groups on the surface[59]). Above 3 h, only lower values were recorded *e.g.* for the 48 h reaction the water contact angle dropped to 83°.

In the case of exposure of C_{18}-methyl **1e** SAMs to $TMSCF_3$ for 3 h, the CA values did not change, which again suggests lack of a reaction (consistent with XPS results).

The results indicate that the reaction parameters, including the concentration of the $TMSCF_3$ reagent and the reaction time, are important for modification of vinyl-terminated SAMs.

5.4.3.3. Ellipsometry

Ellipsometry measurements were used to monitor the onset of film degradation during the reaction of vinyl-terminated SAMs with $:CF_2$ carbene.

No significant differences were measured amongst the films exposed to $TMSCF_3$ (0.6 mM, 1.0 mM, 1.4 mM) for 3 h. However, in the case of the 1.7 mM solution of $TMSCF_3$, the resultant thickness of the modified C_{11}-vinyl **1b** SAM was ~17 Å (compared to ~15 Å for the substrate). This also supports the chemical modification of the surface. Moreover, when a larger concentration of reagent was used (2.7 mM) the film thickness decreased (Appendix 6).

No detectable differences in films thicknesses were observed for SAMs subjected to the 1.7 mM solution of $TMSCF_3$, for 2 h or less. A slight increase in film thickness was noticed in the case of the 3 h reaction product. For the periods of 4 h and 5 h, the lowest thicknesses were obtained indicating film degradation.

The thickness of methyl-terminated SAMs subjected to a 1.7 mM solution of carbene precursor for 3 h remained the same, suggesting a lack of any reaction (consistent with the contact angle and XPS results).

The ellipsometry results are consistent with the XPS and contact angle measurements. The highest conversion of vinyl-terminated SAM for the reaction with $TMSCF_3$ was obtained in the case of 3 h reaction using a 1.7 mM solution of carbene precursor (Appendix 6).

5.4.3.4. Atomic Force Microscopy

Atomic force microscopy images were taken from the vinyl-terminated sample modified with 1.7 mM solution of $TMSCF_3$ for 3 h at 65 °C (**Figure 5.23**).

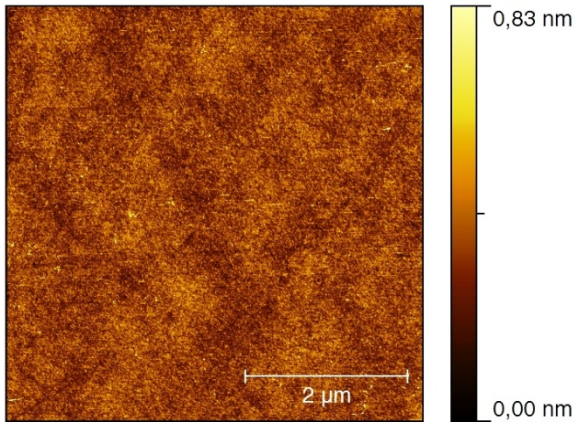

Figure 5.23. AFM image of 5 µm × 5 µm area of C_{11}-vinyl **1b** SAM modified with $:CF_2$ carbene from $TMSCF_3$ (1.7 mM), RMS 79 pm.

The image in **Figure 5.23** shows a very smooth surface with low RMS value. The roughness is similar to the SAM film before modification (Chapter 4). No defects or excess of material was observed.

From these results, it is clear that no detectable changes are observed after film modification with $:CF_2$ carbene. Film roughness increased slightly (from ~60 pm to ~80 pm), which may be caused by the chemical modification on the surface.

5.4.4. Evidence for *gem*-difluorocyclopropane-terminated SAMs

Samples of the modified monolayer film, which exhibited the most intensive F 1s signal, were studied in order to estimate the chemical conversion, and to investigate the nature of the functional groups present on the surface.

The reaction of $TMSCF_3$ with vinyl-terminated SAMs is anticipated to generate a *gem*-difluorocyclopropane-terminated SAM (**Figure 5.24**), consistent with the solution reactions of long chain alkene (**Scheme 5.22**).

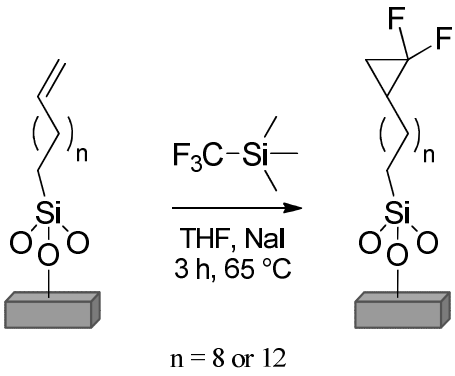

Figure 5.24. Formation of *gem*-difluorocyclopropane-terminated SAMs in the liquid phase.

The highest conversion was observed in the case of the reaction performed for 3 h at 65 °C with 1.7 mM solution of $TMSCF_3$. The progression of the reaction can be monitored by XPS. **Figure 5.25** presents XPS spectra of two different SAM films (**1b** and **1e**) subjected to $TMSCF_3$ using the same reaction conditions.

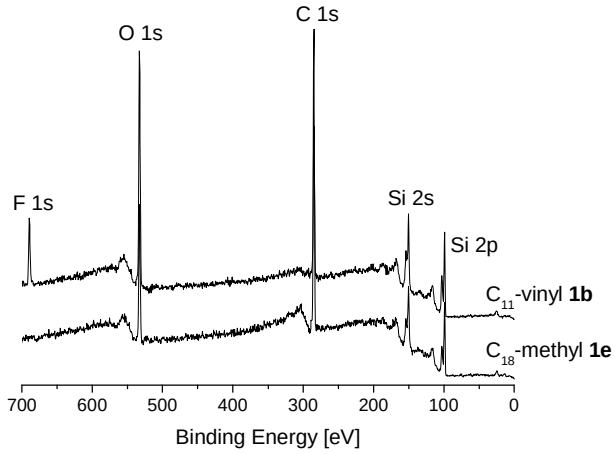

Figure 5.25. The XPS full scans after the reaction of vinyl- **1b** and methyl- **1e** terminated SAMs with $TMSCF_3$.

Successful carbene modification can be observed in the case of C_{11}-vinyl **1b** SAM. In the top spectrum in **Figure 5.25**, a new signal corresponding to fluorine is observed. At the same time, no changes were detected in the case of the methyl-terminated film (bottom spectrum). Such results clearly indicate selective reactivity of the carbene species with terminal double bonds. The position of the F 1s signal at 688.7 eV is characteristic of a C-F species present on the surface.[56] The C 1s region shows three different peaks (**Figure 5.26,** fitting details are provided in Chapter 2, paragraph 2.1.1).

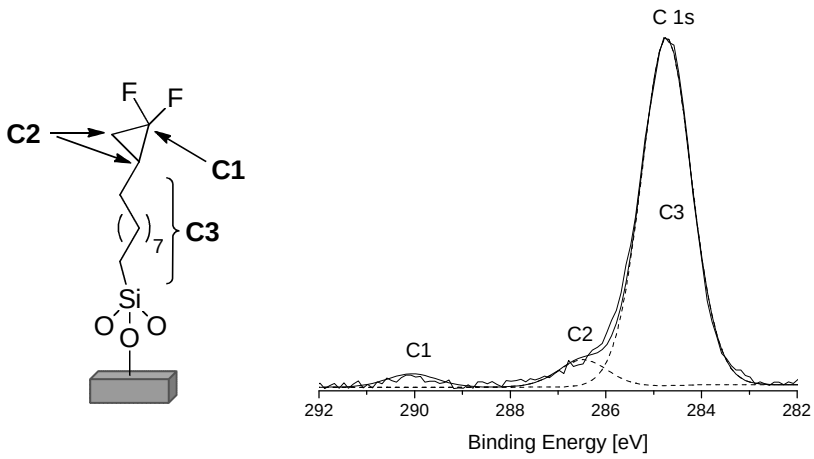

Figure 5.26. Assignment of the C 1s signals according to the formation of *gem*-difluorocyclopropane ring on the surface.

The carbon peak at a binding energy of 290.2 eV is attributed to a $\underline{C}F_2$-$(CH_2)_2$ species and assigned as carbon C1.[56, 60] Peak C2, which has a binding energy of 286.6 eV, is assigned to the two carbon atoms attached to the CF_2 group. The most intense carbon signal (284.6 eV), labelled as carbon C3, is assigned to all of the carbons of the alkyl chain.

Both water contact angle and ellipsometry measurements change after modification of SAMs with :CF_2. The water contact angle increased from 101° to 104°, which is consistent with the addition of difluorocarbene to the surface.[59] Small increases in film thickness, within ~2 Å, were observed (Appendix 6). This might be due to the chemical modification of the surface.

The ratios between the F 1s signal and the C 1s signals (**Figure 5.26**) are consistent with the presence of *gem*-difluorocyclopropane groups. The ratios obtained from C_{11}-vinyl **1b** are listed in **Table 5.2**.

		Ratios		
		$\underline{F}$: $\underline{C}1$	$\underline{F}$: $\underline{C}2$	$\underline{C}1$: $\underline{C}2$
Theor.	C_{11}-vinyl **1b**	2 : 1	1 : 1	1 : 2
Exp.	C_{11}-vinyl **1b**	2.1 : 1	1 : 1	1 : 2

Table 5.2. Theoretical and experimental ratios between F 1s and C 1s signals present on modified SAM.

The yield of the reaction between C_{11}-vinyl **1b** SAM with $TMSCF_3$ can be calculated by taking into account the attenuation factor (paragraph 5.1). Based on the

intensity of the F 1s signal and sum of intensities of the C 1s signals, the difluorocyclopropanation reaction yield is ~47% for the C_{11}-vinyl **1b** SAM.

In order to confirm formation of a *gem*-difluorocyclopropane group in the reaction of vinyl-terminated SAM with :CF_2, a control reaction was performed on a commercially available long chain alkene. Under the same reaction conditions used for the surface chemistry, :CF_2 was generated from $TMSCF_3$ and reacted with 1-decene. The reaction is shown in **Scheme 5.22**.

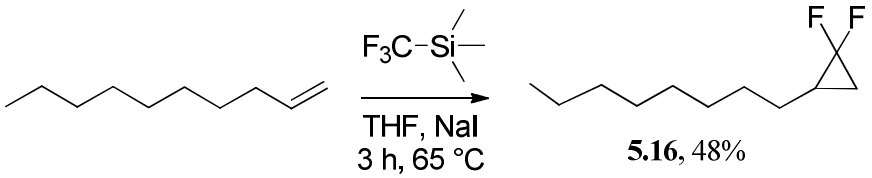

Scheme 5.22. Synthesis of 1,1-difluoro-2-octylcyclopropane **5.16** in the liquid phase.

1,1-Difluoro-2-octylcyclopropane **5.16** (^{19}F NMR, **Figure 5.27**) was obtained in 48% yield (Appendix 7). This lends support that a similar reaction occurred on the vinyl-terminated SAMs.

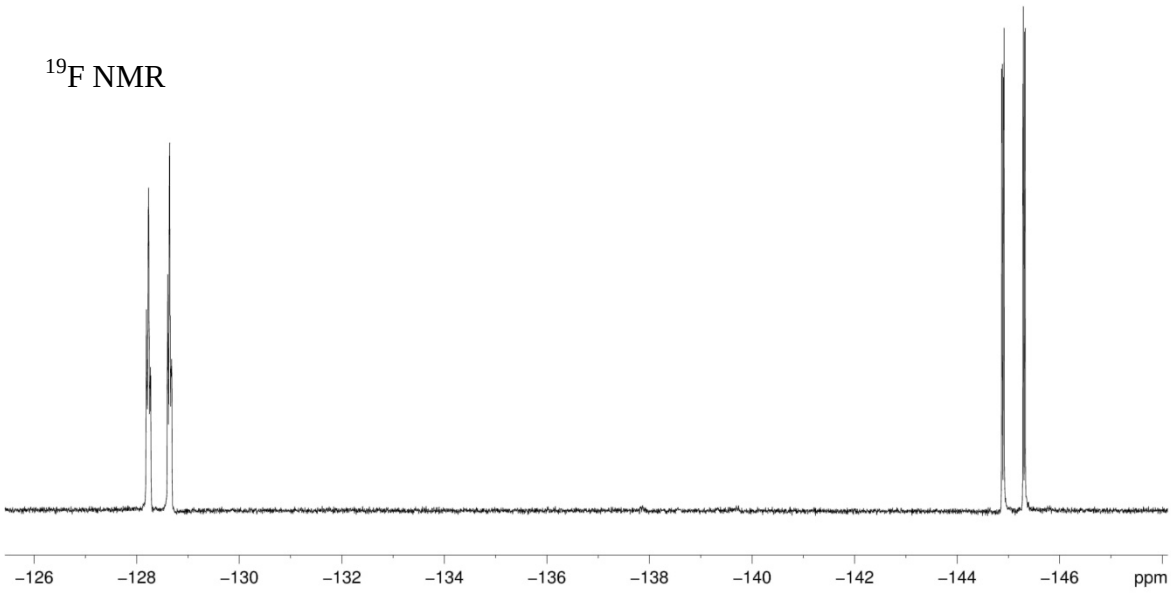

Figure 5.27. ^{19}F NMR of 1,1-difluoro-2-octylcyclopropane **5.16**, prepared in the reaction shown in **Scheme 5.22**.

5.5. Conclusions

Promising modifications of vinyl-terminated SAMs *via* carbene addition has been demonstrated. This new method of C-C bond formation reaction on pre-coated silicon wafers in the liquid phase, opens an attractive route for the selective modification of solid substrates. Moreover, the reaction is not limited to silicon substrates only. Four analytical techniques provided information about SAMs stability under the applied conditions. The balance between modification and degradation of the film was explored and optimised conditions were found. Selectivity for vinyl modification was proven by the lack of a reaction between methyl-terminated SAMs with any of the carbenes. In a control reaction 1,1-dihalo-2-octylcyclopropanes (**5.10**, **5.11** and **5.16**) were obtained with 1-decene was treated in solution.

5.6. Literature

1. A. Ulman, *Chem. Rev.*, 1996, **96**, 1533-1554.
2. A. Ulman, *An Introduction to Ultrathin Organic Films from Langmuir-Blodgett to Self-Assembly*, Academic Press, San Diego, 1991.
3. J. Clayden, N. Greeves and S. Warren, *Organic Chemistry*, 2 edn., Oxford University Press, Oxford New York, 2012.
4. S. R. Wasserman, Y. T. Tao and G. M. Whitesides, *Langmuir*, 1989, **5**, 1074-1087.
5. N. Balachander and C. N. Sukenik, *Langmuir*, 1990, **6**, 1621-1627.
6. Y. S. Cohen, A. Vilan, I. Ron and D. Cahen, *J. Phys. Chem. C*, 2009, **113**, 6174-6181.
7. N. Chanunpanich, A. Ulman, Y. M. Strzhemechny, S. A. Schwarz, A. Janke, H. G. Braun and T. Kraztmuller, *Langmuir*, 1999, **15**, 2089-2094.
8. S. A. Mirji, *Surf. Interface Anal.*, 2006, **38**, 158-165.
9. M. Adamkiewicz, T. O'Hara, D. O'Hagan and G. Hähner, *Thin Solid Films*, 2012, **520**, 6719-6723.
10. J. F. Watts and J. Wolstenholme, *An Introduction to Surface Analysis by XPS and AES*, John Wiley & Sons Ltd, Chichester, West Sussex, 2003.
11. H. S. Hansen, S. Tougaard and H. Biebuyck, *J. Electron. Spectrosc.*, 1992, **58**, 141-158.
12. N. Faucheux, R. Schweiss, K. Lützow, C. Werner and T. Groth, *Biomaterials*, 2004, **25**, 2721-2730.
13. R. A. Jones, *Quarternary Ammonium Salts: Their Use in Phase-Transfer Catalysis*, Academic Press, Trowbridge, UK, 2000.
14. W. von E. Doering and A. K. Hoffmann, *J. Am. Chem. Soc.*, 1954, **76**, 6162-6165.
15. W. E. Parham and E. E. Schweizer, *J. Org. Chem.*, 1959, **24**, 1733-1735.
16. P. Kadaba and J. Edwards, *J. Org. Chem.*, 1960, **25**, 1431-1433.
17. F. Grant and W. Cassie, *J. Org. Chem.*, 1960, **25**, 1433-1434.
18. U. Schöllkopf and P. Hilbert, *Angew. Chem., Int. Ed.*, 1962, **1**, 401-401.
19. D. Seyferth, J. M. Burlitch, R. J. Minasz, J. Yick-Pui Mui, H. D. Simmons, A. J. H. Treiber and S. R. Dowd, *J. Am. Chem. Soc.*, 1965, **87**, 4259-4270.
20. G. Köbrich, H. Büttner and E. Wagner, *Angew. Chem., Int. Ed.*, 1970, **9**, 169-170.
21. M. Makosza and M. Wawrzyniewicz, *Tetrahedron Lett.*, 1969, **10**, 4659-4662.
22. C. M. Starks, *J. Am. Chem. Soc.*, 1971, **93**, 195-199.
23. S. W. Tobey and R. West, *J. Am. Chem. Soc.*, 1964, **86**, 56-61.
24. S. Julia and A. Ginebreda, *Synthesis*, 1977, 682-683.
25. M. Makosza, *Pure Appl. Chem.*, 2000, **72**, 1399-1403.
26. F. Sirovski, C. Reichardt, M. Gorokhova, S. Ruban and E. Stoikova, *Tetrahedron*, 1999, **55**, 6363-6374.
27. F. Sirovski, M. Gorokhova and S. Ruban, *J. Mol. Catal. A: Chem.*, 2003, **197**, 213-222.
28. H. X. Lin, M. F. Yang, P. G. Huang and W. G. Cao, *Molecules*, 2003, **8**, 608-613.
29. J. P. Jayachandran and M.-L. Wang, *Appl. Catal. A*, 2001, **206**, 19-28.
30. V. Rajendran and M. L. Wang, *J. Mol. Catal. A: Chem.*, 2008, **288**, 23-27.
31. M.-L. Wang, Y.-M. Hsieh and R.-Y. Chang, *J. Mol. Catal. A: Chem.*, 2003, **198**, 111-124.
32. H. Ziyat, M. Y. A. Itto, M. A. Ali, A. Riahi, A. Karim and J. C. Daran, *Arkivoc*, 2006, 152-160.
33. S. Ciampi, J. B. Harper and J. J. Gooding, *Chem. Soc. Rev.*, 2010, **39**, 2158-2183.

34. M. Calistri-Yeh, E. J. Kramer, R. Sharma, W. Zhao, M. H. Rafailovich, J. Sokolov and J. D. Brock, *Langmuir*, 1996, **12**, 2747-2755.
35. D. R. Lidle, *CRC Handbook of Chemistry and Physics 90th Edition*, CRC Press, Boca Raton, Florida, 2010.
36. M. K. F. Lo, M. N. Gard, B. R. Goldsmith, M. A. Garcia-Garibay and H. G. Monbouquette, *Langmuir*, 2012, **28**, 16156-16166.
37. J. K. Chen, C. Y. Hsieh, C. F. Huang, P. M. Li, S. W. Kuo and F. C. Chang, *Macromolecules*, 2008, **41**, 8729-8736.
38. S. D. Naik and L. K. Doraiswamy, *Aiche J.*, 1998, **44**, 612-646.
39. D. Seyferth, J. Yick-Pui Mui, M. E. Gordon and J. M. Burlitch, *J. Am. Chem. Soc.*, 1965, **87**, 681-682.
40. D. Seyferth, H. Dertouzos, R. Suzuki and J. Y. P. Mui, *J. Org. Chem.*, 1967, **32**, 2980-2984.
41. D. Seyferth, S. P. Hopper and K. V. Darragh, *J. Am. Chem. Soc.*, 1969, **91**, 6536-6537.
42. D. Seyferth and S. P. Hopper, *J. Org. Chem.*, 1972, **37**, 4070-4075.
43. D. J. Burton and D. G. Naae, *J. Am. Chem. Soc.*, 1973, **95**, 8467-8468.
44. Y. Bessard, U. Muller and M. Schlosser, *Tetrahedron*, 1990, **46**, 5213-5221.
45. W. R. Dolbier, H. Wojtowicz and C. R. Burkholder, *J. Org. Chem.*, 1990, **55**, 5420-5422.
46. D. Babin, F. Pilorge, L. M. Delbarre and J. P. Demoute, *Tetrahedron*, 1995, **51**, 9603-9610.
47. Y. Fujioka and H. Amii, *Org. Lett.*, 2008, **10**, 769-772.
48. F. Tian, V. Kruger, O. Bautista, J.-X. Duan, A.-R. Li, W. R. Dolbier and Q.-Y. Chen, *Org. Lett.*, 2000, **2**, 563-564.
49. X. H. Cai, Y. Zhai, I. Ghiviriga, K. A. Abboud and W. R. Dolbier, *J. Org. Chem.*, 2004, **69**, 4210-4215.
50. W. R. Dolbier, F. Tian, J. X. Duan, A. R. Lia, S. Ait-Mohand, O. Bautista, S. Buathong, J. M. Baker, J. Crawford, P. Anselme, X. H. Cai, A. Modzelewska, H. Koroniak, M. A. Battiste and Q. Y. Chen, *J. Fluor. Chem.*, 2004, **125**, 459-469.
51. Z. L. Cheng and Q. Y. Chen, *J. Fluor. Chem.*, 2005, **126**, 93-97.
52. F. Wang, T. Luo, J. B. Hu, Y. Wang, H. S. Krishnan, P. V. Jog, S. K. Ganesh, G. K. S. Prakash and G. A. Olah, *Angew. Chem., Int. Ed.*, 2011, **50**, 7153-7157.
53. S. Eusterwiemann, H. Martinez and W. R. Dolbier, *J. Org. Chem.*, 2012, **77**, 5461-5464.
54. T. R. Wu, L. Shen and J. M. Chong, *Org. Lett.*, 2004, **6**, 2701-2704.
55. X.-S. Fei, W.-S. Tian and Q.-Y. Chen, *J. Chem. Soc., Perkin Trans. 1*, 1998, 1139-1142.
56. S. Ohnishi, T. Ishida, V. V. Yaminsky and H. K. Christenson, *Langmuir*, 2000, **16**, 2722-2730.
57. A. K. Gnanappa, C. O'Murchu, O. Slattery, F. Peters, T. O'Hara, B. Aszalos-Kiss and S. A. M. Tofail, *J. Phys. Chem. C*, 2008, **112**, 14934-14942.
58. U. Srinivasan, M. R. Houston, R. T. Howe and R. Maboudian, *J. Microelectromech. Syst.*, 1998, **7**, 252-260.
59. M. Motomatsu, W. Mizutani, H.-Y. Nie and H. Tokumoto, *Thin Solid Films*, 1996, **281–282**, 548-551.
60. A. Hozumi, K. Ushiyama, H. Sugimura and O. Takai, *Langmuir*, 1999, **15**, 7600-7604.

6. Chemical Surface Modification in the Vapour Phase

Silane-based self-assembled monolayers (SAMs) formed with long organic chains play an important role in surface chemistry as they can establish physically,[1, 2] thermally[3, 4] and chemically stable films[5] on substrates such as silicon oxide and glass. The functionalisation of solid substrates by self-assembly processes offers the potential to tailor surface properties in a controllable fashion. There are many options to deposit a SAM with fixed properties from solution or to chemically modify a pre-formed SAM in solution.[6-8] While SAM deposition from the vapour phase is known[9] and commonly applied for manufacturing in industry,[10] chemical surface modification from the gas phase is much more limited. Several examples of SAM modification with gas-phase ozone have been reported in the literature,[11-13] however, formation of a new C-C bond on the surface from the vapour phase is challenging and has not previously been reported. The C-C bond formation reaction might serve as a promising route for surface modification in an industrial setting and might be easily adapted for industrial manufacturing.

The aim of this Chapter is to describe a C-C bond functionalisation method of a pre-coated silicon substrate from the gas phase. X-ray photoelectron spectroscopy, atomic force microscopy, ellipsometry and contact angle analysis were performed to investigate the progresses of the gas phase reactions of SAMs and their stability under the applied conditions.

6.1. Fluorinated Precursors

The two commercially available fluorinated molecules, shown in **Figure 6.1**, were used to modify vinyl-terminated SAMs on silicon substrates in the vapour phase. Hexafluoroacetone azine (HFAA) is a colourless liquid with a boiling point of 67-68 °C, whereas hexafluoropropene oxide (HFPO) is a colourless, non-flammable gas with a boiling point of -27.4 °C.[14]

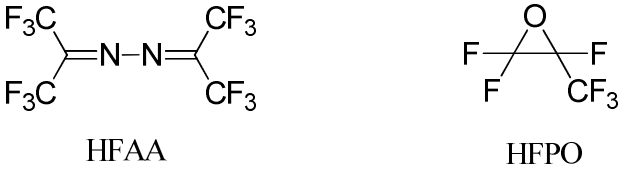

Figure 6.1. Reagents used in SAM functionalisation from the vapour phase.

These compounds were selected to modify vinyl-terminated SAMs because of their established[14, 15] reactivity in the vapour phase. The introduction of a fluorine was particularly attractive as this is anticipated to change the surface properties *e.g.* hydrophobicity. The presence of fluorine on the surface can be readily detected by XPS. Fluorine is the most electronegative element, so it can influence the position of the adjacent carbons' C 1s signals, allowing the formed structure on the surface to be investigated.

6.2. Chemistry on SAMs involving hexafluoroacetone azine

"Carbene-like" chemistry is envisaged to occur when HFAA comes into contact with vinyl-terminated SAMs. The preparation and quality of the SAMs used as starting materials were discussed in Chapter 4. The vapour phase reaction investigated in this section is shown in **Scheme 6.1**.

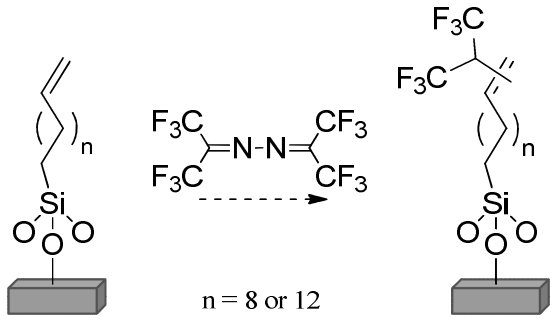

Scheme 6.1. Anticipated vapour phase covalent modification of vinyl-terminated films.

6.2.1. Chemistry of HFAA and sources of *bis*(trifluoromethyl)carbene

The reactivity of HFAA and the intermediates formed during reaction, as well as the mechanism of reaction on a double bond, have been a source of discussion for several years.[16, 17]

In 1966, Gale *et al.*,[16] investigated the chemistry of perfluorodiazo compounds with an emphasis on the formation of fluorinated carbene :$C(CF_3)_2$. It was found that by reacting *bis*(trifluoromethyl)diazomethane (**6.1**) with an excess of *trans*-2-butene in an autoclave at 150 °C, *trans*-1,2-dimethyl-3,3-*bis*(trifluoromethyl) cyclopropane (**6.2**) was obtained in 53% yield (**Scheme 6.2**).

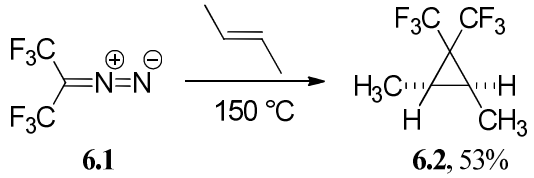

6.1 **6.2**, 53%

Scheme 6.2. The reaction of *bis*(trifluoromethyl)diazomethane (**6.1**) with *trans*-2-butene.

The same carbene can also be formed from *bis*(trifluoromethyl)diazirine (**6.3**). The carbene :$C(CF_3)_2$ is generated through the loss of N_2. It can react with *trans*-2-butene to give *trans*-1,2-dimethyl-3,3-*bis*(trifluoromethyl) cyclopropane (**6.4**, 57%), *trans*- 6,6,6-trifluoro-5-trifluoro-methyl-2-hexene (**6.5**, 39%) and *cis*-5,5,5-trifluoro-4-trifluoromethyl-3-methyl-2-pentene (**6.6**, 4%) (**Scheme 6.3**).[16]

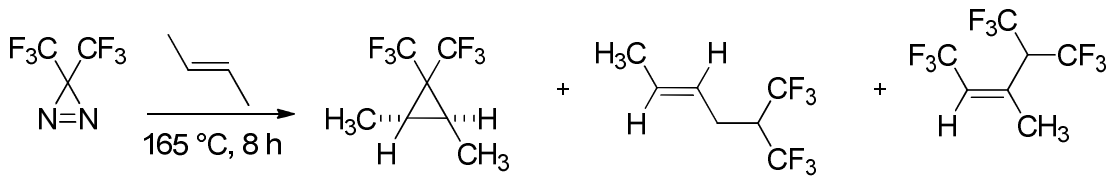

6.3 **6.4**, 57% **6.5**, 39% **6.6**, 4%

Scheme 6.3. Thermal reaction of *bis*(trifluoromethyl)diazirine (**6.3**) with *trans*-2-butene.

It was also found that pyrolysis of *bis*(trifluoromethyl)diazirine (**6.3**) over quartz at 300 °C gave two products, hexafluoropropene (**6.7**) and hexafluoroacetone azine (**6.8**) (**Scheme 6.4**).[16]

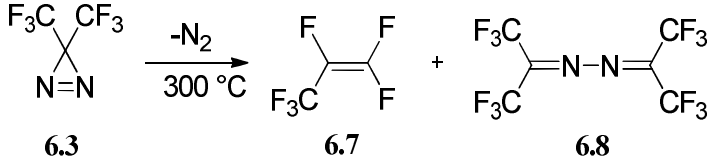

6.3 **6.7** **6.8**

Scheme 6.4. The products obtained after pyrolysis of *bis*(trifluoromethyl)diazirine (**6.3**).

In 1968, Middleton *et al.*,[18] investigated thermal reactions of diazo compounds with saturated hydrocarbons. They found that a range of products formed when either *bis*(trifluoromethyl)diazomethane (**6.1**) or *bis*(trifluoromethyl)diazirine (**6.3**) was heated with cyclohexane. In both cases only a small amount of the expected carbene insertion product **6.9** was obtained (**Scheme 6.5**).

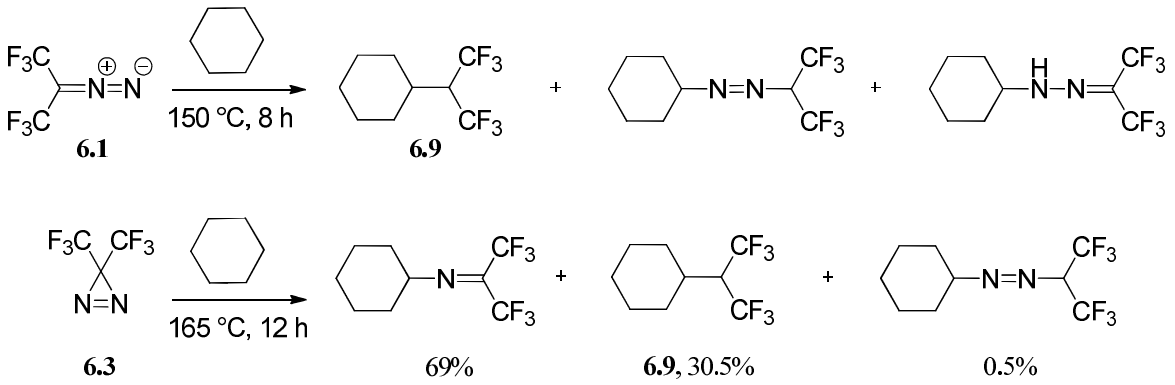

Scheme 6.5. Products of thermal reactions of *bis*(trifluoromethyl) diazomethane (**6.1**) and *bis*(trifluoromethyl)diazirine (**6.3**) with cyclohexane.

They also found[18] that hexafluoroacetone azine (HFAA) reacts with cyclohexane at 165 °C to give the carbene insertion product **6.10** (**Scheme 6.6**). Middleton and co-workers[18] considered that HFAA may offer the best source of $:C(CF_3)_2$ for an insertion reaction with saturated hydrocarbons. However, it was suspected that the free carbene might not be directly involved in the reaction. Unlike *bis*(trifluoromethyl)diazomethane (**6.1**) and *bis*(trifluoromethyl)diazirine (**6.3**), HFAA did not react with benzene at 165 °C to give any carbene addition products.[16, 18]

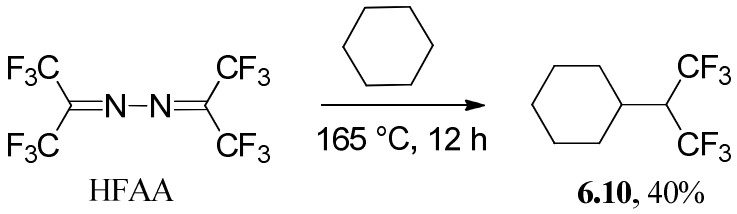

Scheme 6.6. The addition reaction of hexafluoroacetone azine with cyclohexane.

One year later, Forshaw *et al.*,[19] reported that the thermal reaction of HFAA with olefins of CH_2=CHR type (where R = -H, $-CH_3$, $-CH_2CH_3$) gave 'criss-cross' (1,3- ; 4,2-) addition products (**6.11**, **6.12**, **6.13**) (**Scheme 6.7**). They also claimed that HFAA is stable

up to 240 °C and under the conditions used by Middleton *et al.*,[18] the formation of :C(CF$_3$)$_2$ carbene was unlikely (**Scheme 6.6**).

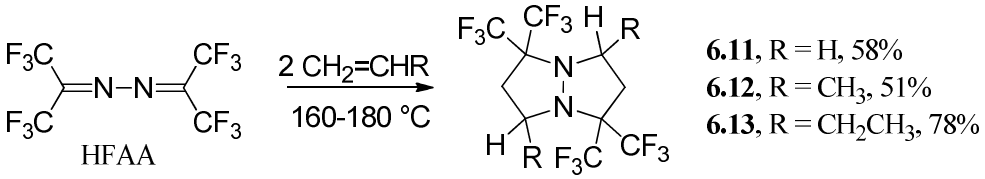

6.11, R = H, 58%
6.12, R = CH_3, 51%
6.13, R = CH_2CH_3, 78%

Scheme 6.7. Formation of the 'criss-cross' (1,3- ; 4,2-) products (**6.11**, **6.12**, **6.13**) in the reaction of hexafluoroacetone azine with olefins.

In 1971, Forshaw and Tipping[20] proposed a mechanism for the formation of the 'criss-cross' adduct. They suggested that the reaction involves a bimolecular two-step process with the formation of 'diradical' species (**Scheme 6.8**). A 'diradical' mechanism was supported by the fact that the reaction occurs in the vapour phase under thermal and photochemical conditions.[20]

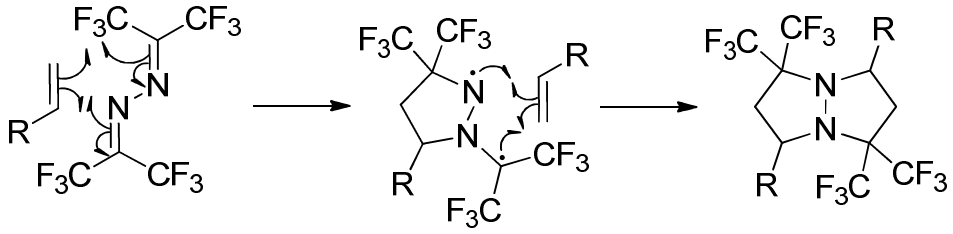

Scheme 6.8. Radical mechanism proposed for the formation of 'criss-cross' adducts.

In the same year Middleton[17] re-examined the reaction of HFAA with cyclohexane in the temperature range of 129 – 170 °C. The observed products confirmed Forshaw's and Tipping's[19] observation that the hexafluoroacetone azine does not initially create :C(CF$_3$)$_2$ carbene. He confirmed that the azine reacts mainly through a radical mechanism, however, :C(CF$_3$)$_2$ carbene is also formed but in a small amount.

6.2.2. Thermal stability of SAMs

Chemical modification of SAMs in the vapour phase involves elevated temperatures, thus it is crucial to learn about SAM stability. Alkyltrichlorosilane based self-assembled monolayers on silicon are considered to form very stable films.[4] In 1986, Cohen and Sagiv[21] demonstrated that octadecyltrichlorosilane (OTS) films were stable up to 140 °C in air. Kluth *et al.*,[22] investigated the thermal behaviour of SAMs formed from methyl-terminated trichlorosilanes. They found that films, independent of their chain length, were stable at 460 °C under vacuum for 30 min. Above this temperature, the monolayer began to decompose through C-C bond cleavage, resulting in a gradual decrease in chain length. One year later, the same group[23] performed similar experiments with a film prepared from pentadecyltrichlorosilane molecules (C_{15}) where the last four carbon atoms of the chain were deuterated. It was found that the deuterated carbon atoms desorb before the hydrogenated carbon atoms, confirming film decomposition through C-C bond cleavage.

Srinivasan[24] investigated the thermal stability of two types of SAM coatings formed from the hydrocarbon precursor, octadecyltrichlorosilane [CH_3-$(CH_2)_{17}$-$SiCl_3$, OTS] and the fluorinated precursor, 1H,1H,2H,2H-perfluorodecyltrichlorosilane [CF_3-$(CF_2)_7$-$(CH_2)_2$-$SiCl_3$, FDTS]. Both films were stable when kept at 450 °C for 5 min under a N_2 atmosphere. However, in air, the OTS film started to degrade at 150 °C, but the FDTS film remained intact up to 400 °C. This observation was explained by the fact that the degradation of a fluorinated alkyl chain is more difficult due to the higher energy of a C-F bond compared with a C-H bond. Similar stabilities of OTS and FDTS films were observed by Seo and Sung.[25] Kim *et al.*,[26] claimed that OTS films were stable in air up to about 200 °C. However, the temperature under which SAMs were stable was about 250 °C lower in air than under vacuum, which supports the observation that water and oxygen in air can accelerate C-C bond cleavage. Kulkarni *et al.*,[27] demonstrated that OTS SAMs were stable in air up to 250 °C and were completely decomposed around 400 °C.

Klein *et al.*,[28] have recently published their results regarding the thermal stability of SAMs based on non-fluorinated and fluorinated molecules. They investigated thermal degradation of films in a dry and oxygen-rich environment as well as under vacuum. Samples were analysed after being kept for 1 h at an elevated temperature. In a dry and oxygen-rich environment OTS SAMs were stable up to 120 °C. Between 120-250 °C, C-C bond cleavage was observed. Above 250 °C, the remaining films were converted to a

'graphitic' coating with C=C bonds. The same situation was observed in the case of fluorinated SAMs, which were stable up to 300 °C. Above 350 °C, fluorine atoms were removed from the remaining molecules, and the films were converted into a 'graphitic' layer. However, they observed that under vacuum the fluorinated SAMs were stable up to 550 °C, while above this temperature, entire molecules were removed from the surface, because of Si-O-Si bond cleavage.

These stability experiments were performed under rather harsh conditions, where samples were tested *e.g.* at high temperatures under vacuum or in an oxygen-rich environment. In the present work it was important to establish how resistant a coated silicon wafer is at 160 °C, and how long it can resist without significant degradation. The exposure time to high temperatures studied by others[24] was usually short and the longest exposure experiment (which lasted for 1 h) was carried out by Klein *et al*.[28] Consequently a temperature of 160 °C was chosen in this study with the known reactivity of HFAA at this temperature.[18] Two different SAM films formed from decyltrichlorosilane **1d** (CH_3-$(CH_2)_9$-$SiCl_3$, C_{10}-methyl) and octadecanetrichlorosilane **1e** (CH_3-$(CH_2)_{18}$-$SiCl_3$, C_{18}-methyl), were used in order to test their resistance to temperature. Investigated films were prepared according to the liquid phase process discussed in Chapter 4.

Ten individual SAM coatings of each **1d** and **1e** were freshly prepared on silicon substrates. Each of the substrates was placed in a separate glass vial. The vials were then purged with nitrogen and sealed. Then, they were placed in a heating block, pre-heated to 160 °C. The wafers were kept at this temperature for fixed periods of time (1 h, 2 h, 3 h, 4 h, 5 h, 6 h, 13 h, 19 h, 24 h, 48 h). After each period a wafer of **1d** and **1e** was taken out and characterised.

6.2.3. Results and Discussion

Contact angle goniometry and ellipsometry were used to monitor the thermal stability of methyl-terminated SAMs.

6.2.3.1. Water Contact Angle

The water contact angles were measured before the SAM wafers were exposed to 160 °C and then immediately after the experiment. The contact angle results are shown in **Figure 6.2**.

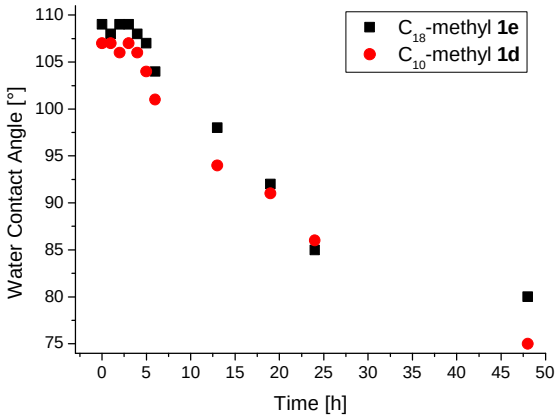

Figure 6.2. Water contact angle (°), of C_{18}-methyl **1e** and C_{10}-methyl **1d** SAMs before and after thermal degradation at 160 °C (Appendix 8).

The water contact angle data provides information about surface coverage during various stages of degradation. Both of the examined films exhibited high water contact angles before heat-treatment, 109° and 107° for **1e** and **1d**, respectively. **Figure 6.2** shows that the films remained intact for the first 5 h and the measured CA values remained above 105°, suggesting the presence of a hydrophobic coating on the surface. However, the contact angle gradually decreased when the samples were heated for 13 h or more, suggesting film degradation. Both methyl-terminated films behaved in the same way, which is in accordance with observations made by Kluth *et al*.[22]

6.2.3.2. Ellipsometry

The thickness of the films was measured for all samples. **Figure 6.3** shows how SAMs' thickness changed with temperature over time.

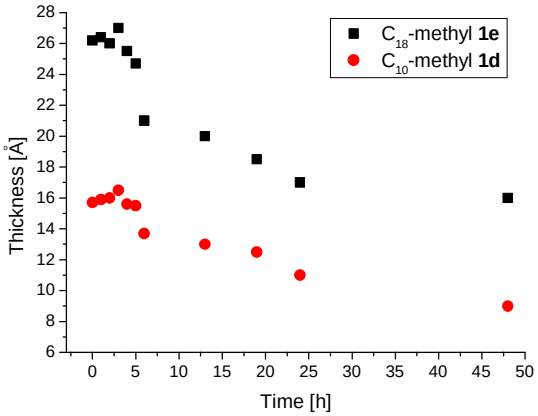

Figure 6.3. Values of thicknesses for silicon wafers with C_{18}-methyl **1e** and C_{10}-methyl **1d** SAMs before and after thermal degradation (Appendix 8).

For the first 5 h, the film thickness did not change significantly. Small variations within ~1 Å were not considered significant as they are within experimental error. From 6 h onwards, the film thickness gradually decreased. Observed changes in film thickness are in good agreement with the measured contact angle results (**Figure 6.2**).

Results obtained from both techniques clearly indicate SAM degradation, which was manifest by a decreasing contact angle and decreasing thickness. It was found that the monolayers were stable up to 5 h at 160 °C. After 6 h they started to decompose. However, the stability of the examined films was better than that found for the hydrocarbon SAMs reported in the literature. Previous experiments showed that SAMs were stable only for *e.g.* 1 h at 120 °C in a dry, oxygen-rich environment[28] or for 5 min at 450 °C in a nitrogen atmosphere.[24] The conditions, in these previous experiments, favoured the formation of radicals, which may cause film decomposition *via* C-C bond cleavage as proposed by Kluth *et al.*[22, 23] Experiments described in this section were performed at lower temperatures under a nitrogen atmosphere, which significantly increased the durability of the SAMs. There is no obvious reason why the films decompose after 5 h at 160 °C. At such a low temperature, it is unlikely that the C-C bonds break without a catalyst. However, the experiments were not performed in a glove-box, thus the reaction environment might have low level air contamination. This could explain the slow decomposition of the film *via* C-C bond cleavage. Alternatively, a small amount of water may have been trapped between the self-assembling molecules and the substrate, during the SAM formation process, which might lead to the cleavage of the Si-O bond.[29] It is also possible that both mechanisms work in parallel to contribute to a slow degradation.

6.2.4. Optimisation of the reaction conditions for SAMs modification

Chemical modification of vinyl-terminated self-assembled monolayers in the vapour phase is rare. This kind of chemistry significantly differs from traditional solution chemistry. In the case of SAMs, one reactant is covalently bonded to a surface. Low accessibility and restricted conformational freedom of the terminal functional group might influence the formation or nature of the product – the new film. The optimisation of the reaction conditions between hexafluoroacetone azine and vinyl-terminated SAMs is now described in detail. The aim was to obtain a maximum conversion with minimum film degradation. All films were fully characterised.

6.2.4.1. Procedure for the reaction of HFAA with SAMs

Silicon wafers, coated with vinyl- or methyl- terminated SAMs, were placed in one of the two chambers of a glass reaction vessel (100 mL capacity). HFAA was added (50 µL, 100 µL, 150 µL, 200 µL, 300 µL and 400 µL) into the second chamber under a nitrogen atmosphere. There was no direct contact between the liquid HFAA and the pre-coated silicon wafer. The reaction vessel was sealed and heated at fixed temperatures (80 °C, 120 °C, 160 °C) for defined time periods (10 min, 20 min, 30 min, 1 h, 2 h, 5 h, 48 h). After each reaction, the samples were sonicated (15 min) sequentially in toluene, dichloromethane, and then deionised water to remove any by-products formed during the reaction.

6.2.4.2. Results and Discussion

In order to monitor reaction progress on vinyl-terminated SAMs, thickness, surface coverage and chemical composition were determined by X-ray photoelectron spectroscopy (XPS), static water contact angle measurements, ellipsometry and atomic force microscopy (AFM).

As described earlier, self-assembled monolayers are stable at elevated temperatures. SAMs prepared according to the procedure described in Chapter 4 can withstand 160 °C for 5 h under a nitrogen atmosphere, which was verified experimentally. However, the stability of SAMs under elevated temperatures in the presence of other chemicals is unknown. To optimise the reaction conditions, several experiments were performed. The work was divided into three parts in order to optimise each parameter

separately. The first experiment focused on finding the lowest possible temperature, under which SAMs efficiently react with HFAA, because higher temperatures in the presence of additional chemicals can destroy the films.[28, 30] In the second part the optional reaction time was investigated. And finally, the third part focused on finding the optimal amount of starting material required for the most efficient conversion.

6.2.4.2.1. X-ray Photoelectron Spectroscopy

Optimisation of reaction temperature

The first experiment was designed to find the optimum temperature for the reaction between vinyl-terminated SAMs and HFAA. C_{11}-vinyl **1b** SAMs were reacted with HFAA (100 µL in the container) for 20 min at fixed temperatures (80 °C, 120 °C, 160 °C).

XPS analysis proved to be a useful tool for monitoring the reaction progress/conversion on SAMs. The product of the reaction between vinyl-terminated SAMs and HFAA was expected to contain a fluorinated terminal group. However, it is also known that HFAA can form a nitrogen containing adduct, thus regions of the spectrum where fluorine and nitrogen peaks appear, were carefully analysed. The XPS survey spectra taken from samples after the reactions at 80 °C, 120 °C and 160 °C are shown in **Figure 6.4** and **Figure 6.5**.

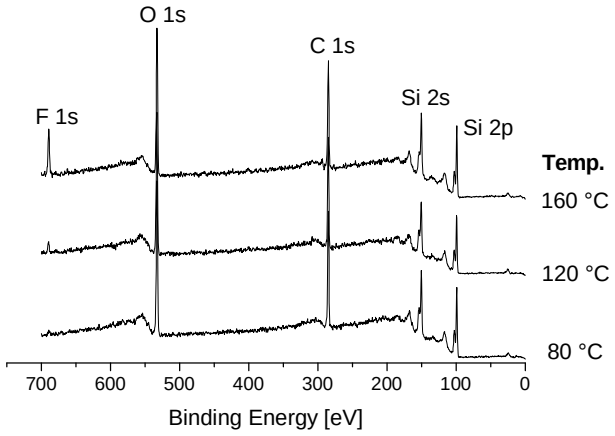

Figure 6.4. The XPS survey spectra taken from C_{11}-vinyl **1b** SAMs reacted with HFAA at different temperatures.

The vinyl-terminated SAMs are expected to give rise to XPS signals showing the elements silicon, carbon and oxygen. After the modification a new signal, with a binding energy of 688.9 eV, appeared on the XPS in the case of the reactions performed at 120 °C and 160 °C. The new signal can be assigned to fluorine. However, there were significant

differences in peak intensities. The intensity of the F signal for the reaction carried out at 120 °C was much smaller than the F signal observed for the reaction at 160 °C. XPS counts electrons ejected from a sample surface and the peak intensity measures how much of the material is at the surface.[31] Thus the intensity of the fluorine signal is a crude measure of reaction conversion. The more fluorine is observed on the surface, the more double bonds have reacted with HFAA.

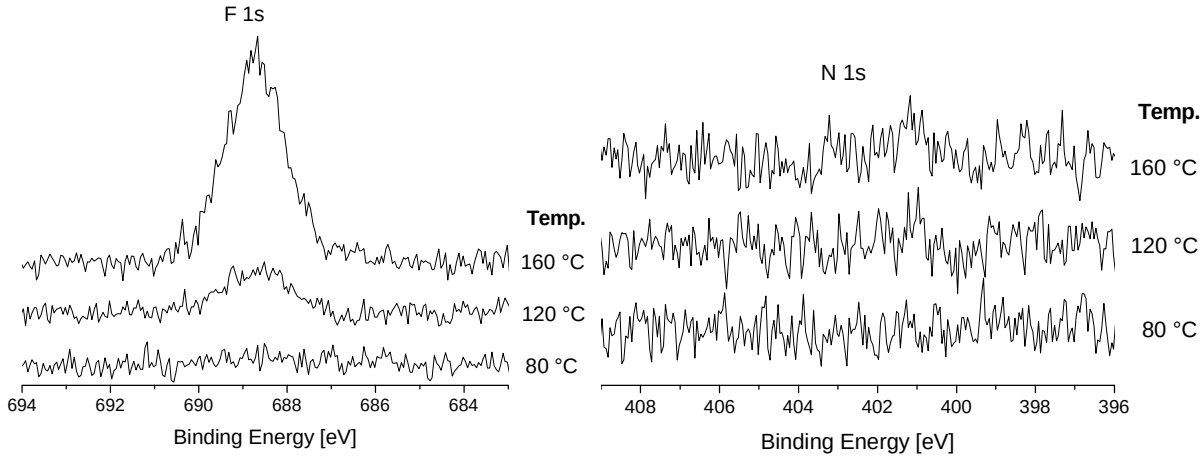

Figure 6.5. The XPS high resolution scans of F 1s and N 1s regions taken from C_{11}-vinyl **1b** SAMs reacted with HFAA at different temperatures.

From the high resolution scans, it was observed that the fluorine signal is symmetric. The position (688.9 eV) and symmetric shape of the peak suggests that the F present on the surface has a single chemical environment, consistent with a CF_3 group.[32] The experiments led to the conclusion that the highest conversion is achieved when the reaction is performed at 160 °C.

It is also known that HFAA can form a nitrogen-containing 'criss-cross' adduct, which consists of one HFAA molecule reacting with two alkenes (**Scheme 6.7**). However, the absence of a nitrogen signal on XPS (**Figure 6.5**), suggest that such a species is not relevant in this reaction. The formation of such a bicyclic ring product is presumably impeded by the intramolecular nature of the reaction on the surface. This gets some support from the observation of Koloski *et al*.[33] The authors explored nucleophilic displacement reactions on benzyl halide SAMs. In those experiments a benzyl chloride (Bz-Cl) film, formed from (*p*-chloromethylphenyl)trichlorosilane $ClCH_2$-C_6H_4-$SiCl_3$, was used as a starting material. Next, NaI was introduced as an I^- source to displace Cl^-. It was found that only half of the Cl atoms were replaced with I, which was explained by the

steric hindrance of the incoming halogen. However, when a less-hindered film was used, Bz-ECl, formed from *p*-chloromethyl(phenylethyl)trichlorosilane $ClCH_2$-C_6H_4-$CH_2CH_2SiCl_3$, a complete conversion to the iodinated product was obtained.[33] Thus steric hindrance and conformational limitations are significant for surface reactions.

Optimisation of reaction time

A series of experiments was designed to explore how long a film can be subjected to react with HFAA at 160 °C without degradation. From the thermal stability experiment, it was shown that SAMs under a nitrogen atmosphere can withstand an elevated temperature of 160 °C for 5 h. However, for a chemical reaction the additional reagent (HFAA) was present in the environment, and this may accelerate SAM decomposition. Accordingly, C_{11}-vinyl **1b** SAMs were reacted with HFAA (50 µL) at 160 °C for fixed periods of time (10 min, 20 min, 30 min, 1 h, 2 h, 5 h, 48 h). The reaction progress was monitored by XPS and the results are shown in **Figure 6.6**.

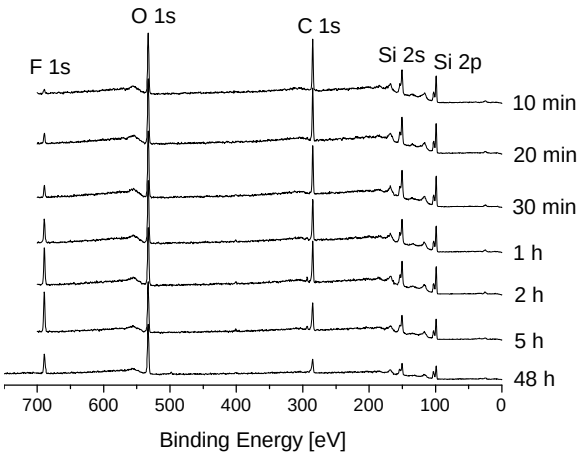

Figure 6.6. XPS survey spectra taken after the reaction between C_{11}-vinyl **1b** SAMs and HFAA for fixed periods of time at 160 °C.

It was observed that the intensity of the F signal on the surface increased with longer reaction times. The smallest peak was recorded on the surface after 10 min, whereas for a reaction time of 2 h, the most intense peak was detected. However, with increasing F signal, the C signal decreased. This is obvious by comparing the spectra of *e.g.* 2 h and 5 h reactions. From this experiment, it was found that SAMs remained stable when the reaction time was not longer than 20 min. Above 20 min, film degradation was already obvious. This was also confirmed by other analytical methods discussed later in this Chapter. Moreover, when the reaction time was longer than 30 min, a small signal at a

binding energy of 400.9 eV, was detected. This new signal was assigned to nitrogen. The high resolution spectra of the N 1s region are shown in **Figure 6.7**.

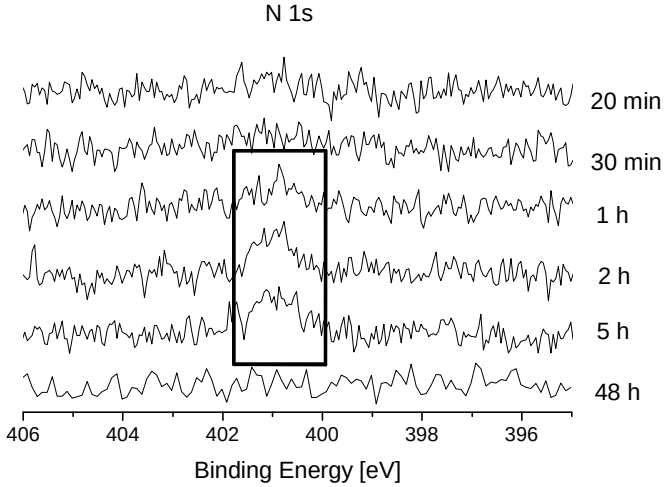

Figure 6.7. High resolution scans of N 1s region for the reaction performed at fixed periods of time on C_{11}-vinyl **1b** SAMs, when exposed to HFAA at 160 °C.

The N 1s signal is highlighted in the black frame in **Figure 6.7**. A nitrogen peak appeared in samples which were reacted with HFAA for 1 h, 2 h and 5 h. However, no nitrogen was detected on a surface after 48 h, most likely due to significant film degradation. The presence of nitrogen might suggest formation of a 'criss-cross' adduct. This phenomenon can by explained as follows: the film subjected to HFAA for 10 min, 20 min and 30 min was still well-packed and the molecules were close to each other, preventing the formation of an intramolecular 'criss-cross' adduct. However, for longer exposure times degradation became significant. It was claimed earlier[23] that films decompose through C-C bond cleavage, but the molecules do not degrade simultaneously. If some of the molecules present on the surface had already been shorter by a few carbons, but some others remained intact, their double bonds could form the 'criss-cross' adduct because of reduced steric hindrance.

Another interesting observation is the fact that with an increasing amount of fluorine on the surface, the carbon signal decreases *e.g.* reaction time of 2 h and 5 h. The theoretical ratio of the F atoms to the C atoms, per single modified molecule, is constant. Differences in recorded ratios of the F signal to the C signal may suggest that unmodified hydrocarbon molecules decompose faster than those with a fluorinated terminal group. The C-F bond is much stronger than the C-C and C-H bonds,[24] thus C-C bond cleavage will occur first in non-fluorinated molecules. Finally, fluorine-modified molecules also

decompose (see spectrum of reaction after 48 h), possibly due to exposure of their hydrocarbon alkyl chains to attacking species. **Scheme 6.9** illustrates the proposed degradation steps. This observation may suggest that a small change in film/molecule composition, such as introducing a fluorinated terminal group, increases film stability.

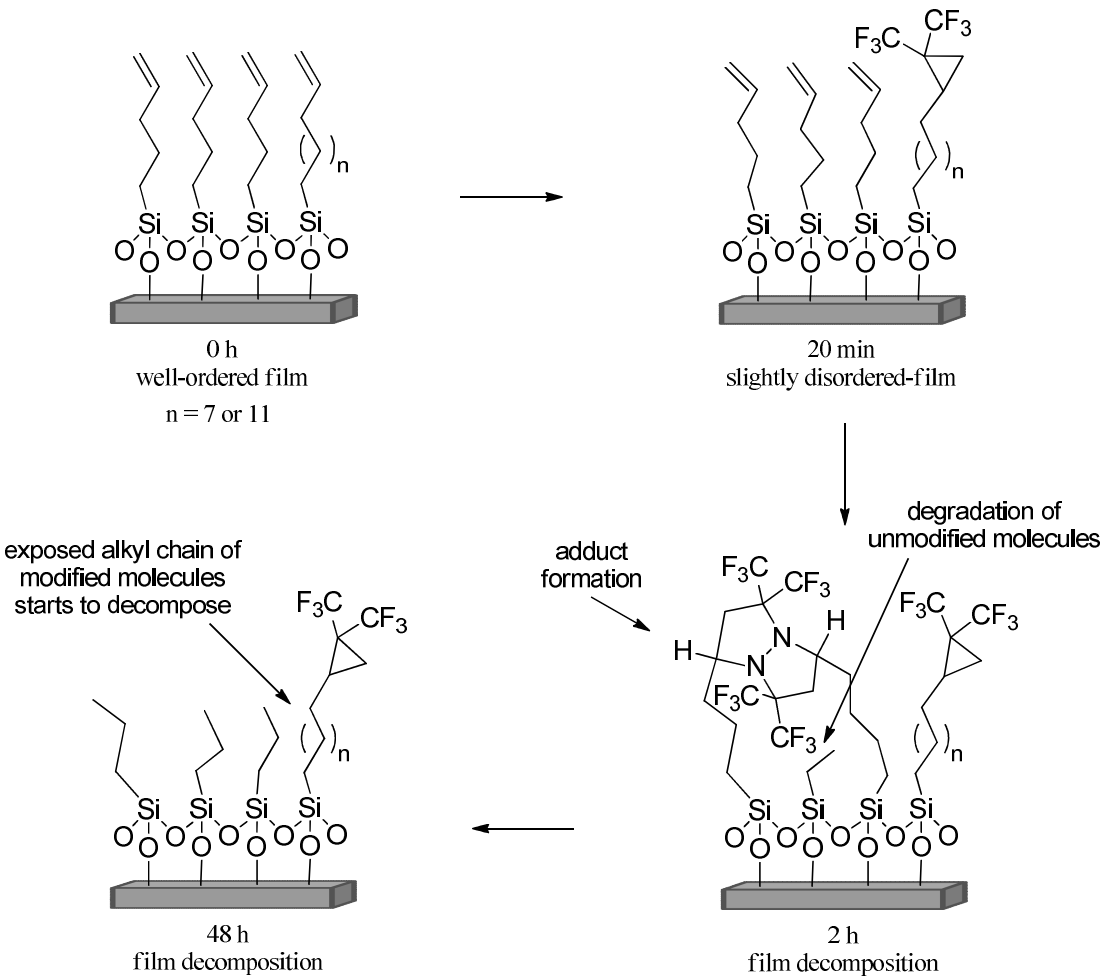

Scheme 6.9. Proposed mechanism of film degradation as well as possible groups formed on the surface.

Optimisation of HFAA amount

The next experiment was performed to investigate how the concentration of HFAA in the reactor affects both the stability and conversion of SAMs. Different volumes of HFAA, from 50 to 400 µL, were used to modify C_{11}-vinyl **1b** SAMs in the 100 mL container. The reactions were performed under a nitrogen atmosphere at 160 °C for 20 min. Under these conditions the entire liquid HFAA evaporated into the gas phase. The XPS survey spectra are shown in **Figure 6.8**.

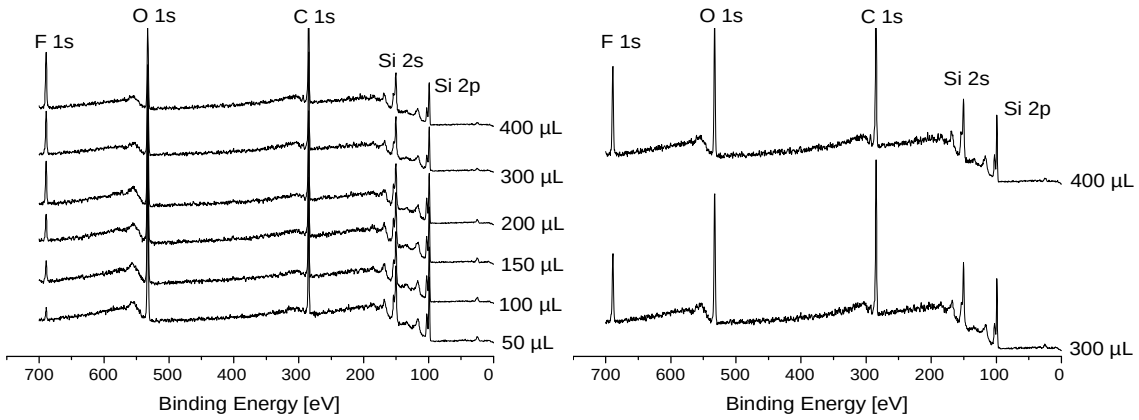

Figure 6.8. The XPS survey scans taken from C_{11}-vinyl **1b** SAMs reacted with different volumes of HFAA.

The XPS surveys scans shown in **Figure 6.8** indicate a gradual increase of the F signal. The least intense F peak was observed when 50 µL of HFAA was used, while the most intense peak was detected in the case of 400 µL of HFAA. 500 µL of HFAA and more, were not investigated in this study, because film degradation was already significant when 400 µL of HFAA was used in the reaction vessel. Film decomposition was concluded by the decreasing intensity of the C 1s signal of the modified SAM (**Figure 6.8**, right spectra).

It was clear that the higher the concentration of HFAA, the more fluorine was present on the surface as indicated by the increasing intensity of the F signal on the XPS survey scans (**Figure 6.8**). High resolution scans of the fluorine region showed a symmetric fluorine signal, and significantly no nitrogen was observed in all samples tested.

Exposure of methyl-terminated SAMs to HFAA

In order to explore the degree of selective reactivity of HFAA with the C=C double bond versus direct CH_2 insertion, several experiments were performed on methyl-terminated SAMs: C_{10}-methyl **1d**, C_{18}-methyl **1e**, C_{12}-methyl **1f**. The samples were treated with 200 µL of HFAA for 20 min at 160 °C. The XPS results are shown in **Figure 6.9**.

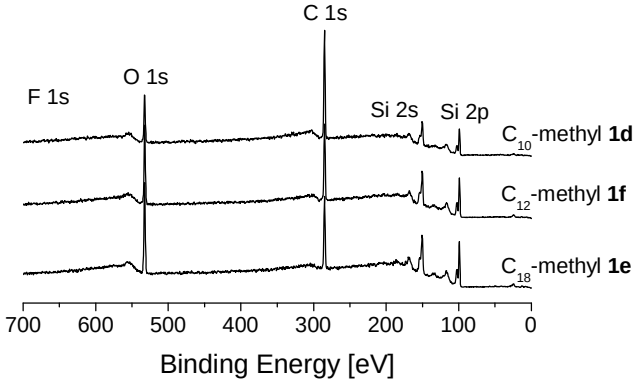

Figure 6.9. The XPS survey scans of the reaction between HFAA and methyl-terminated **1d**, **1e**, and **1f** SAMs (20 min, 160 °C).

From the XPS survey scans, only silicon, carbon and oxygen were detected. There was no evidence for the accumulation of fluorine or nitrogen on the surface. High resolution scans of the F 1s and the N 1s region are shown in **Figure 6.10**.

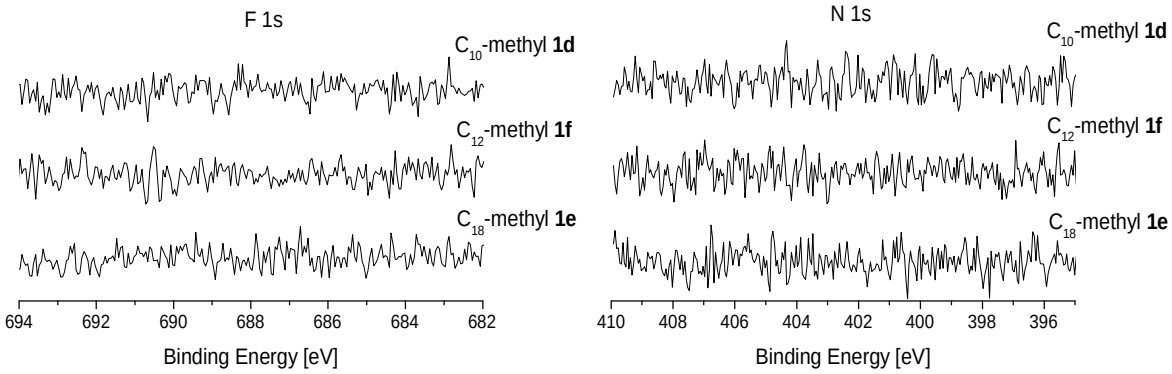

Figure 6.10. High resolution scans of F 1s and N 1s regions taken from methyl-terminated **1d**, **1e**, and **1f** SAMs after the reaction with HFAA (20 min, 160 °C).

The lack of a reaction suggests that unlike vinyl-terminated SAMs, the methyl-terminated films are resistant to HFAA.

Additionally, films formed from the longest self-assembling molecule, C_{18}-methyl **1e**, were also contacted with gaseous HFAA (50 µL in 100 mL container) at 160 °C for 2 and 5 h. The methyl-terminated film was stable even after 2 h of exposure to HFAA and no decomposition was observed. However, after 5 h exposure the intensity of the carbon signal significantly decreased. This observation is consistent with the observation reported by Middleton *et al.*[17] They claimed that HFAA is stable under elevated temperatures. However, after 5 h at 160 °C HFAA might start to decompose and the various species formed from its decomposition might initiate SAM degradation.

Bromination of residual C=C bonds on *bis*(trifluoromethyl)-terminated SAMs

The following experiment was designed to investigate whether vinyl-terminated SAMs treated with HFAA, still contain reactive terminal double bonds.

Vinyl-terminated SAMs were exposed to HFAA (300 µL) for 20 min at 160 °C. After the reaction wafers were fully characterised and then re-used in a bromination reaction.[30] C_{11}-Vinyl **1b** SAMs were also brominated, as described in Chapter 5 (**Scheme 6.10**).

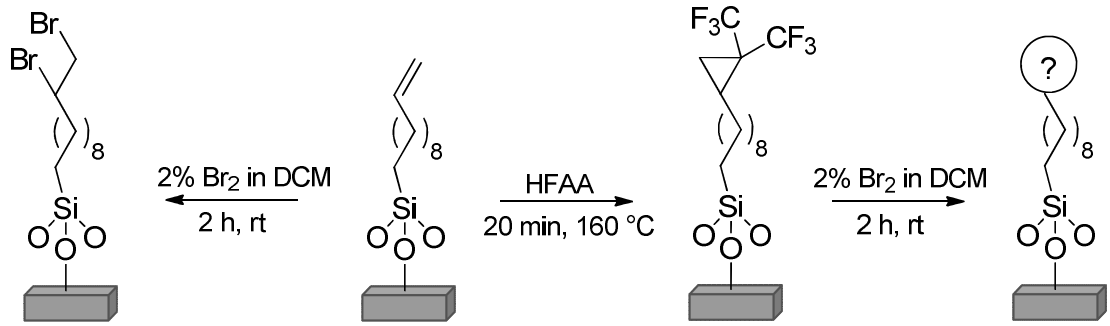

Scheme 6.10. Schematic representation of bromination reaction performed on C_{11}-vinyl **1b** and HFAA treated SAM.

The XPS results obtained after the bromination reaction performed on C_{11}-vinyl **1b** and HFAA treated SAM **1b** are shown in **Figure 6.11**.

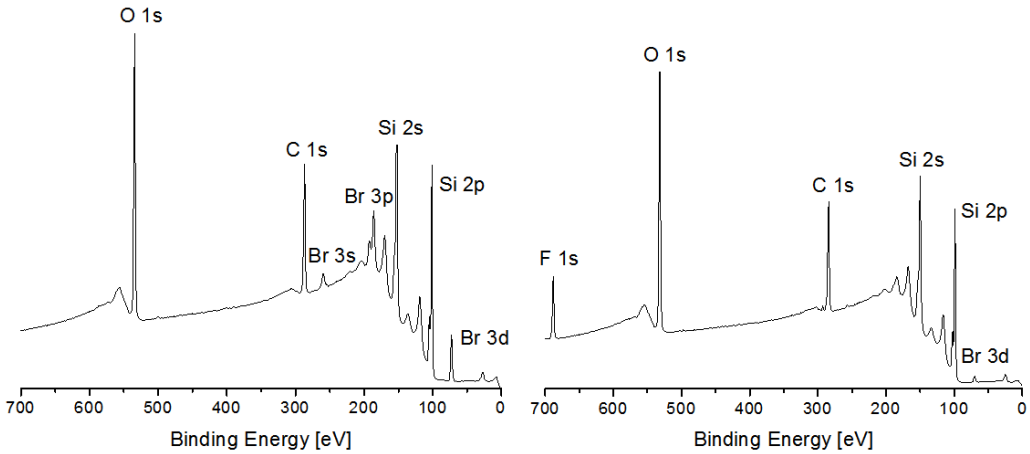

Figure 6.11. The XPS survey scans of bromine treated C_{11}-vinyl **1b** SAM (left spectrum) and HFAA/bromine treated SAM **1b** (right spectrum).

The XPS survey scan, obtained after bromination of C_{11}-vinyl **1b** SAM, recorded new signals in the range of 50 to 260 eV. All of the signals come from Br, due to reaction of Br_2 presumably with a terminal double bond (left spectrum). On the spectrum obtained after bromination of HFAA treated SAM (right spectrum), apart from Si, C, O and F, a small Br 3d signal (71 eV) was detected. However, the intensity of Br 3d signal in both

samples is different. The Br 3d signal recorded after direct bromination of C_{11}-vinyl **1b** SAM, is an order of magnitude more intense than the Br 3d signal recorded after HFAA/bromination of C_{11}-vinyl **1b** film. As expected a significantly lower level of Br was detected in the case of the second film.

6.2.4.2.2. Water Contact Angle

The water contact angle of C_{11}-vinyl **1b** SAMs, which were modified in the vapour phase, was 101°. While, the CA values of methyl-terminated films were 105° for **1d** and 109° for **1e**. In order to monitor the reaction progress and to verify the measurable onset of film degradation, water contact angles were recorded for all films.

The CA values obtained from the reaction of C_{11}-vinyl **1b** SAMs with HFAA (100 µL) at 80 °C and 120 °C were 101°, suggesting no or only very low conversions. However, after the reaction performed at 160 °C, the water contact angle increased from 101° to 106°, which is consistent with an increased amount of fluorine in the film.[32]

The water contact angles, obtained from the films which were reacted with HFAA (50 µL) for different periods of time (10 min, 20 min, 30 min, 1 h, 2 h, 5 h) at 160 °C are shown in **Figure 6.12**.

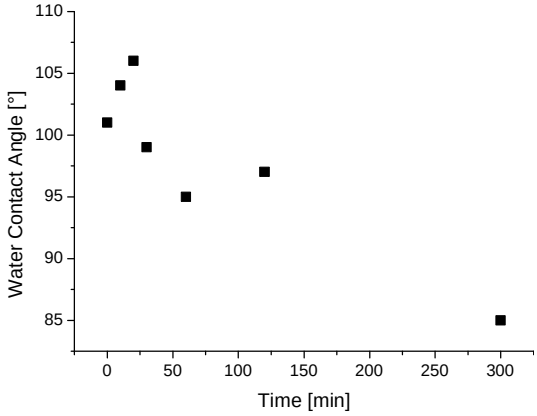

Figure 6.12. The water contact angles measured after the reaction performed for fixed periods of time at 160 °C on C_{11}-vinyl **1b** SAMs.

After a 10 min reaction the observed CA was 104°. The highest value of 106°, was measured after 20 min reaction. For exposure times longer than 20 min, the CA gradually decreased to the lowest value of 50°, which was recorded after a 48 h reaction.

The water contact angle measurements are an indicator of the time for the onset of SAM degradation when different amounts of HFAA were used in the vapour phase

reaction. For the HFAA levels in the range of 50 to 300 µL, all recorded values were 106°. The water contact angle only decreased when 400 µL of HFAA was used.

In the case of exposure of methyl-terminated films to HFAA, the CA values did not change at all up to 2 h. The lowest contact angle was measured for the C_{18}-methyl **1e** SAM **1e**, when the reaction was performed for a 5 h duration. The contact angle dropped from 109° to 104° during this time (see Appendices 9 and 10).

The water contact angle of the HFAA pre-treated SAM, after the bromination reaction, decreased from 106° to 100°. This change, can be explained by the presence of a small amount of Br on the surface.

The water contact angles suggest that the two parameters, reaction time and temperature, are important for optimising the modification of vinyl-terminated SAMs. However, the concentration of HFAA is also important. Film degradation was observed when a treshold volume of HFAA were present in the reaction vessel. Volumes of HFAA between 50 and 300 µL within the 100 mL container gave a constant water contact angle of 106°. This might suggest that the substrate is modified uniformly across the entire surface. No differences in the CA were observed in the case of methyl-terminated SAMs, which suggest that only the C=C double bond can react with HFAA. All of the obtained CA values were in good agreement with XPS data.

6.2.4.2.3. Ellipsometry

Ellipsometry measurements were used to monitor the film thickness, which allowed to determine the onset of film degradation under the applied reaction conditions. The thicknesses were recorded for all films exposed to HFAA.

No significant differences in SAM thicknesses were noticed when the reactions were performed at different temperatures (80 °C, 120 °C, 160 °C). All of the recorded values confirmed the presence of monolayer films.

In the case of experiments performed for different periods of time (10 min to 48 h), the observable degradation of the films occurred for reaction periods longer than 20 min. The measured thicknesses of films exposed to HFAA for longer than 20 min at 160 °C were always below 10 Å (Appendix 9), suggesting significant film decomposition. Lower thicknesses were also measured when the highest volume of HFAA (400 µL) were used to modify the SAMs. The recorded values changed *e.g.* for the C_{15}-vinyl **1c** SAM, from 20 Å to 18 Å.

In the case of methyl-terminated SAMs, measured thicknesses also indicated monolayer films for the reaction periods of 20 min and 2 h. Changes in film thicknesses were observed only for the exposure time of 5 h. The measured value of C_{18}-methyl **1e** film decreased from 26 Å to 19 Å.

The ellipsometry measurements were useful for optimising the reaction times and volumes of HFAA used. Changes in film thicknesses were easily observable by comparing SAMs thicknesses recorded before and after modification.

6.2.4.2.4. Atomic Force Microscopy

Atomic force microscopy (AFM) images were taken from the samples modified for 20 min at 160 °C. In **Figure 6.13**, SAM film of C_{11}-vinyl **1b** scanned before and after reaction with HFAA (300 µL) are illustrated.

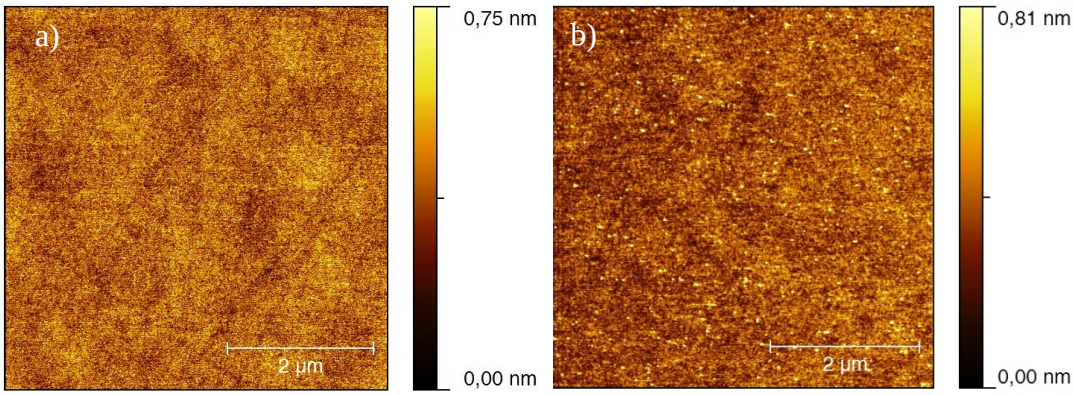

Figure 6.13. AFM images of 5 µm × 5 µm area of, a) C_{11}-vinyl **1b** prepared from solution, RMS 71.9 pm, and b) C_{11}-vinyl **1b** after the vapour phase reaction with HFAA (20 min, 160 °C), RMS 118 pm.

Both images show a very smooth film with low RMS values. However, the average roughness of the modified SAM is slightly higher than before the reaction. The observed values increased from ~72 pm to ~120 pm. This is probably due to the new functional group formed on the SAM film. The SAM reaction with HFAA will lead to a formation of a bulkier group than the vinyl group. Thus the SAMs' homogeneity, and therefore, the order of the molecules and their organisation in the film might change.

A summary of water contact angles and ellipsometry results, obtained after chemical modification of vinyl- and methyl-terminated SAMs are listed in Appendices 9 and 10.

6.2.5. Evidence for *bis*(trifluoromethyl)cyclopropane-terminated SAMs

It is anticipated that the reaction of hexafluoroacetone azine with vinyl-terminated SAMs in the vapour phase generates a *bis*(trifluoromethyl)cyclopropane-terminated film (**Scheme 6.11**). In this section the evidence towards formation of the *bis*(trifluoromethyl)cyclopropane head group will be discussed, based on the results obtained from the sample exhibiting the highest conversion.

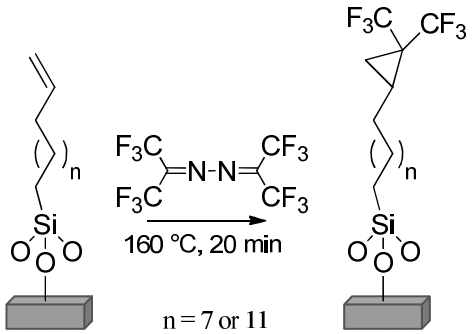

Scheme 6.11. Putative formation of *bis*(trifluoromethyl)cyclopropane-terminated SAMs in the vapour phase reaction with HFAA.

The highest reaction conversions were obtained when 300 µL of HFAA were used to treat a C_{11}-vinyl **1b** or C_{15}-vinyl **1c** SAMs at 160 °C for 20 min. XPS spectra of two different samples, C_{18}-methyl **1e** and C_{15}-vinyl **1c** terminated SAMs, were compared after exposure to HFAA under the same conditions (**Figure 6.14**).

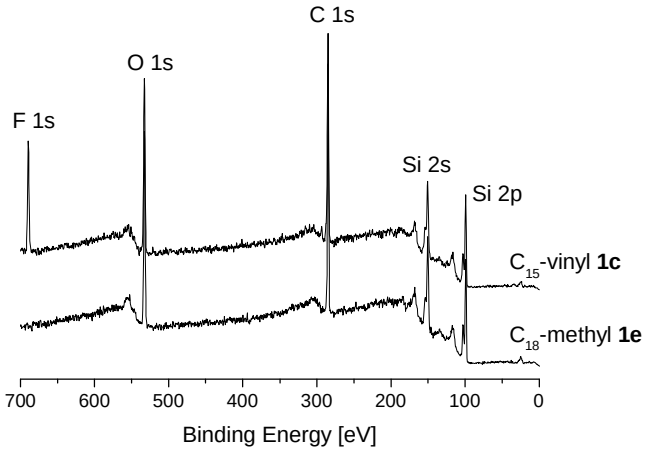

Figure 6.14. The XPS full scans after the reaction of C_{18}-methyl **1e** and C_{15}-vinyl **1c** terminated film with HFAA in vapour phase.

A new fluorine signal can be clearly observed after treatment of the SAM film, which contained a terminal C=C double bond (top spectrum). This change was not observed in the case of the methyl-terminated SAM (bottom spectrum). High resolution scans of the F 1s and C 1s regions taken from the C_{15}-vinyl **1c** SAM are shown in **Figure 6.15**.

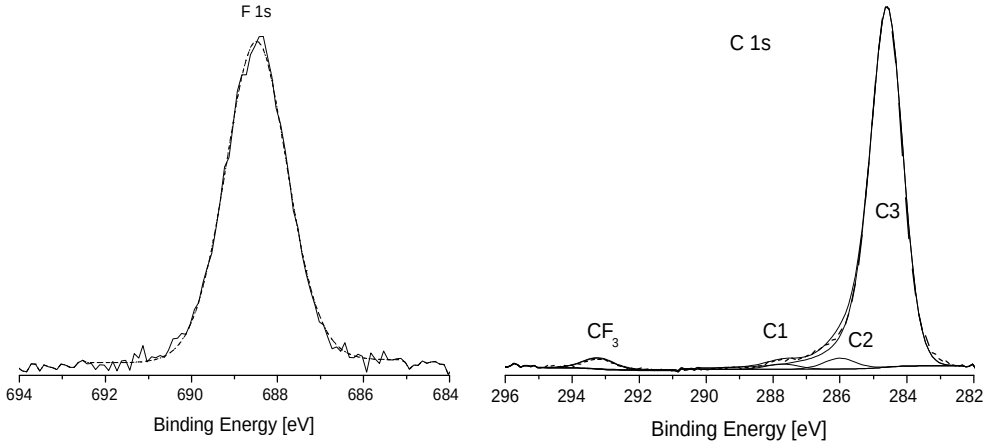

Figure 6.15. The XPS high resolution scans of the F 1s and C 1s region of C_{15}-vinyl **1c** SAM after the reaction with HFAA (for details see text).

The symmetric fluorine signal suggests the presence of fluorine atoms of the same environment on the surface of the film and corresponds to the CF_3 group. The position of the F 1s peak at 688.9 eV is characteristic of a fluorinated organic coating.[34, 35] The carbon region is more complex and four different signals can be distinguished. The most intensive signal with a binding energy of 284.6 eV corresponds to carbon-carbon bonds of hydrocarbon alkyl chain present on the surface.[9, 36] The signals at 286.0 eV and 287.7 eV correspond to the carbon atoms adjacent to the fluorinated group.[37, 38] While the signal at 293.3 eV corresponds to the carbon of the $\underline{C}F_3$ group.[38, 39]

Film modification was also consistent with the observed changes in the water contact angle. Unmodified vinyl-terminated SAMs exhibited a water contact angle of ~101°,[9] while after modification the water contact angle increased to 106°. This is consistent with an increase of hydrophobic groups on the surface. Moreover the water contact angle of CF_3-terminated SAMs was reported to be 106°.[32, 40] From the ellipsometry results, no significant differences were observed in film thicknesses, however a significant change is not expected.

The presence of *bis*(trifluoromethyl)cyclopropane groups on the surface is also consistent with the theoretical and experimental ratios of the F 1s signal and the C 1s signals (**Figure 6.16,** fitting details are provided in Chapter 2, paragraph 2.1.1).

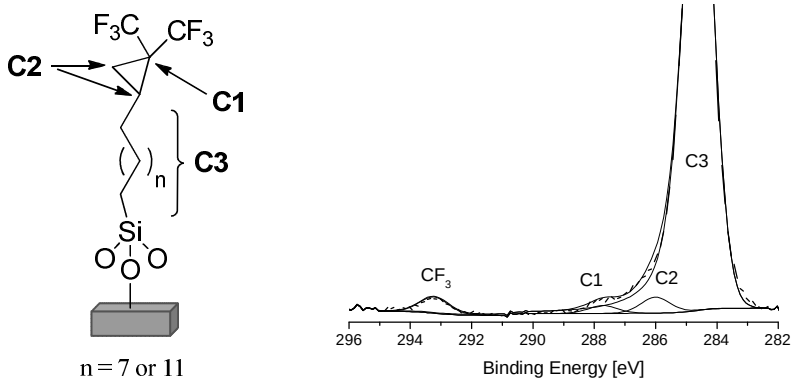

Figure 6.16. Assignment of the C 1s signals according to the possible structure formed on the surface.

The carbon peak, that is the most shifted peak towards higher binding energies from the region of 282.5-288.5 eV, was assigned as carbon C1 (287.7 eV). According to the proposed structure, this can be assigned to the CF_3 groups – $\underline{C}(CF_3)_2$. A second carbon peak, with a binding energy of 285.8 eV, was assigned to the C2 carbons (two carbons of cyclopropane ring). And last, the most intensive signal C3, was assigned to all carbons from an alkyl chain (284.6 eV). The ratios obtained from C_{11}-vinyl **1b** and C_{15}-vinyl **1c** SAMs are presented in **Table 6.1**.

		Ratios		
		$\underline{F}$: $\underline{C}F_3$	$\underline{C}F_3$: $\underline{C}1$	$\underline{C}F_3$: $\underline{C}2$
Theor.	C_{11}-vinyl **1b**	3 : 1	2 : 1	1 : 1
	C_{15}-vinyl **1c**	3 : 1	2 : 1	1 : 1
Exp.	C_{11}-vinyl **1b**	3.11 : 1	1.84 : 1	0.97 : 1
	C_{15}-vinyl **1c**	3.06 : 1	2.05 : 1	1.01 : 1

Table 6.1. Theoretical and experimental ratios between the F 1s and C 1s signals present on modified SAMs.

Based on the intensity of the F 1s signal and the sum of intensities of the C 1s signals, the reaction conversion of HFAA with C_{11}-vinyl **1b** or C_{15}-vinyl **1c** can be estimated as 32% and 27%, respectively. However, these values are overestimated because not all C 1s electrons were detected, thus taking into account the attenuation factor

(Chapter 5, paragraph 5.1), the conversion for C_{11}-vinyl **1b** is estimated to be ~27% and the conversion for C_{15}-vinyl **1c** is estimated to be ~23%.

A proposed mechanism for the formation of *bis*(trifluoromethyl)cyclopropane group on the surface is presented in **Scheme 6.12**. The radical, bimolecular, two-step mechanism of 'criss-cross' adduct formation, proposed by Forshaw and Tipping[20] has been used as a starting point.

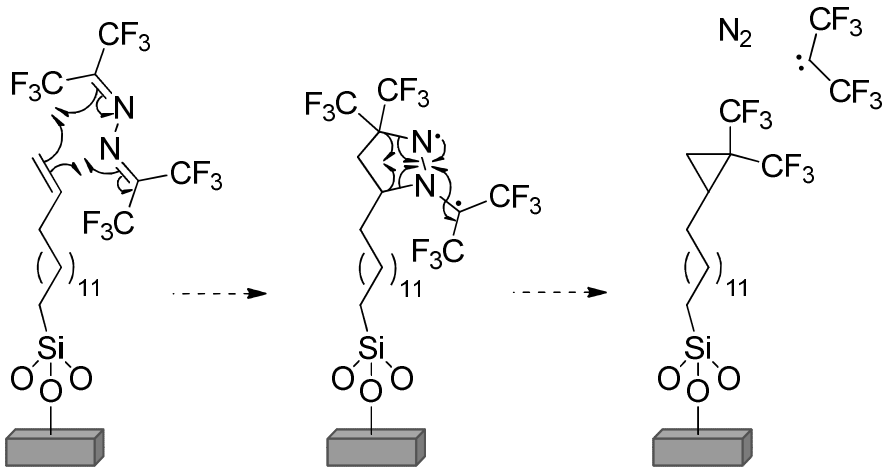

Scheme 6.12. Putative mechanism for the formation of *bis*(trifluoromethyl)cyclopropane terminated SAMs in the vapour phase.

By this process a second molecule would attack the intermediate diradical and form a 'criss-cross' adduct as shown in **Scheme 6.8**. However, the unique steric aspect of SAMs is expected to limit this and thus the intermediate will decompose to a cyclopropane with N_2 as a by-product. Only, after a 2 h reaction on vinyl-terminated films, a small amount of nitrogen was detected by XPS. The presence of nitrogen might suggest formation of the 'criss-cross' adduct, but this was only possible when the SAM had undergone degradation, and steric hindrance is less of a problem. A control vapour phase reaction between HFAA and 1-decene was performed under exactly the same conditions as reactions on SAMs (**Scheme 6.13**). In the reaction mixture, the 'criss-cross' adduct **6.14**, 1-decene and some unidentified compounds were formed. The reaction procedure can be found in Appendix 11.

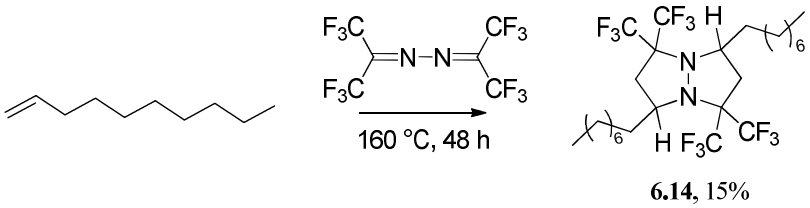

6.14, 15%

Scheme 6.13. Formation of 'criss-cross' adduct in the vapour phase reaction between HFAA and 1-decene.

6.3. Chemistry of SAMs exposed to hexafluoropropene oxide (HFPO)

A second reagent was explored in vapour phase reactions of SAMs. Hexafluoropropene oxide (HFPO) is known to generate :CF_2 carbene by heating, thus its reaction with vinyl-terminated SAMs was also investigated (**Scheme 6.14**).

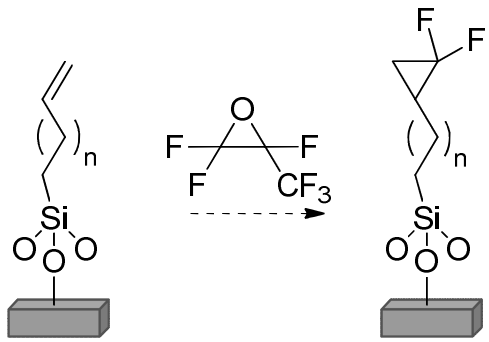

n = 8 or 12

Scheme 6.14. Exploration of a vapour phase reaction between vinyl-terminated SAM and HFPO.

6.3.1. Chemistry of HFPO

HFPO is commonly used as an intermediate in industrial chemistry to manufacture organofluorine products. HFPO reacts with strong nucleophiles such as amines,[41, 42] fluorinated alkoxides,[43] alcohols, thiols and water.[42] It is also a convenient source of difluorocarbene, :CF_2,[14, 44] which is a major focus in this study.

HFPO reacts with olefins to give cyclopropanes (**6.15**), formed by addition of difluorocarbene :CF_2 to a double bond. Trifluoroacetyl fluoride (**6.16**) is generated as a by-product (**Scheme 6.15**).[45]

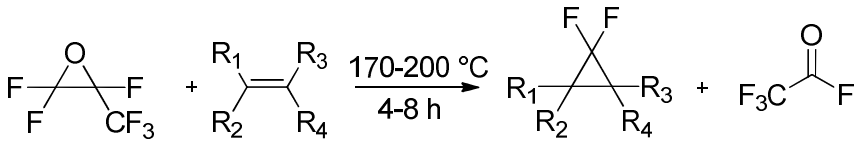

Scheme 6.15. Formation of difluorocyclopropane from hexafluoropropene oxide and alkene at 170-200 °C.[45]

Prolonged heating of the reacting mixture (**Scheme 6.15**) causes isomerisation of the cyclopropane product, which was proven experimentally by Sargeant.[45] Mahler and Resnick[44] reported that the half-life of HFPO is 6 h at 165 °C. At this temperature, difluorocarbene and trifluoroacetyl fluoride are formed.[44] The authors also found that HFPO fragmentation is reversible, $:CF_2$ can react with $CF_3C(O)F$ to give the starting fluorinated epoxide.

6.3.2. Optimisation of the reaction conditions

HFPO has been selected in this study because:

1. The reactivity of this compound is known as it has already been used in industry as a fluorinating agent.[14]
2. HFPO is a gas, thus, deposition of SAMs and its further chemical modification could be carried out in the vapour phase.
3. The results obtained could be used as a comparison to SAMs modified with a $:CF_2$ carbene generated from the Ruppert-Prakash reagent,[46] discussed in Chapter 5.

6.3.2.1. Procedure for the reaction of HFPO with SAMs

Vinyl- and methyl- terminated SAM substrates were placed in a glass reaction vessel (100 mL capacity). The air from the container was evacuated using a vacuum pump (~4 mbar). The container was then placed in a cooling bath (acetone/dry ice, -78 °C) and HFPO gas was transferred (~1 g). The reaction mixture was then warmed to room temperature and subsequently heated at fixed temperatures (160 °C, 175 °C, 185 °C, 190 °C) for defined periods (15 min, 20 min).

6.3.2.2. Results and Discussion

The reaction progress was monitored by X-ray photoelectron spectroscopy and contact angle goniometry.

6.3.2.2.1. X-ray Photoelectron Spectroscopy

Optimisation of reaction temperature

This experiment was designed to explore the optimum temperature for the reaction between vinyl-terminated SAMs and HFPO. According to the literature[44] the half-life of HFPO is 6 h at 165 °C. Thus, C_{11}-vinyl **1b** SAMs were reacted with HFPO for 20 min at 160 °C, 175 °C and 185 °C. Higher temperatures (175 °C and 185 °C) were tested in order to increase the conversion. The XPS survey spectra and the F 1s high resolution regions recorded after the reaction are shown in **Figure 6.17**.

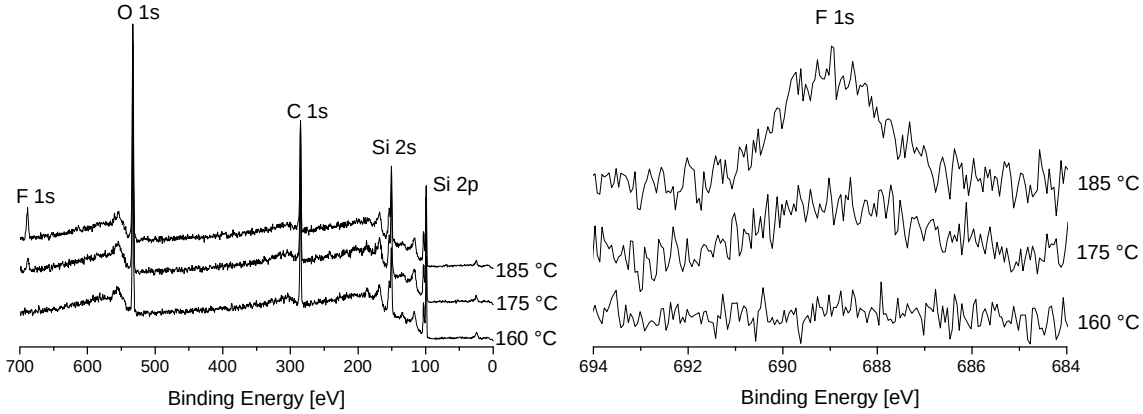

Figure 6.17. The XPS survey spectra and the F 1s region after 20 min reaction between HFPO and C_{11}-vinyl **1b** SAMs.

The most intense fluorine signal was observed in the case of the reaction performed at 185 °C. A less intense fluorine peak was observed when the temperature was lowered by 10 °C. No fluorine signal was detected at 160 °C. From these results it was clear that the highest temperature gave the highest conversion. However, after 20 min at 185 °C the film started to degrade. This was revealed by the intensity drop of the C 1s signal.

Slightly modified reaction conditions were also tested. The reaction temperature was increased from 185 °C to 190 °C, and the reaction time was shortened by 5 min (from 20 min to 15 min). By these changes it was hoped to increase the reaction conversion and to reduce film degradation. The obtained XPS result is shown in **Figure 6.18**.

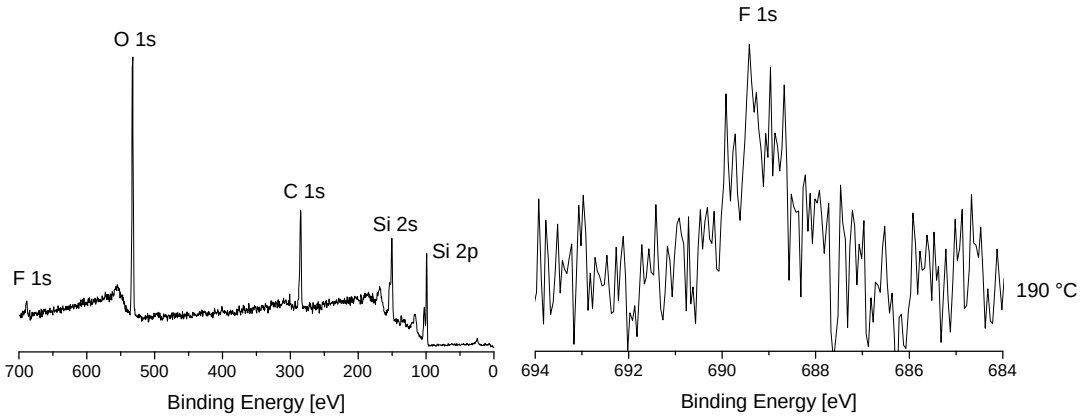

Figure 6.18. XPS survey spectrum and the F 1s high resolution region after reaction of HFPO at 190 °C for 15 min with C_{11}-vinyl **1b** SAM.

A small fluorine signal can be observed on the XPS survey scan and on the F 1s single scan region. However, the carbon signal has significantly decreased, indicating significant SAM degradation (**Figure 6.19**).

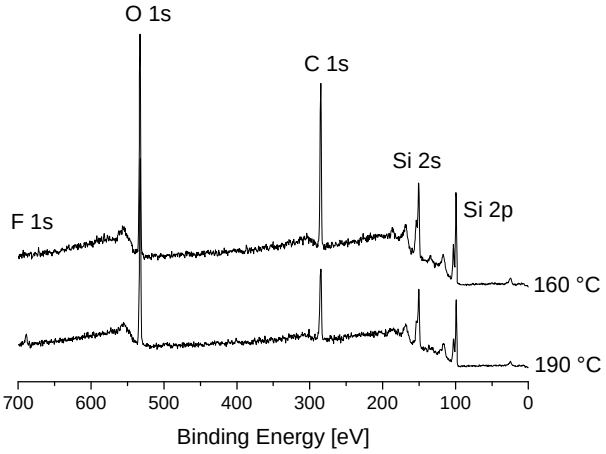

Figure 6.19. The XPS full scans after the reaction of C_{11}-vinyl **1b** SAM with HFPO at 160 °C (top spectrum) and at 190 °C (bottom spectrum).

From the thermal experiment, it is concluded that the optimum temperature to modify the SAM film with HFPO was 185 °C.

6.3.2.2.2. Water Contact Angle

The water contact angles were recorded for all wafers reacted with HFPO. The CA value of C_{11}-vinyl **1b** SAM used in the reaction was 101°. After modification this value decreased to 100°, 95°, 70° and 65° for reaction temperatures of 160 °C, 175 °C, 185 °C and 190 °C, respectively (**Figure 6.20**).

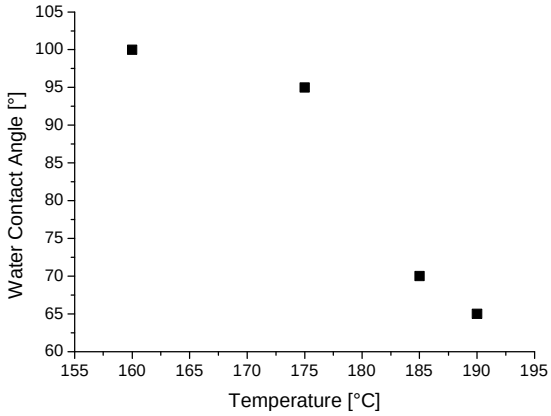

Figure 6.20. The water contact angles measured after the reaction of HFPO with C_{11}-vinyl **1b** SAMs at fixed temperatures.

From the results it can be deduced that the SAMs degrade with increasing temperature in the presence of HFPO. However, when more fluorine was observed on the XPS spectrum a lower contact angle was measured, suggesting that the reaction by-products accelerate film decomposition. An exception was the reaction at 190 °C, where the F signal was low, most likely due to significant film degradation. This was confirmed by the low intensity of the carbon signal compared to its intensity after reaction at 160 °C (**Figure 6.19**).

HFPO requires a high temperature to generate the $:CF_2$ carbene species. At 160 °C, fluorine was not observed, thus, the water contact angle did not change, suggesting the presence of a hydrophobic coating on the surface, which is in good agreement with the XPS data. Most likely at this temperature HFPO did not generate enough carbene to be able to react with the SAM, due to the short reaction time (20 min). Longer reaction times are required, due to the half-life of HFPO (6 h at 165 °C),[44] however, SAMs do not survive such a long reaction period at high temperature, thus no further conditions were tested.

6.3.2.3. Prolonged carbene generation with HFPO

A prolonged carbene generation experiment was designed as a consequence of the high temperature and long reaction time requirements, to generate $:CF_2$ carbene from HFPO. The experimental set-up used is presented in **Figure 6.21**.

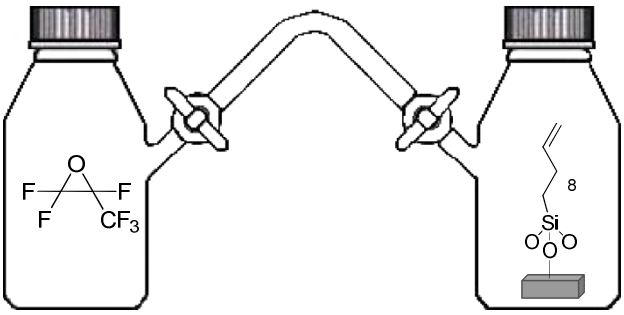

Figure 6.21. Schematic representation of the prolonged carbene generation experiment.

A modified, glass bottle (100 mL) containing HFPO (~1g), was heated for 6 h at 165 °C. In the second bottle a wafer with C_{11}-vinyl **1b** SAM was placed and then the air from the bottle was evacuated by vacuum pump. Next, the bottle with the wafer was pre-heated to 165 °C and then the gas from the first bottle was transferred to the second reactor. After the transfer, the bottle containing the silicon wafer was heated at 165 °C for an additional 20 min. Next the SAM film was characterised by XPS analysis and contact angle goniometry.

No changes in the SAM properties were observed after exposure of the vinyl-terminated film to HFPO. No fluorine was detected by XPS and there was no change in the water contact angle. This lack of reaction can be explained by the fact that the HFPO fragmentation species do not survive transfer to the second container.[44]

6.3.2.4. Control experiment with methyl- and vinyl- terminated SAMs and HFPO

In order to investigate SAM resistance to HFPO, the following experiment was performed. Vinyl- and methyl- terminated SAMs (**1b**, **1d** and **1e**) were reacted with HFPO for 4 h at 50 °C. An example of the XPS results of vinyl- and methyl- terminated films after the reaction are shown in **Figure 6.22**.

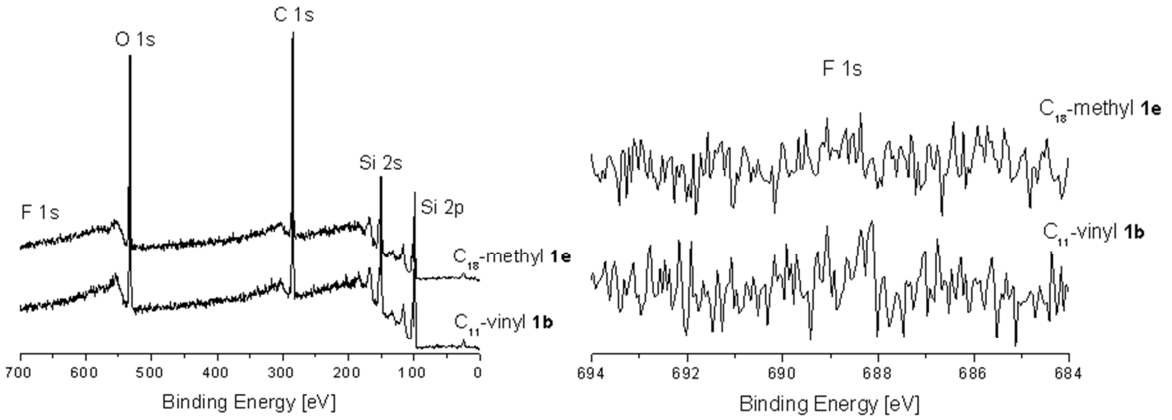

Figure 6.22. XPS survey spectra and the F 1s high resolution scan of vinyl- and methyl-terminated SAMs after the reaction with HFPO for 4 h.

No fluorine signals were observed in the case of all three control wafers. The water contact angles remained the same after treatment, 101° for C_{11}-vinyl **1b** SAM, 107° for C_{10}-methyl **1d** and 109° for C_{18}-methyl **1e** SAM. These results suggest that at low temperature (50 °C) in HFPO, the SAMs are very stable and the HFPO is unreactive. This lack of reaction and degradation suggests that the fragmentation species of HFPO *e.g.* difluorocarbene and trifluoroacetyl fluoride, might be responsible for initiation of the degradation of the SAMs.

6.4. Conclusions

A novel surface modification route *via* addition of fluorinated species from the vapour phase using HFAA has been demonstrated. Evidence for the successful surface modification was obtained by XPS analysis. A fluorine signal was clearly observed after reaction on vinyl-terminated SAMs and no reaction occurred with methyl-terminated SAMs. These reactions show the potential of vapour phase chemistry for the modification of pre-formed SAMs by C-C bond forming reaction on solid substrates. Moreover, the demonstrated reactions are selective, thus they could possibly be used to modify films with a variety of functionalities, in a regiospecific manner.

6.5. Literature

1. Y. A. Cheng, B. Zheng, P. H. Chuang and S. Hsieh, *Langmuir*, 2010, **26**, 8256-8261.
2. B. D. Booth, S. G. Vilt, J. Ben Lewis, J. L. Rivera, E. A. Buehler, C. McCabe and G. K. Jennings, *Langmuir*, 2011, **27**, 5909-5917.
3. R. Maoz, H. Cohen and J. Sagiv, *Langmuir*, 1998, **14**, 5988-5993.
4. R. Maboudian, W. R. Ashurst and C. Carraro, *Sens. Actuator A-Phys.*, 2000, **82**, 219-223.
5. A. Ulman, *Chem. Rev.*, 1996, **96**, 1533-1554.
6. N. Herzer, C. Haensch, S. Hoeppener and U. S. Schubert, *Langmuir*, 2010, **26**, 8358-8365.
7. S. Dutta, M. Perring, S. Barrett, M. Mitchell, P. J. A. Kenis and N. B. Bowden, *Langmuir*, 2006, **22**, 2146-2155.
8. M. Qu, Y. Zhang, J. He, X. Cao and J. Zhang, *Appl. Surf. Sci.*, 2008, **255**, 2608-2612.
9. M. Adamkiewicz, T. O'Hara, D. O'Hagan and G. Hähner, *Thin Solid Films*, 2012, **520**, 6719-6723.
10. Y. X. Zhuang, O. Hansen, T. Knieling, C. Wang, P. Rombach, W. Lang, W. Benecke, M. Kehlenbeck and J. Koblitz, *J. Microelectromech. Syst.*, 2007, **16**, 1451-1460.
11. L. R. Fiegland, M. M. Saint Fleur and J. R. Morris, *Langmuir*, 2005, **21**, 2660-2661.
12. M. A. Hallen and H. D. Hallen, *J. Phys. Chem. C*, 2008, **112**, 2086-2090.
13. A. Razgon, R. G. Bergman and C. N. Sukenik, *Langmuir*, 2008, **24**, 2545-2552.
14. H. Millauer, W. Schwertfeger and G. Siegemund, *Angew. Chem., Int. Ed.*, 1985, **24**, 161-179.
15. T. P. Forshaw and A. E. Tipping, *J. Chem. Soc.-Perkin Trans. 1*, 1972, 1059-1062.
16. D. M. Gale, W. J. Middleton and C. G. Krespan, *J. Am. Chem. Soc.*, 1966, **88**, 3617-3623.
17. W. J. Middleton, *J. Am. Chem. Soc.*, 1971, **93**, 423-425.
18. W. J. Middleton, D. M. Gale and C. G. Krespan, *J. Am. Chem. Soc.*, 1968, **90**, 6813-6816.
19. T. P. Forshaw and A. E. Tipping, *Chem. Commun.*, 1969, 816-817.
20. T. P. Forshaw and A. E. Tipping, *J. Chem. Soc. C*, 1971, 2404-2408.
21. S. R. Cohen, R. Naaman and J. Sagiv, *J. Phys. Chem.*, 1986, **90**, 3054-3056.
22. G. J. Kluth, M. M. Sung and R. Maboudian, *Langmuir*, 1997, **13**, 3775-3780.
23. G. J. Kluth, M. Sander, M. M. Sung and R. Maboudian, *J. Vac. Sci. Technol. A*, 1998, **16**, 932-936.
24. U. Srinivasan, M. R. Houston, R. T. Howe and R. Maboudian, *J. Microelectromech. Syst.*, 1998, **7**, 252-260.
25. E. K. Seo and M. M. Sung, *Ultramicroscopy*, 2007, **107**, 995-999.
26. H. K. Kim, J. P. Lee, C. R. Park, H. T. Kwak and M. M. Sung, *J. Phys. Chem. B*, 2003, **107**, 4348-4351.
27. S. A. Kulkarni, S. A. Mirji, A. B. Mandale and K. P. Vijayamohanan, *Thin Solid Films*, 2006, **496**, 420-425.
28. R. J. Klein, D. A. Fischer and J. L. Lenhart, *Langmuir*, 2011, **27**, 12423-12433.
29. M. Calistri-Yeh, E. J. Kramer, R. Sharma, W. Zhao, M. H. Rafailovich, J. Sokolov and J. D. Brock, *Langmuir*, 1996, **12**, 2747-2755.
30. S. R. Wasserman, Y. T. Tao and G. M. Whitesides, *Langmuir*, 1989, **5**, 1074-1087.

31. N. Fairley, *CasaXPS Manual 2.3.15 XPS AES ToF-MS SNMS Dynamic-SIMS*, Casa Software Ltd., Devon, 2009.
32. A. Ulman, *An Introduction to Ultrathin Organic Films from Langmuir-Blodgett to Self-Assembly*, Academic Press, San Diego, 1991.
33. T. S. Koloski, C. S. Dulcey, Q. J. Haralson and J. M. Calvert, *Langmuir*, 1994, **10**, 3122-3133.
34. S. Ohnishi, T. Ishida, V. V. Yaminsky and H. K. Christenson, *Langmuir*, 2000, **16**, 2722-2730.
35. T. J. Lenk, V. M. Hallmark, C. L. Hoffmann, J. F. Rabolt, D. G. Castner, C. Erdelen and H. Ringsdorf, *Langmuir*, 1994, **10**, 4610-4617.
36. S. A. Mirji, *Surf. Interface Anal.*, 2006, **38**, 158-165.
37. A. Hozumi, K. Ushiyama, H. Sugimura and O. Takai, *Langmuir*, 1999, **15**, 7600-7604.
38. A. K. Gnanappa, C. O'Murchu, O. Slattery, F. Peters, T. O'Hara, B. Aszalos-Kiss and S. A. M. Tofail, *Appl. Surf. Sci.*, 2011, **257**, 4331-4338.
39. T. Nishino, Y. Urushihara, M. Meguro and K. Nakamae, *J. Colloid Interface Sci.*, 2004, **279**, 364-369.
40. V. DePalma and N. Tillman, *Langmuir*, 1989, **5**, 868-872.
41. H. Kawa and N. Ishikawa, *J. Fluor. Chem.*, 1980, **16**, 365-372.
42. D. Sianesi, A. Pasetti and F. Tarli, *J. Org. Chem.*, 1966, **31**, 2312-2316.
43. E. J. Soloski, C. Tamborski and T. Psarras, *J. Fluor. Chem.*, 1978, **11**, 601-612.
44. W. Mahler and P. R. Resnick, *J. Fluor. Chem.*, 1974, **3**, 451-452.
45. P. B. Sargeant, *J. Org. Chem.*, 1970, **35**, 678-682.
46. F. Wang, T. Luo, J. B. Hu, Y. Wang, H. S. Krishnan, P. V. Jog, S. K. Ganesh, G. K. S. Prakash and G. A. Olah, *Angew. Chem., Int. Ed.*, 2011, **50**, 7153-7157.

7. Summary

This thesis has described the preparation and chemical modification of self-assembled monolayers on SiO_x/Si substrate. Three vinyl-terminated trichlorosilane surfactants were successfully synthesised. The shorter silanes, 9-decenyltrichlorosilane (CH_2=CH-$(CH_2)_8$-$SiCl_3$) and 10-undecenyltrichlorosilane (CH_2=CH-$(CH_2)_9$-$SiCl_3$) were obtained in a two-step reaction, while the longer 14-pentadecenyltrichlorosilane (CH_2=CH-$(CH_2)_{13}$-$SiCl_3$) was prepared following a six step synthetic route. All molecules were obtained in moderate to good yields. The final surfactants, as well as synthetic intermediate, were characterised by NMR and mass spectrometry. The vinyl-terminated silanes, and commercially available methyl-terminated precursors, were then used to prepare self-assembled monolayers on silicon substrates. SAM deposition from solution was performed according to literature procedures. Conditions for the vapour phase process were optimised in order to obtain SAMs with comparable quality to the films obtained from the liquid process. Vapour phase preparations were optimised for each SAM. The shorter surfactant molecules require lower temperature and longer reaction time (60 °C, 4 days), compared to the longer silanes (70 °C, 3 days). The properties of these monolayers were characterised by XPS, contact angle goniometry, ellipsometry and AFM. In all cases XPS analysis revealed the presence of silicon, carbon and oxygen. The measured water contact angles were >100° indicating hydrophobic surfaces, while the thicknesses were in the range of 13-26 Å suggesting the presence of monolayers.

Well defined monolayers were further modified with carbenes (:CCl_2, :CBr_2 and :CF_2) generated in solution. Hexafluoroacetone azine (HFAA) and :CF_2 carbene (generated from HFPO) were used to modify SAMs in the vapour phase. Successful modifications were observed for all reactions performed in the liquid and vapour phases. The progress of the reactions was monitored with XPS, by observing changes of new peak intensities (Br, Cl or F). The modification was also confirmed by changes in water contact angles, which decreased from 101° to 80° and 85° for Cl and Br terminated film, respectively. In the case of fluorine modified SAMs the water contact angle increased from 101° to 106° and 104° for CF_3 and CF_2 terminated SAMs, respectively. For optimised reaction conditions ellipsometry indicated monolayers. However, for extended reaction times film decomposition was observed and it was much faster in the vapour phase than in solution.

The selective reactivity of the carbenes with double bonds, was confirmed by lack of reaction with methyl-terminated SAMs. Moreover, controlled cyclopropanation reactions in solution and the vapour phase were performed with 1-decene. The resulting molecules, 1,1-dichloro-2-octylcyclopropane, 1,1-dibromo-2-octylcyclopropane and 1,1-difluoro-2-octylcyclopropane, were obtained in good yields. However, the vapour phase cyclopropanation reaction with HFAA resulted in the formation of a criss-cross adduct. The structure of the new terminal groups formed on the SAMs were investigated by comparison of XPS ratios between halogen and carbon signals, which appeared after modification. In the case of all reactions the ratios were consistent with the formation of cyclopropane rings on the surface.

This study demonstrates a novel vapour phase C-C bond forming reaction and the potential of carbene chemistry for the solution and vapour phase modification of pre-formed SAMs on solid substrates. These new methods might be used for selective modification of surfaces rich in functional groups to obtain desired terminal groups on a surface which cannot be attached to the surfactant molecule before deposition. Carbene chemistry on SAMs can be further explored in order to introduce more complex functionalities onto different surfaces and can find application in *e.g.* biosensors fabrication.

Appendix 1 - General experimental procedure for the reaction of CHCl3 and CHBr3 on SAMs

To a round-bottom flask (10 mL) equipped with a small stirring bar and cooled to 0 °C, NaOH (100 mg, 200 mg, 300 mg, 400 mg, 500 mg) and $CHCl_3$ or $CHBr_3$ (1 mL) were added. Next, a solution of benzyltriethylammonium chloride (BTEAC, 0.1 mmol) in dichloromethane (1 mL) was added and the reaction mixture was stirred for 10 min at 0 °C. Next, the silicon wafers (1 cm × 1.5 cm), pre-coated with vinyl-terminated SAMs, prepared according to the procedure described in Chapter 4, were immersed in the reaction mixture and the liquids were stirred at room temperature for a fixed period of time (30 min, 1 h, 2 h, 3 h, 4 h, 5 h). After the reaction, the wafers were washed several times with distilled water and then sonicated sequentially in dichloromethane, toluene and DI water for a minimum of 15 min in each solvent. Then the wafers were dried under a nitrogen atmosphere and stored in a desiccator until they have been characterised.

Appendix 2 - Table A1 - SAMs modification with $CHCl_3$ and $CHBr_3$

The results obtained after the reaction of vinyl- and methyl- terminated SAMs with $CHCl_3$ and $CHBr_3$. Each value is an average of measurements taken from two samples. The errors are based on standard deviation.

Precursor Molecule	Carbene Precursor	NaOH [mg]	Time [h or min]	Film Thickness [Å]		Film Contact Angle [°]	
				Before	After	Before	After
C_{11}-vinyl **1b**	$CHCl_3$	100	30 min	~15	14.9±0.1	101±1	100±1
C_{11}-vinyl **1b**	$CHCl_3$	200	30 min	~15	15.1±0.1	101±1	98±1
C_{11}-vinyl **1b**	$CHCl_3$	300	30 min	~15	15.4±0.2	101±1	90±1
C_{11}-vinyl **1b**	$CHCl_3$	400	30 min	~15	12.9±0.1	101±1	87±1
C_{11}-vinyl **1b**	$CHCl_3$	500	30 min	~15	9.7±0.2	101±1	79±1
C_{11}-vinyl **1b**	$CHBr_3$	100	30 min	~15	15.6±0.1	101±1	101±1
C_{11}-vinyl **1b**	$CHBr_3$	200	30 min	~15	15.4±0.2	101±1	93±1
C_{11}-vinyl **1b**	$CHBr_3$	300	30 min	~15	14.9±0.3	101±1	92±1
C_{11}-vinyl **1b**	$CHBr_3$	400	30 min	~15	10.2±0.4	101±1	84±1
C_{11}-vinyl **1b**	$CHBr_3$	500	30 min	~15	9.2±0.1	101±1	80±1
C_{11}-vinyl **1b**	$CHCl_3$	300	1 h	~15	15.0±0.2	101±1	93±1
C_{11}-vinyl **1b**	$CHCl_3$	300	2 h	~15	14.8±0.3	101±1	90±1
C_{11}-vinyl **1b**	$CHCl_3$	300	3 h	~15	16.4±0.1	101±1	85±1
C_{11}-vinyl **1b**	$CHCl_3$	300	4 h	~15	13.7±0.1	101±1	82±1
C_{11}-vinyl **1b**	$CHCl_3$	300	5 h	~15	9.5±0.2	101±1	75±1
C_{11}-vinyl **1b**	$CHBr_3$	300	1 h	~15	15.2±0.1	101±1	91±1
C_{11}-vinyl **1b**	$CHBr_3$	300	2 h	~15	16.1±0.2	101±1	82±1
C_{11}-vinyl **1b**	$CHBr_3$	300	3 h	~15	16.6±0.3	101±1	80±1
C_{11}-vinyl **1b**	$CHBr_3$	300	4 h	~15	11.6±0.4	101±1	72±1
C_{11}-vinyl **1b**	$CHBr_3$	300	5 h	~15	9.9±0.1	101±1	70±1
C_{15}-vinyl **1c**	$CHCl_3$	300	3 h	~19	19.6±0.2	105±1	85±1
C_{15}-vinyl **1c**	$CHBr_3$	300	3 h	~19	19.1±0.3	105±1	80±1
C_{18}-methyl **1e**	$CHCl_3$	300	3 h	~26	26.2±0.1	109±1	109±1
C_{18}-methyl **1e**	$CHBr_3$	300	3 h	~26	25.6±0.3	109±1	109±1

Appendix 3 - Synthesis of 1,1-dichloro-2-octylcyclopropane 5.10

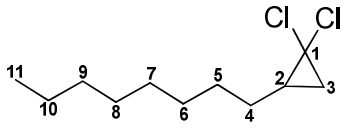

Sodium hydroxide (3.0 g, 75 mmol, 12 eq) and BTEAC (0.02 g, 0.1 mmol) were added to dichloromethane (6 mL) at room temperature. The mixture was cooled to 0 °C and then chloroform (6 mL) was added in a single portion. The reaction mixture was stirred for 10 min, then 1-decene (0.88 g, 6.3 mmol, 1 eq) was added dropwise over a period of 30 min. The mixture was stirred for 8 h at rt and then quenched by the addition of water (20 mL). The aqueous layer was extracted into dichloromethane (3 × 10 mL), and the combined organic extracts were dried over $MgSO_4$. The product was purified by silica gel chromatography (hexane), affording 1,1-dichloro-2-octylcyclopropane **5.10** (0.69 g, 49%) as a colourless oil. ^{1}H NMR (400 MHz, $CDCl_3$) δ_H 1.63-1.40 (6H, m), 1.37-1.21 (10H, m), 1.06-1.01 (1H, m), 0.88 (3H, t, *J* 6.6 Hz, C$\underline{H}_3$) ^{13}C NMR (100 MHz, $CDCl_3$) δ_C 32.0, 31.0, 30.5, 29.6, 29.4, 29.3, 28.7, 26.9, 22.8, 14.3; *HRMS m/z* (CI): calculated for $C_{11}H_{20}{}^{35}Cl_2$ [M^+] 222.0937, found 222.0938.

Appendix 4 - Synthesis of 1,1-dibromo-2-octylcyclopropane 5.11

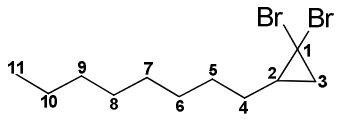

Sodium hydroxide (3.0 g, 75 mmol, 12 eq) and BTEAC (0.02 g, 0.1 mmol) were added to dichloromethane (6 mL) at room temperature. The mixture was cooled to 0 °C and then bromoform (6 mL) was added in a single portion. The reaction mixture was stirred for 10 min, then 1-decene (0.88 g, 6.3 mmol, 1 eq) was added dropwise over a period of 30 min. The mixture was stirred for 8 h at rt and then quenched by the addition of water (20 mL). The aqueous layer was extracted into dichloromethane (3 × 10 mL), and the combined organic extracts were dried over $MgSO_4$. The product was purified by silica gel chromatography (hexane), affording 1,1-dibromo-2-octylcyclopropane **5.11** (1.05 g, 54%) as a colourless oil. ^{1}H NMR (400 MHz, $CDCl_3$) δ_H 1.78-1.68 (1H, m), 1.66-1.41 (6H, m), 1.39-1.23 (10H, m), 0.88 (3H, t, *J* 6.5 Hz, C$\underline{H}_3$) ^{13}C NMR (100 MHz, $CDCl_3$) δ_C 32.6, 31.9, 31.5, 29.8, 29.5, 29.3, 29.2, 28.5, 28.3, 22.7, 14.1; *HRMS m/z* (CI): calculated for $C_{11}H_{19}{}^{79}Br_2$ $[M-H]^+$ 308.9848, found 308.9845.

Appendix 5 - General experimental procedure for the reaction of TMSCF3 on SAMs

To a round bottom flask (10 mL) equipped with a stirring bar, NaI (0.2 eq) and $TMSCF_3$ (0.6 mM, 1.0 mM, 1.4 mM, 1.7 mM, 2.7 mM) in THF (2 mL) were added. Next, the silicon wafers (1 cm × 1.5 cm), pre-coated with vinyl-terminated SAMs, were immersed in the reaction mixture and the solution was stirred at 65 °C for fixed periods of time (2 h, 3 h, 4 h, 5 h). After the reaction, the wafers were washed several times with distilled water and then sonicated sequentially in dichloromethane, toluene and DI water for a minimum of 15 min in each solvent. Then the wafers were dried under a nitrogen atmosphere and stored in a desiccator until they have been characterised.

Appendix 6 - Table A2 - SAMs modification with $TMSCF_3$

The results obtained after the reaction of vinyl- and methyl- terminated SAMs with $TMSCF_3$. Each value is an average of measurements taken from two samples. The errors are based on standard deviation.

Precursor Molecule	$TMSCF_3$ [mM]	Time [h]	Film Thickness [Å]		Film Contact Angle [°]	
			Before	After	Before	After
C_{11}-vinyl **1b**	0.6	3 h	~15	15.6±0.2	101±1	101±1
C_{11}-vinyl **1b**	1.0	3 h	~15	15.7±0.3	101±1	101±1
C_{11}-vinyl **1b**	1.4	3 h	~15	16.1±0.1	101±1	103±1
C_{11}-vinyl **1b**	1.7	3 h	~15	17.1±0.1	101±1	104±1
C_{11}-vinyl **1b**	2.7	3 h	~15	14.0±0.2	101±1	100±1
C_{11}-vinyl **1b**	1.7	2 h	~15	16.0±0.3	101±1	103±1
C_{11}-vinyl **1b**	1.7	3 h	~15	17.5±0.1	101±1	104±1
C_{11}-vinyl **1b**	1.7	4 h	~15	13.9±0.2	101±1	103±1
C_{11}-vinyl **1b**	1.7	5 h	~15	13.4±0.3	101±1	100±1
C_{11}-vinyl **1b**	1.7	48 h	-	-	101±1	83±1
C_{15}-vinyl **1c**	1.7	3 h	~19	19.2±0.1	103±1	104±1
C_{18}-methyl **1e**	1.7	3 h	~26	26.0±0.2	109±1	109±1

Appendix 7 - Synthesis of 1,1-difluoro-2-octylcyclopropane 5.16

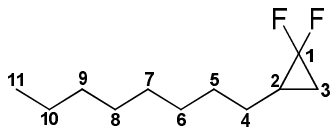

Sodium iodide (0.64 g, 4.3 mmol, 0.2 eq), 1-decene (3.0 g, 21.4 mmol, 1 eq) and THF (40 mL) were placed in a round-bottom flask. $TMSCF_3$ (7.6 mL, 53.5 mmol, 2.5 eq) was then added. The reaction mixture was heated at 65 °C for 2 h and then concentrated *in vacuo*. The crude was extracted into diethyl ether (3 × 25 mL), and the combined organic layers were washed sequentially with water (25 mL), sodium sulphite solution (25 mL), saturated sodium bicarbonate solution (25 mL), dried over $MgSO_4$ and then the solvent was removed *in vacuo*. The product was purified over silica gel (hexane), to afford 1,1-difluoro-2-octylcyclopropane **5.13** (1.9 g, 48%) as a colourless oil; ^{1}H NMR (400 MHz, $CDCl_3$) δ_H 1.52-1.18 (17H, m), 0.88 (3H, t, *J* 6.6 Hz, C$\underline{H}_3$); ^{13}C NMR (100 MHz, $CDCl_3$) δ_C 114.7 (1C, t, *J* 283.2, Hz $\underline{C}F_2$), 31.9, 29.4, 29.2, 29.1, 28.8, 26.8, 26.7, 22.7-22.4 (1C, m), 15.9 (1C, t, *J* 11.2 Hz), 14.0; ^{19}F NMR (282 MHz, $CDCl_3$) δ_F -145.1 (1F, ddd, *J* 154.2, 12.8, 4.6 Hz), -128.1- (-128.7) (1F, m); *HRMS m/z* (CI): calculated for $C_{11}H_{19}F_2$ $[M\text{-}H]^+$ 189.1449, found 189.1444.

Appendix 8 - Table A3 - thermal degradation of SAMs

Water contact angle and thickness values of C_{18}-methyl **1e** and C_{10}-methyl **1d** before and after thermal degradation. Each value is an average of measurements taken from two samples. The errors are based on standard deviation.

Precursor Molecule	Reaction Temperature	Time	Film Thickness [Å]		Film Contact Angle [°]	
			Before	After	Before	After
C_{10}-methyl **1d**	160 °C	1 h	~15	15.9±0.3	107±1	107±1
C_{10}-methyl **1d**	160 °C	2 h	~15	16.0±0.2	107±1	106±1
C_{10}-methyl **1d**	160 °C	3 h	~15	16.5±0.3	107±1	107±1
C_{10}-methyl **1d**	160 °C	4 h	~15	15.6±0.1	107±1	106±1
C_{10}-methyl **1d**	160 °C	5 h	~15	15.5±0.1	107±1	104±1
C_{10}-methyl **1d**	160 °C	6 h	~15	13.7±0.2	107±1	101±1
C_{10}-methyl **1d**	160 °C	13 h	~15	13.0±0.1	107±1	94±1
C_{10}-methyl **1d**	160 °C	19 h	~15	12.5±0.1	107±1	91±1
C_{10}-methyl **1d**	160 °C	24 h	~15	11.0±0.2	107±1	86±1
C_{10}-methyl **1d**	160 °C	48 h	~15	9.0±0.2	107±1	75±1
C_{18}-methyl **1e**	160 °C	1 h	~26	26.4±0.3	109±1	108±1
C_{18}-methyl **1e**	160 °C	2 h	~26	26.0±0.2	109±1	109±1
C_{18}-methyl **1e**	160 °C	3 h	~26	27.0±0.2	109±1	109±1
C_{18}-methyl **1e**	160 °C	4 h	~26	25.5±0.1	109±1	108±1
C_{18}-methyl **1e**	160 °C	5 h	~26	24.7±0.1	109±1	107±1
C_{18}-methyl **1e**	160 °C	6 h	~26	21.0±0.2	109±1	104±1
C_{18}-methyl **1e**	160 °C	13 h	~26	20.0±0.1	109±1	98±1
C_{18}-methyl **1e**	160 °C	19 h	~26	18.5±0.1	109±1	92±1
C_{18}-methyl **1e**	160 °C	24 h	~26	17.0±0.1	109±1	85±1
C_{18}-methyl **1e**	160 °C	48 h	~26	16.0±0.2	109±1	80±1

Appendix 9 - Table A4 - vinyl-terminated SAMs modification with HFAA

The results obtained after the reaction of C_{11}-vinyl **1b** and C_{15}-vinyl **1c** SAMs with HFAA. Each value is an average of measurements taken from two samples. The errors are based on standard deviation.

Precursor Molecule	Reaction Temperature	HFAA [µL]	Time [h or min]	Film Thickness [Å]		Film Contact Angle [°]	
				Before	After	Before	After
C_{11}-vinyl **1b**	160 °C	150	48 h	~15	<10	101±1	55±1
C_{11}-vinyl **1b**	160 °C	50	48 h	~15	<10	101±1	50±1
C_{11}-vinyl **1b**	160 °C	50	5 h	~15	<10	101±1	83±1
C_{11}-vinyl **1b**	160 °C	50	2 h	~15	<10	101±1	97±1
C_{11}-vinyl **1b**	160 °C	50	1 h	~15	<10	101±1	95±1
C_{11}-vinyl **1b**	160 °C	50	30 min	~15	<10	101±1	99±1
C_{11}-vinyl **1b**	160 °C	50	20 min	~15	13.1±0.2	101±1	106±1
C_{11}-vinyl **1b**	160 °C	50	10 min	~15	13.1±0.3	101±1	104±1
C_{11}-vinyl **1b**	120 °C	50	20 min	14.9±0.1	12.4±0.4	101±1	101±1
C_{11}-vinyl **1b**	120 °C	100	20 min	15.3±0.1	15.3±0.1	101±1	101±1
C_{11}-vinyl **1b**	80 °C	50	20 min	13.6±0.2	12.4±0.3	101±1	101±1
C_{11}-vinyl **1b**	80 °C	100	20 min	14.7±0.1	15.3±0.2	101±1	101±1
C_{11}-vinyl **1b**	160 °C	100	20 min	~15	16.1±0.1	101±1	106±1
C_{11}-vinyl **1b**	160 °C	150	20 min	14.6±0.1	15.2±0.2	101±1	106±1
C_{11}-vinyl **1b**	160 °C	200	20 min	14.9±0.1	15.3±0.1	101±1	106±1
C_{11}-vinyl **1b**	160 °C	300	20 min	15.1±0.2	16.7±0.3	101±1	106±1
C_{11}-vinyl **1b**	160 °C	400	20 min	15.4±0.1	13.1±0.2	101±1	100±1
C_{15}-vinyl **1c**	160 °C	200	20 min	19.1±0.1	20.4±0.1	101±1	106±1
C_{15}-vinyl **1c**	160 °C	300	20 min	19.1±0.2	21.7±0.1	101±1	106±1
C_{15}-vinyl **1c**	160 °C	400	20 min	20.2±0.1	18.1±0.1	101±1	103±1

Appendix 10 - Table A5 - methyl-terminated SAMs modification with HFAA

The results obtained after the reaction of C_{10}-methyl **1d**, C_{18}-methyl **1e** and C_{12}-methyl **1f** SAMs with HFAA. Each value is an average of measurements taken from two samples. The errors are based on standard deviation.

Precursor Molecule	Reaction Temperature	HFAA [µL]	Time [h or min]	Film Thickness [Å]		Film Contact Angle [°]	
				Before	After	Before	After
C_{10}-methyl **1d**	160 °C	100	20 min	15.2±0.2	10.9±0.3	105±1	103±1
C_{10}-methyl **1d**	120 °C	50	20 min	-	-	105±1	105±1
C_{10}-methyl **1d**	120 °C	100	20 min	-	-	105±1	105±1
C_{10}-methyl **1d**	80 °C	50	20 min	-	-	105±1	105±1
C_{10}-methyl **1d**	80 °C	100	20 min	-	-	105±1	105±1
C_{10}-methyl **1d**	160 °C	200	20 min	13.2±0.3	15.3±0.2	105±1	105±1
C_{18}-methyl **1e**	160 °C	200	20 min	27.1±0.1	26.2±0.1	109±1	109±1
C_{18}-methyl **1e**	160 °C	50	5 h	26.2±0.1	19.1±0.1	109±1	104±1
C_{18}-methyl **1e**	160 °C	50	2 h	26.3±0.1	25.4±0.1	109±1	109±1
C_{12}-methyl **1f**	160 °C	200	20 min	13.9±0.2	15.5±0.2	106±1	106±1

Appendix 11 - Synthesis of 2,6-dioctyl-4,4,8,8-tetrakis(trifluoromethyl)-1,5-diazobicyclo[3,3,0]octane 6.14

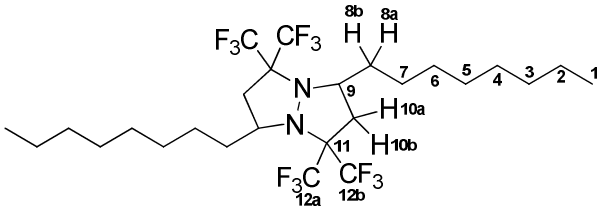

Hexafluoroacetone azine (1.0 g, 3.1 mmol, 1 eq) and 1-decene (0.9 g, 6.2 mmol, 2 eq) were placed in an autoclave and heated at 160 °C for 48 h. The reaction mixture was purified by silica gel chromatography (hexane), to give the 'criss-cross' adduct **6.14** as a colourless oil (278 mg, 15%). ^{1}H NMR (300 MHz, $CDCl_3$) δ_H 3.62-3.48 (2H, m, C*H*$(CH_2)_7CH_3$), 2.75 (2H, dd, *J* 13.8, 6.1 Hz, $(CF_3)_2C$*H2* 10a), 2.45 (2H, dd, *J* 13.8, 9.7 Hz, $(CF_3)2CC$*H2* 10b), 1.89-1.75 (2H, m, C*H*$_2(CH_2)_6CH_3$ 8a), 1.37-1.14 (26H, m, C*H*$_2$(C*H*$_2)_6CH_3$ 8b), 0.88 (6H, t, *J* 6.5 Hz, C*H*$_3$); ^{13}C NMR (75 MHz, $CDCl_3$) δ_C 123.7 (q, *J* 2.8 Hz, *C*F_3 12a), 123.5 (q, *J* 2.9 Hz, *C*F_3 12b), 69.0 (m, $(CF_3)_2$*C*), 56.6 (*C*H: C9), 41.1 ($(CF_3)_2C$*C*H_2: C10), 33.0 (*C*$H_2(CH_2)_6CH_3$: C8), 32.0, 29.7, 29.6, 29.3, 25.9, 22.8 (*C*H_2, C2-C7), 14.2 (*C*H_3); ^{19}F NMR (282 MHz, $CDCl_3$) δ_F -67.6 (6F, q, *J* 18.0, 8.6 Hz, C*F*$_3$ a), -73.6 (6F, q, *J* 18.0, 8.6 Hz, C*F*$_3$ b); *HRMS m/z* (CI): calculated for $C_{26}H_{41}F_{12}N_2$ $[M+H]^+$ 609.3073, found 609.3064.